T.R.
GEBZE TECHNICAL UNIVERSITY
GRADUATE SCHOOL OF NATURAL AND APPLIED SCIENCES

SYNTHESIS OF STYRENE BASED POLYMERS BEARING PENDANT FLUORESCENT GROUPS AND THEIR USE IN THE PREPARATION OF ELECTROSPUN NANOFIBERS

SÜMEYRA BAYIR
A THESIS SUBMITTED FOR THE DEGREE OF
DOCTOR OF PHILOSOPHY
DEPARTMENT OF CHEMISTRY

GEBZE
2017

T.R.

GEBZE TECHNICAL UNIVERSITY

GRADUATE SCHOOL OF NATURAL AND APPLIED SCIENCES

SYNTHESIS OF STYRENE BASED POLYMERS BEARING PENDANT FLUORESCENT GROUPS AND THEIR USE IN THE PREPARATION OF ELECTROSPUN NANOFIBERS

SÜMEYRA BAYIR

A THESIS SUBMITTED FOR THE DEGREE OF

DOCTOR OF PHILOSOPHY

DEPARTMENT OF CHEMISTRY

THESIS SUPERVISOR

PROF. DR. AYŞE GÜL GÜREK

II. THESIS SUPERVISOR

ASSOC. PROF. DR. MEHMET ATİLLA TAŞDELEN

GEBZE

2017

T.C.
GEBZE TEKNİK ÜNİVERSİTESİ
FEN BİLİMLERİ ENSTİTÜSÜ

FLORESANS GRUPLARINA SAHİP STİREN POLİMERLERİNİN SENTEZİ VE ELEKTROEĞİRİLMİŞ NANOFİBERLERİNİN ÜRETİLMESİ

SÜMEYRA BAYIR

DOKTORA TEZİ
KİMYA ANABİLİM DALI

DANIŞMANI
PROF. DR. AYŞE GÜL GÜREK
II. DANIŞMANI
DOÇ DR. MEHMET ATİLLA TAŞDELEN

GEBZE
2017

GEBZE TEKNİK ÜNİVERSİTESİ	**DOKTORA JÜRİ ONAY FORMU**

GTÜ Fen Bilimleri Enstitüsü Yönetim Kurulu'nun 29/03/2017 tarih ve 2017/19 sayılı kararıyla oluşturulan jüri tarafından 13/04/2017 tarihinde tez savunma sınavı yapılan SÜMEYRA BAYIR'ın tez çalışması KİMYA Anabilim Dalında DOKTORA tezi olarak kabul edilmiştir.

JÜRİ

ÜYE (TEZ DANIŞMANI)	: Prof. Dr. Ayşe GÜL GÜREK
ÜYE	: Prof. Dr. Hayal BÜLBÜL SÖNMEZ
ÜYE	: Yrd. Doç. Dr. Erdinç DOĞANCI
ÜYE	: Yrd. Doç. Dr. İlke ANAÇ
ÜYE	: Yrd. Doç. Dr. Ozan TOPRAKÇI

ONAY

Gebze Teknik Üniversitesi Fen Bilimleri Enstitüsü Yönetim Kurulu'nun

...../...../..... tarih ve ...../..... sayılı kararı.

İMZA/MÜHÜR

SUMMARY

In the present thesis, styrene based polymers bearing different fluorescence active functional groups were synthesized and employed for the preparation of electrospun nanofibers. This research methodology is empirical and consists of four chapters based different types of fluorescent groups; i) pyrene functional, ii) dansyl-functional, iii) porphyrin-functional, and iv) coumarin-functional styrene copolymers.

For this purpose, in the first step, styrene copolymers with chloromethyl side groups were synthesized via nitroxide mediated radical polymerization method, which is a well-known controlled polymerization method, using styrene and vinylbenzyl chloride as monomers. In the second step, the obtained polymers with the chloride side groups were converted into azide by treating sodium azide. In the final step, azide side groups of the styrene polymers were converted into pyrene, dansyl, and porphyrin using copper(I)-catalyzed azide alkyne cycloaddition (CuAAC) click chemistry technique. Additionally, the chloride side groups of the styrene copolymer were converted into coumarin via etherification reaction. The obtained functional styrene copolymers with different fluorescent groups were employed in the production of nanofibers via electrospinning method. These functional nanofibers, depending on their fluorescence active functional groups, are thought to have potentials to be used in optic chemical sensors, electrochromic fibers, and ultrafiltration.

Key Words: Styrene, Vinylbenzyl Chloride, Click Chemistry, Functional Polymers, Electrospinning, Nanofiber.

ÖZET

Bu tez çalışması dört bölümden oluşmakta ve her bölüm floresans özellikte farklı moleküle (piren, dansil, porfirin ve kumarin) sahip stiren kopolimerlerin sentezini ve elektroeğirme yöntemi ile bu kopolimerlerin nanofiberlerinin hazırlanmasını içermektedir. Bu kapsamda sentezlenen polimerler; piren yan gruplarına sahip stiren polimeri, dansil yan gruplarına sahip stiren polimeri, porfirin yan gruplarına sahip stiren polimeri ve kumarin yan gruplarına sahip stiren polimeridir.

Bu amaçla öncelikle stiren ve vinilbenzil klorür monomerleri kullanılarak kontrollü bir polimerleşme yöntemi olan nitroksi ortamlı radikalik polimerleşme yöntemi ile klorür yan gruplarına sahip polistiren sentezlendi. Sonra, elde edilen polimerlerin klorür yan grupları sodyum azidür ile azidür gruplarına dönüştürüldü. Son adımda ise azidür yan gruplarına sahip stiren polimerleri oldukça etkili bir fonksiyonlandırma yöntemi olan bakır(I) katalizörlü azid-alkin siklo-katılma (CuAAC) click tepkimesi kullanılarak piren, dansil ve porfirin grupları ile fonksiyonlandırılırken, eterleştirme reaksiyonu ile klorürür yan gruplarına sahip stiren polimerleri kumarin ile fonksiyonlandırıldı. Elde edilen farklı fonksiyonel gruplara sahip bu stiren polimerleri elektroeğirme yöntemi ile nanofiber üretiminde kullanıldı. Bu tez kapsamında hazırlanan elektroeğirilmiş polistiren nanofiberlerinin sahip oldukları foksiyonel gruplara bağlı olarak optik kimyasal sensör, elektrokromik lif üretimi ve ultrafiltrasyon alanlarında kullanım potansiyeline sahip olacakları düşünülmektedir.

Anahtar Kelimeler: Stiren, Vinilbenzil Klorür, Click Kimyası, Fonksiyonel Polimerler, Elektroeğirme, Nanofiber.

ACKNOWLEDGEMENTS

I would like to express my special appreciation and thanks to my advisors Prof. Dr. Ayşe Gül Gürek and Assoc. Prof. Dr. Mehmet Atilla Taşdelen.

I would also like to thank Asst. Prof. Dr. Erdinç Doğancı, Zeynep M. Şahin, Büşra Şengez, Figen Aynalı, Magdalena Tonta, Dr. Muhammet Aydın, Enis Taşcı, Nursel Olgaç, Mustafa Uygun, Fırat Kayabaşı, and Ahmet Üner for their supports and helps doing my Ph.D. thesis.

I would especially like to thank Faruk Yılmaz for encouraging my research and for supporting me during these past four years, and also thanks to Mesut Görür for his guidance and supporting during my Ph.D. thesis.

I would also like to thank Assoc. Prof. Dr. Tamer Uyar, Dr. Aslı Çelebioglu, and Anitha Senthamizhan for their supports in application studies.

I would also like to thank TUBITAK (113Z577) for the financial support.

I would also like to thank my friend Fatma Sağır for supporting and encouraging me throughout this experience.

Finally a special thanks to my family, my mother, and father for all of the sacrifices that you've made on my behalf.

TABLE of CONTENTS

LIST of ABBREVIATIONS and ACRONYMS

Abbreviations and Acronyms		**Explanations**
aq	:	Aqua
dB	:	Decibel
h	:	Hour
kV	:	Kilovolt
mL	:	Mililiter
nm	:	Nanometer
v/v	:	Volume/volume
w/v	:	Weight/volume
BPO	:	Benzoyl peroxide
CVD	:	Chemical Vapor Deposition
CuAAC	:	Copper-Catalyzed Azide-Alkyne Cycloaddition
DCM	:	Dichloromethane
DMAc	:	Dimethyl acetamide
DMF	:	Dimethyl formamide
DNT	:	Dinitrotoluene
DSC	:	Differential Scanning Calorimetry
EMI	:	Electromagnetic interference
EPS	:	Expanded polystyrene
FNFM	:	Fluorescent nanofibrous membrane
FTIR	:	Fourier-transform Infrared Spectroscopy
GPC	:	Gel Permeation Chromatography
GTU	:	Gebze Technical University
HEPA	:	High-efficiency particulate air
IMU	:	Istanbul Medeniyet University
MWNT	:	Multi-layer carbon nanotube
NMP	:	Nitroxide Mediated Radical Polymerization
NMR	:	Nuclear Magnetic Resonance Spectroscopy
NSF	:	National Science Foundation
PANI	:	Polyaniline

PEO	:	Poly(ethylene oxide)
PMDETA	:	*N,N,N′,N″,N″*-Pentamethyldiethylenetriamine
ppb		Parts-per-billion
PS	:	Polystyrene
PSA		Polysulfonamide
Pd	:	Palladium
Pt	:	Platinum
QCM	:	Quartz crystal microbalance
Rh	:	Rhodium
RT	:	Room Temperature
SAS-CI	:	Statistical Analysis Software- Customer Intelligence
SEM	:	Scanning Electron Microscopy
TEM	:	Transmission Electron Microscopy
TEMPO	:	2,2,6,6-Tetramethyl-1-piperidinyloxy
Tg	:	Glass transition temperature
TGA	:	Thermal Gravimetric Analysis
TMOPP	:	Tetrakis (4-methoxyphenyl)porphyrin
TNT	:	Trinitrotoluene
TPA-PBPV	:	Triphenylamine-alt-biphenylenevinylene
UNAM	:	National Nanotechnology Research Center
UV-vis	:	Ultraviolet–visible
VOC	:	Volatile organic compound

LIST of FIGURES

LIST of TABLES

1. INTRODUCTION

Nanofibers have generated increasing research interest in recent years. As an important nanomaterial, nanofibers have great specific surface area due to their very small diameter sizes. Therefore, nanofibers have superior physical (hardness, tensile strength etc.) and chemical (number of functional groups per unit surface area) properties compared to ordinary polymer fibers [1]. Besides these unique merits, nanofibers have a potential to be used in a variety of fields requiring materials with unexcelled properties, since polymers can have very different functional groups and can be loaded with various materials.

A number of processing methods such as, chemical synthesis [2-4], nanolithography [5-6], electrospinning [7-10], and physical drawing [11-17] have been developed for the preparation of polymer nanofibers. Among these methods, electrospinning is the most currently used fabrication method with its high production rate and low cost [10,18]. In this method, polymer solutions or melts are exposed to high-voltage electric fields between a metallic needle and a conductive collector and drawn into fibers from micron to several nanometer diameters [19]. This method can be applied to a broad range of polymers that can be dissolved or melted. The method may seem as a simple and straightforward method, but in fact it is a very complicated procedure and depends on various molecular, process and technical parameters that must be tackled carefully. The most prominent advantage of electrospinning is that a variety of non-fiber forming materials can be incorporated into nanofiber nonwovens. Besides, very sensitive biological entities, like virus, bacteria and cell, can be immobilized into nanofiber materials. Electrospun nanofibers can be employed in a variety of applications depending on the functional groups they have. Fiber diameters have a great influence on the effectiveness of nanofibers. Thin and defect-free fibers are required to increase the effectiveness of nanofibers.

Many natural and synthetic polymer nanofibers were obtained by electrospinning method, including, acrylate [20] and methacrylate polymers [21,22], vinyl polymers [23,24], polystyrene (PS) [25], polyamide (PA) [26,27], polyurethane (PU) [28,29], polyesters [30-32], polybenzimidazole [33], polycarbonate [34], polyethylene glycol [35,36], polyaniline [37], natural polymers [38-42] and their composites [43-44]. In addition, various

nanomaterials, pigments, and materials having various functional groups were added to polymer solutions and used in the production of composite nanofibers [45].

Amorphous polystyrene is transparent and stiff material with a high electrical resistance and low dielectric loss. It is one of the most widely employed commodity polymer in a variety of applications, such as packaging, insulation, and filtration. Many studies have been conducted on the preparation of electrospun nanofibers from polystyrene and their applications, depending on the functional groups they have.

Polymer nanofibers can be used in a wide range of applications like filtermaterials [46,47], wound dressing materials, nano-composites, non-woven fabrics, tissue engineering, ultrafiltration, ion exchange, enzyme immobilization, optic chemical sensors, catalysis immobilization, electromagnetic interference (EMI) shielding, electrochromic fibers [48], and many others.

Nanofibers with fluorescence characteristics are preferred in optical chemical sensor applications due to the high surface area, high sensitivity and fast responses of fluorescence sensors [49]. It is known that the pyrene, dansyl, porphyrin, and coumarin fluorescence structures react with some chemicals in the solution medium or in air by suppressing the fluorescence activity or changing the fluorescence properties. In addition, nanofibers increase the sensitivity of the added sensor molecules and reduce the response time due to their high surface area and porous structure.

Tao and his friends performed a work on electrospun silica nanofibers modified with porphyrin to detect the TNT in vapor [50]. Wand and coworkers obtained a PS fluorogenic nanofibrous sensing material from polystyrene/pyrene blends to detect the buried explosives [51]. Hua et al. fabricated electrospun polyacrylonitrile nanofibers coated with pyrene to detect the TNT based on fluorescence quenching mechanism [52].

In this thesis, pyrene, dansyl, porphyrin, and coumarin functional styrene copolymers were synthesized using Nitroxide Mediated Radical Polymerization (NMP) and copper(I)-catalyzed azide alkyne cycloaddition (CuAAC) “click” chemistry techniques. The obtained styrene polymers were employed in the production of nanofibers via electrospinning method. The chemical structures of the synthesized polymers were investigated via ^{1}H NMR and FT-IR spectroscopic

methods. Average molecular weights of the synthesized polymers and polydispersity indices were determined via gel permeation chromatography (GPC) and also synthesized monomers have been analytically characterized by mass spectrometry. Morphological and structural characterizations of the nanofibers were performed via scanning electron microscope (SEM). Thermal properties of the polymers were studied via differential scanning calorimetry (DSC) and thermogravimetric analysis (TGA). Fluorescence measurements of the fluorescence-active nanofibers were conducted using fluorescence spectrophotometer.

2. THEORETICAL PART

2.1. Nanofibers

National Science Foundation (NSF) and fiber science related literature, defines the term nanofibers as fibers having at least one dimension of 100 nanometer (nm) or less, but generally nanofibers are considered as having a diameter of less than one micron according to nonwoven industry [53].

2.1.1. Nanofiber Structure and Properties

Nanofbers have different commercial applications due to their properties such as high surface area, high porosity, and tight pore sizes [54]. Figure 2.1 shows how much smaller nanofibers are compared to a human hair, which is 50-150 µm and the size of a pollen particle compared to nanofibers [55].

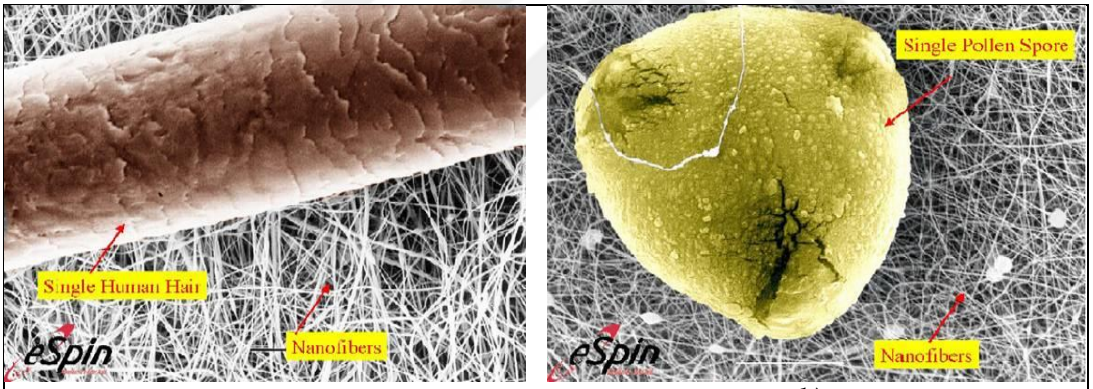

Figure 2.1: Comparison between a) human hair, nanofiber web and b) entrapped pollen spore on nanofiber web.

2.1.2. Nanofiber Production Methods

There are various methods for nanofibers production; such as drawing, phase separation, template synthesis, self assembly, and electrospinning, which have explained in the following sections.

2.1.2.1. Drawing Method

In this method, it is worked with a small micrometer radius micropipette. A micropipette (a device for the precise process under a microscope) with the help of a micro-manipulator is immersed in the line in contact with the surface of the polymer solution and micro-pipette is withdrawn from the liquid at a constant speed. In this way, fibers are collected on the surface (Figure 2.2) [56].

Drawing method requires little equipment, but due to lack of continuity of the process is disadvantageous in terms of practical applications. In addition, fibers can not be obtained below 100 nm and also diameter of nanofibers can not be controlled.

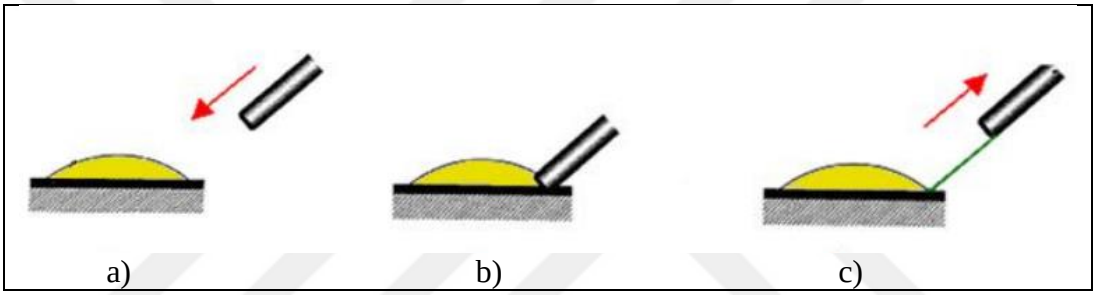

Figure 2.2: The preparation of fibers by the drawing method. (a) a millimeter drop of polymer solution is applied on the substrate material, b) micropipette moves down toward the edge of the drop, c) there is contact and the fiber is to pull out of polymer droplet by drawing back of micropipette.

2.1.2.2. Phase Separation Method

Nanofibers by phase separation method are produced on the basis of thermodynamic separation of two liquid phases. A schematic representation of phase separation is shown in Figure 2.3 [57]. This method generally takes place in five stages, respectively [58].

i) Dissolution of the polymer
ii) Gelation
iii) Solvent extraction
iv) Freezing
v) Freeze-drying

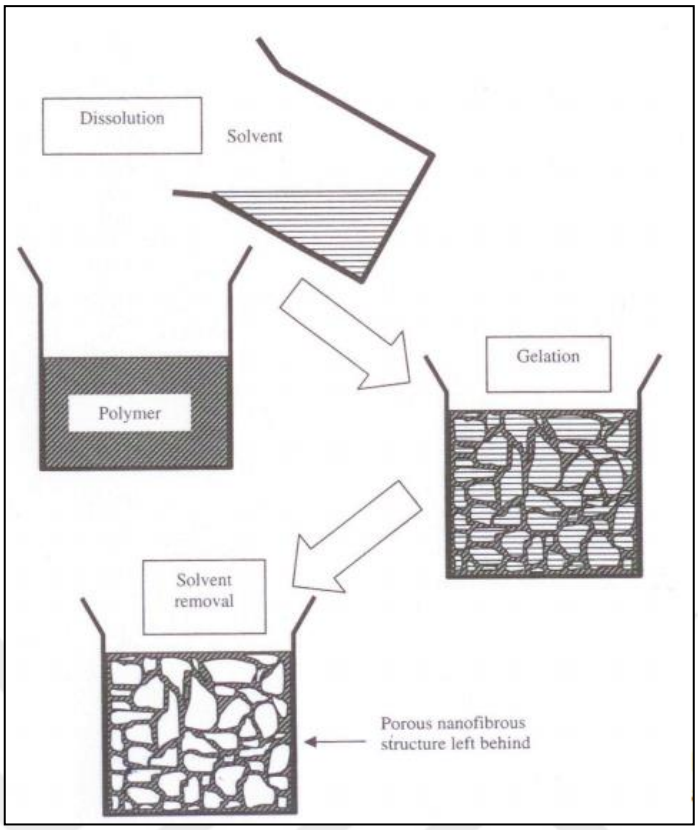

Figure 2.3: Fiber production with the phase separation method.

The polymer type, solvent, concentration, phase separation temperature, cooling and heating stages are important parameters. This method is a time consuming and complicated method. Controlling the fiber diameter is both very difficult and also this method is available only for certain polymers [53].

2.1.2.3. Template Synthesis Method

In this method, nanofibers are produced through nano-porous membranes (Figure 2.4) [57]. This specific membranes with 5-50 mm thickness have cylindrical porous structures. Nano cylinders, nanotubes, and nanofibers are obtained depending on the material and chemical structures of the pores [59]. The length of the produced nanofibers can be controlled by the use of alumina molds.

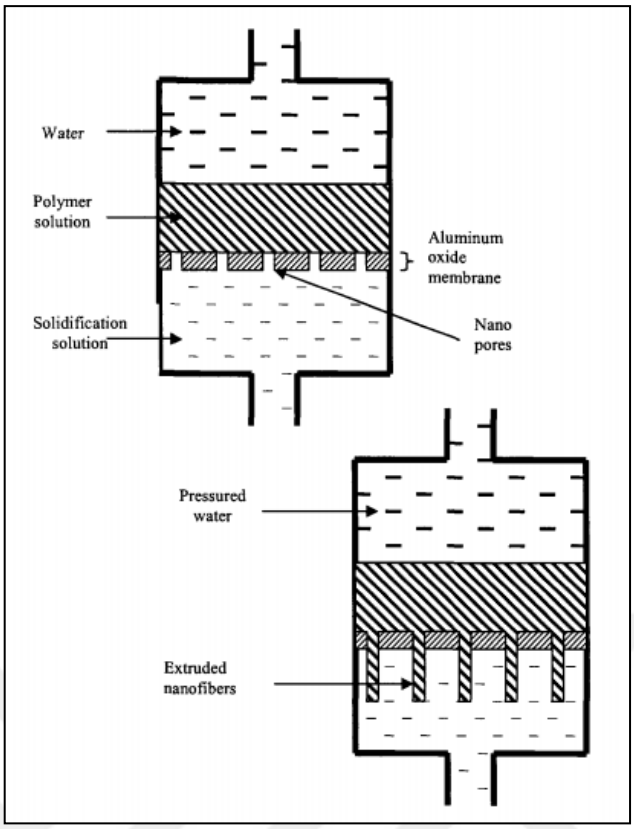

Figure 2.4: Schematic representation of the template synthesis method.

2.1.2.4. Self Assembly Method

In self assembly method, atoms or molecules are arranged in specific order spontaneously by hydrogen bonding, hydrophobic forces and weak and non-covalent interactions such as electrostatic attraction [60]. The self-assembly of a dendritic dipeptide is schematically illustrated in Figure 2.5 [61]. This method is complicated, required longer time and has a low production capacity.

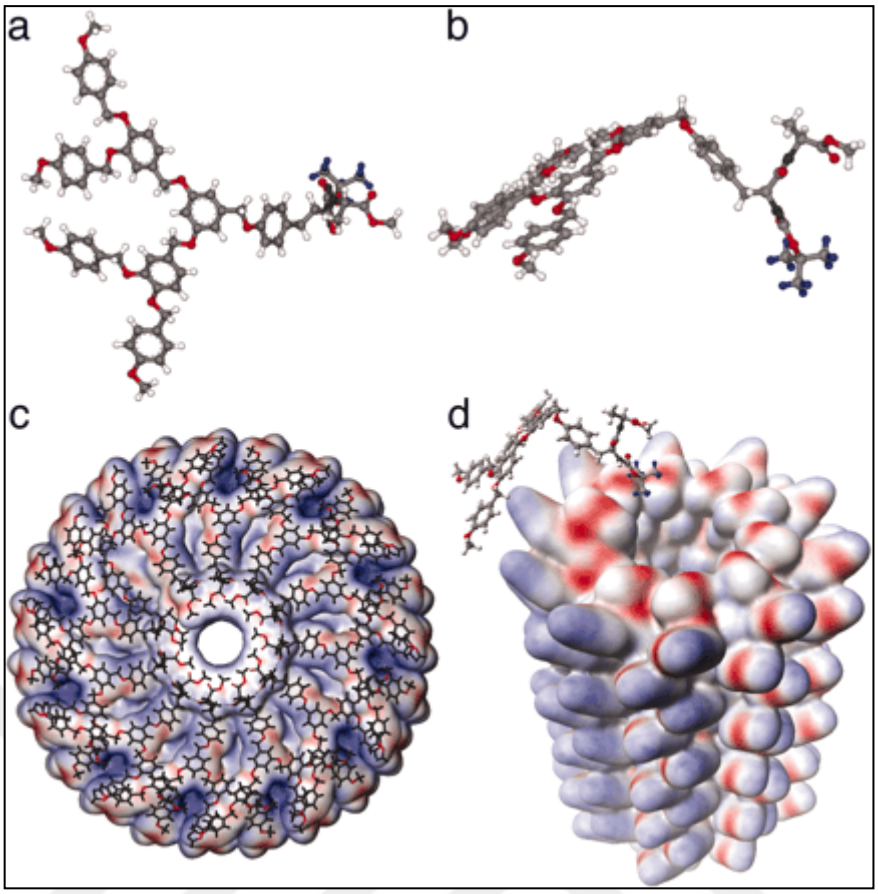

Figure 2.5: Self assembly of a dendritic dipeptide into helical pores (a-d).

2.1.2.5. Electrospinning Method

Electrospinning is also known as electrostatic spinning. The scientific basis of this method based on the search of Lord Rayleigh in 1882 about how much electrical charge is needed to overcome the surface tension of a drop [62]. The first important patent on the electrospinning of plastics was taken by Anton Formhals in 1934 [63]. Despite these operational procedures it has not gained enough commercial importance for a long time. In 1970, Simm and his colleagues patented the production of fibers having a diameter less than 1 mm [64]. Electrospun fibers found their first commercial applications in the filter applications. The interest in this field began to grow in the 1990s with the work of Reneker group [65].

Electrospinning method is suitable to put materials together with different functional groups for different applications and different settings. Many natural and synthetic polymer nanofibers have been prepared by electrospinning method.

Among them, acrylate [66] and methacrylate polymers [67], vinylic polymers [68], polystyrene [69], polyamide [70], polyurethane [71], polyesters [72,73], polybenzimidazole [74], polycarbonate [75], polyethyleneglycol [76], polyaniline [77], natural polymers [78, 79] and composites [80] have been widely studied. In addition, numerous nanomaterials, pigments and many materials having functional groups are used in the production of composite nanofibers by adding to the polymer solution [81].

Electrospinning is the most advantageous method for the production of nanofibers when compared with other methods. It is cheap and fast method that can be applied most effectively and easily. Applying a high potential voltage to the liquid polymer solution, fibers in the nanoscale are obtained. Advantages and disadvantages of nanofiber production methods are summarized in Table 2.1 [56,82,83].

Table 2.1: Comparison of nanofiber production methods.

Method	**Advantages**	**Limitations**	**Fiber diameter**	**Fiber size**
Drawing	• Minimum equipment is required.	• Discontinuous process.	2-100 nm	10 micron
Template synthesis	• Different fiber diameters	• Fiber size arrangement is limited	100 nm	10 micron
Phase separation	• Tailorable mechanical properties, pore size and interconnectivity • Batch-to-batch consistency • Minimum equipment is required.	• Low yield • Matrix directly fabricated • Limited to a few polymers	50-500 nm	Porous structure
Self assembly	• Achieves fiber diameters on lowest scale	• Only short fibers can be created. • Low yield. • Matrix directly fabricated. • Limited to a few polymers.	7-100 nm	1-20 micron
Electro-spinning	• Low cost • Continuous production capability • Nano-size fibers (high surface/volume) • Production of aligned nanofibers • Tailorable mechanical properties	• Large nanometer to micron scale fiber • Use of organic solvents • No control over 3D pore structure	3-1000 nm	Different sizes (m)

2.2. Nanofiber Production with Electrospinning Method

The experimental setup for electrospinning method (Figure 2.6) basically consists of three parts [84].

i) High voltage power supply,

ii) Supply unit (syringe, metal needle etc.),

iii) Grounded collector surface (conductive plate, rotating cylinder etc.).

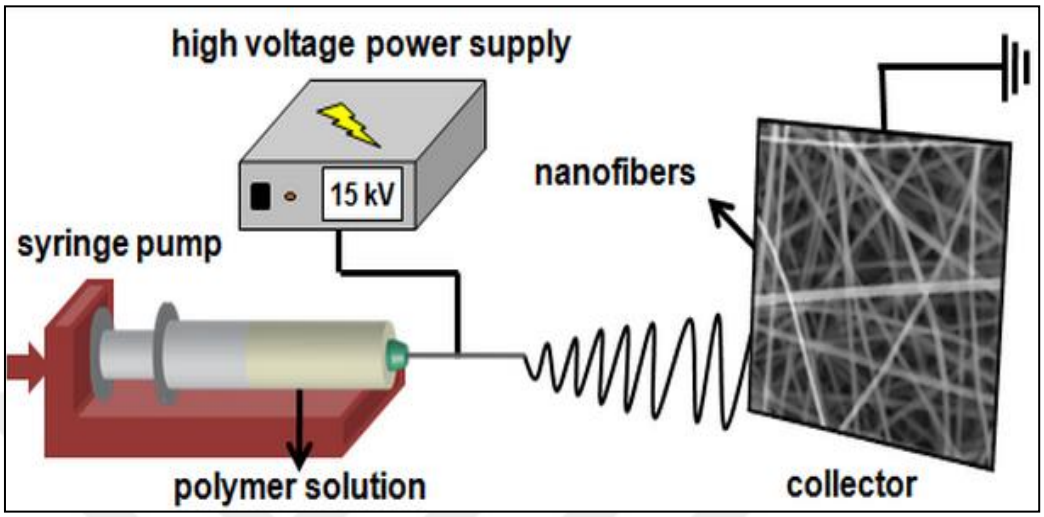

Figure 2.6: Schematic illustration of electrospining method.

In the process of electrospinning, the polymer solution is charged with electricity and a magnetic field is generated between two electrodes through high voltage at kV level. Prior to forming field the polymer solution is in the form of drops in the pipette or syringe tip, after forming field it takes conical shape (Taylor cone) due to the electric charges. When electrical forces overcome the surface tension and viscosity of the polymer solution, thin polymer solution is suitable for commercial production (Figure 2.7) [85]. In this process, the polymer solution is extruded under the influence of electric field from the surface. Polymer solution drawn by electric power is accelerated, but momentum is slowing after a while because of the resistance to viscosity or it is stable at zero, which shows an unstable behavior. Upon elongation of polymer jet and evaporation of the solvent the diameter of the fibers is reduced, loading is increasing and is divided into smaller diameters due to reduced diameter.

In the electrospinning method; viscosity of the solution, surface tension, conductivity, voltage value, feed amount, the distance between the pipette tip and the collector, atmospheric conditions are the most important factors that determine properties of the obtained nanofibers. Due to providing a very high surface area,

the nanoscale diameter of the obtained fiber allows its use in special areas such as filtration, drug delivery, controlled drug release, protective textiles, and fuel cells.

Stages of the electrospinning method;

i) droplet formation,
ii) formation of the Taylor cone,
iii) the formation of electro shooting jets
iv) the extension of the jet in stable area,
v) formation of the unstable area,
vi) solidification in the form of fiber.

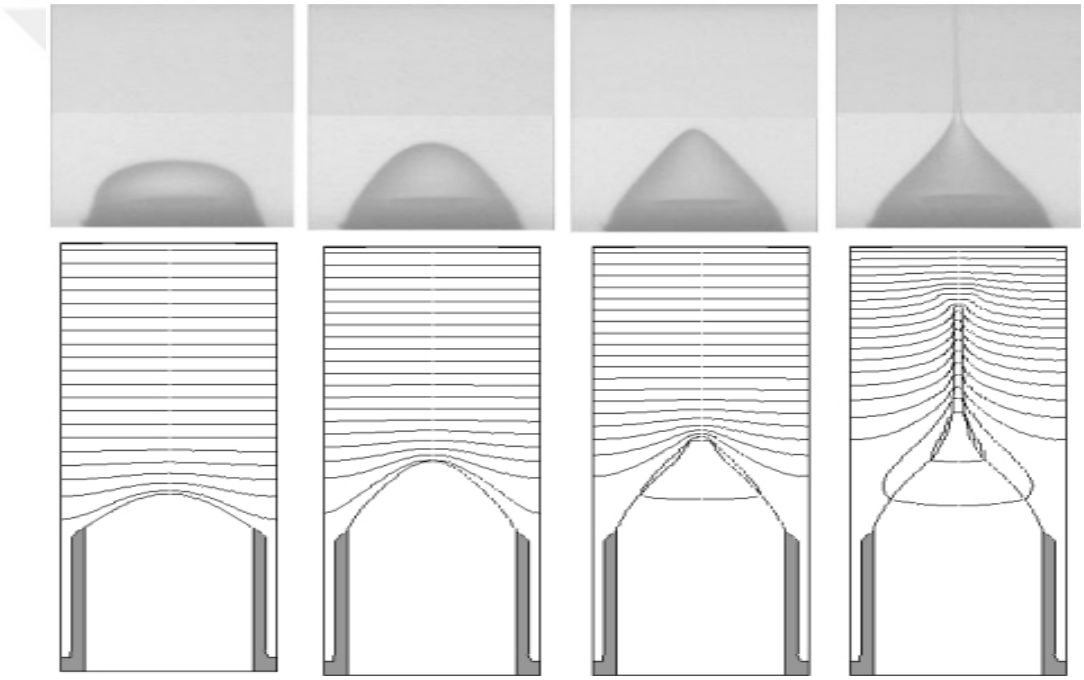

Figure 2.7: Formation of Taylor cone.

2.3. Parameters Affecting the Process of Electrospinning

These parameters are:

i) Solution parameters,
ii) Processing conditions,
iii) Environmental parameters.

Table 2.2: Parameters affecting the nanofiber formation.

Solution parameters	**Processing conditions**	**Environmental parameters**
Surface tension	Applied voltage	Temperature
Molecular weight and viscosity	Flow rate of solution	Humidity
Dielectric constant of solvent	Distance between a needle and a collector	Pressure
Conductivity of the solution	Diameter of the needle	Atmosphere type

2.3.1. Solution Parameters

The high value of the viscosity of the solution used during the process of electrospinning causes obstruction of the needle tip, on the other hand a low valueof viscosity by the action of solution gravity causes to drip from the needle tip and prevention of production. Because of this, the polymer solution should have a molecular weight to provide the required viscosity [86]. A greater amount of polymer will be in solution with increasing concentration. This situation will also positively affect the formation of continuous polymer jet. Several studies show that polymer solutions with low concentrations form more beaded structure, although in higher concentrations forms more uniform fibers are formed [87].

During the process of electrospinning, charge must be applied to overcome the surface tension. In electrospinning method, beaded structures can be seen due to the high surface tension. To reduce the surface tension, low surface tension solvents or surfactants may be added [88].

The total charge density increases when using a solution with a high dielectric constant. This allows an easy elongation of the polymer jet. Fiber diameter and bead formation are reduced.

If conductivity of the solution is increased, the polymer jet may carry more load. To increase conductivity, conductive solvents, ionic or nonionic surfactants, organic or inorganic salts may be added into polymer solution. Additional ions increase the conductivity of the solution, provide formation of fibers without beads and also decrease the fiber diameter.

2.3.2. Processing Conditions

The applied voltage causes an electrical charge of the polymer solution. The shape of the drop in the syringe tip with increasing voltage turns into different shapes and causes more loading of the jet. Consequently jet is accelerated. Voltage rise decreases the fiber diameter. The nanofiber diameter decreases with the increase of the applied voltage after a certain point, voltage increase will cause more polymer feeding (Figure 2.8) [89]. Taylor cone begins to form in the needle and can cause unwanted beads while pulling more polymer solution [90].

Fiber diameters can increase or beading can be observed, due to increase of the amount of solution taken from the syringe with increasing solution flow rate.

With increasing amount of withdrawn solution would not be enough time to evaporate the solvent. Thus, the solvent remaining in the fibers can cause the fibers sticking to each other [91].

When the distance between the needle and collector is reduced, it may not be sufficient time to evaporate the solvent due to reducing of the time required for collecting the polymer jets. Adhesions and beadings will be observed between fibers. When the distance is increased, lower diameter fibers will be achieved due to increase the path of the jet [92]. Decreasing the diameter of the syringe needle or capillary causes blocking, decrease in the number of beads, and fiber diameter.

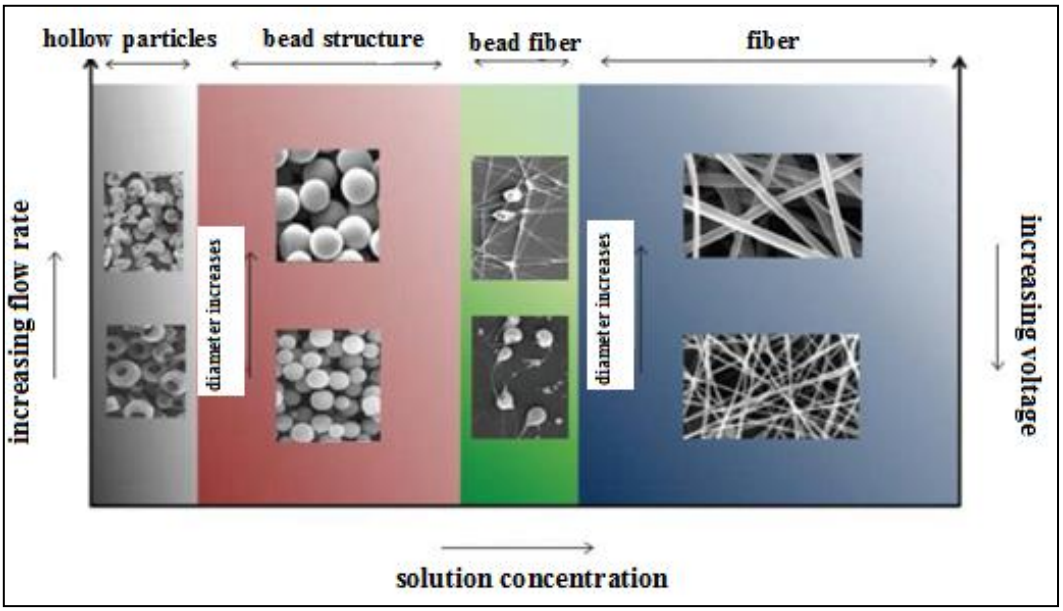

Figure 2.8: The effect of various parameters to the fiber structure.

In the electrospinning process, conductive materials are often used as collectors. Aluminium foil is the most widely used conductive material. The collector types used in electrospinning process are given in Table 2.3 [86, 93].

Table 2.3: The collector types used in electrospinning method.

Collector	**Collector shape**
Plane plate collector	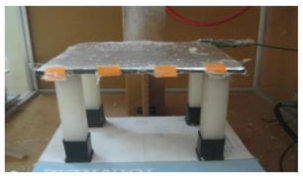
Grid type collector	
Drum rotatory collector	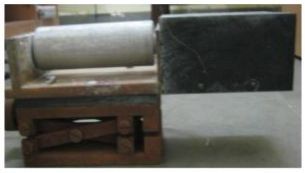
Edge type collector	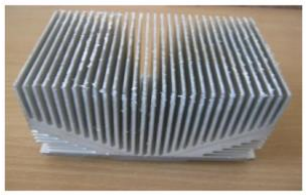

2.3.3. Environmental Parameters

Increase in temperature causes an increase in evaporation rate of the solvent, viscosity decrease, and increase in the solubility. All this helps elongation of the polymer jet and more uniform distribution of nanofiber structures.

In electrospinning method performed in a humid environment, porous structures are formed by condensation of water molecules on the fiber. Also humidity, reduces the evaporation rate of the solvent. Acrylic fibers at 60% relative humidity which was determined by experimental studies can not fully dry. [94].

During the electrospinning method, air composition is very important in the environment. The behavior of the gas in the electric field differ from each other. For example, helium is broken down in the electric field and prevents

electrospinning. When the pressure drops below the atmospheric value, the polymer solution in the needle will tend to flow out. This situation will lead to the formation of an unstable jet [95].

2.4. Applications of Electrospun Nanofibers

Electrospun nanofibers have potential use in many areas depending on the properties of the used polymers due to their high surface area.

Electrospun nanofibers, can be used as a template in the preparation of grooved hollow fiber. In this method, the polymeric nanofibers as the template like the poly(lactic acid) [96], nylon-4/6, and poly(tetramethylene adipamide) which can be easily pyrolyzed, are coated with materials (polymers, metals and other materials) to be prepared nanotubes. In an alternative selective form of fiber templates, after extraction or degradation hollow (grooved) fibers are obtained.

Electrospun nanofibers of a biodegradable and soluble poly(lactic acid) (PLA) was covered with poly(p-xylylene) using chemical vapor deposition method (CVD) by Hou. Then, grooved poly(p-xylylene) nanofibers were obtained as a result of PLA pyrolysis. As a result of TEM analysis, inner diameter of the obtained poly(p-xylylene) nanofibers were in the range of 5-50 nm, and the outer diameters were found between 50-250 nm [97].

Electrospun PLA nanofibers were immersed into the solution of titanium (IV) isopropoxide and then were subjected to hydrolysis and condensation process at 1: 1 isopropanol / water solvent system, by Caruso and his friends. Researchers, after drying of electrospun PLA nanofibers loaded with the metal nanoparticles precursor, titanium dioxide nanotubes were obtained with the PLA degradation by calcining for 10 hours at 723 K. As a result of SEM analysis, it was shown that the surface of the tube was quite smooth [98].

2.4.1. Filtration and Adsorption Techniques

Micron pore size filters are not enough for the filtration of very small particles, nanoporous filtration materials are a need [99]. Coalescence and aerosol filters are the most important applications of nanofiber nonwoven materials. Coalescence filters are quite effective for separating emulsions containing water

droplets smaller than 50 μm [100]. For example, they are used to remove small water droplets from aircraft fuel. If these water droplets are not removed, cause the formation of ice crystals at high altitudes [101]. In addition, thin aerosol particles may be filtered efficiently using nanofiber nonwoven filters [61]. For coalescence filtering, fiber diameter and wettability are important factors to be considered.

Shin et al. used electrospun polystyrene nanofibers, which were prepared using recycled expanded polystyrene (EPS), to filter the water droplets from water-in-oil emulsion. They also report that when 24.4% polysulfonamide (PSA) nanofibers were used in composite materials, filtration efficiency increased from 68% to 88%. In contrast, the pressure drop was increased at a significant rate [102]. In another study of Shin, optimum result was received when electrospun nylon-6 nanofibers were mixed with glass microfibers at 1.6% (w/w) ratio and there was no excessive pressure drop [103]. Shin and Chase have examined the effects of factors such as the fiber diameter, wettability, and thickness of the filter on coalescing filtration efficiency in their work by mixing electrospun nylon-6, polyamide and polyacrylonitrile nanofibers with glass microfibers. In this study, polyamide nanofiber filter with the smallest thickness showed the best separation efficiency (77%), on the other hand nylon nanofibers with high wettability value (49.0 dynes cm^{-1}) have provided optimum filtration efficiency (maximum separation efficiency with a minimum pressure drop). Also the separation efficiency increased with the increase of the thickness of the filter, whereas it was also encountered with more pressure drop [100].

The pollutants transported by air and water, hazardous biological agents, and allergens control have vitally important in the processes of food control, pharmaceuticals, and biotechnology. High-efficiency particulate air (HEPA) have minimum 99.97% filtration efficiency for particles over 0.3 μM size [104]. In contrast, electrospun nylon-6 nanofilters had 99.993% efficiency in the tests conducted with the test particles of 0.3 μm of diameter at 5 cm/s velocity (face velocity) [105]. Graham and colleagues, had accumulated a thin (1-5 μm thick) nanofiber material on a nonwoven support and and examined the effects of its filtration characteristics. Only conventional nonwoven substrates showed dept filtration characteristics, when used without nanofiber material (particles dispersed in the filter medium). In contrast, filtration characteristics turned from

dept loading to surface loading when used nanofilter and thereby filtration efficiency was improved [106].

2.4.2. Catalyst and Enzyme Carriers

The most dangerous biological agents in heating, ventilation, and air conditioning systems are *Staphylococcus*, *Serratia*, *Klebsiella*, *Cladosporium* and *Aspergillus* species. Jeong et al, prepared electrospun nanofibers of polyurethane cationomer containing quaternary ammonium groups and these fibers had strong antimicrobial activity against to *Staphylococcus aureus* and *Escherichia coli* bacteria and also they reported that they can be used for air filtration [107]. Metallic silver and silver oxide has been reported to be safe and effective antimicrobial agents when used in low levels [104]. Son et al, have indicated that cellulose acetate electrospun nanofibers containing silver nanoparticles had a strong antimicrobial activity [108].

Electrospun nanofibers can be used effectively in the preparation of nanotubes containing catalytically active metal nanoparticles. When used as template and a relatively large surface area of the nanofibres due to providing the preparation of carbon nanofibers were used successfully in heterogeneous catalyst applications. Graeser et al. prepared Pd and Rh nanofibers by adding Pd and Rh salts to solutions of poly (D, L-lactic acid) and poly(ethylene oxide) (PEO) polymer. The obtained nanofibers were coated with poly(p-xylylene) using chemical vapor deposition method. At high temperatures, Rh and Pd containing poly (p-xylylene) nanotubes were obtained with degradation of the carrier polymer in nanofibers and chemical conversion of the metal salts. This catalyst system was found to be highly active at the hydrogenation reactions [109]. Xie et al. prepared polyvinylpyrrolidone nanofibers containing $Zn(Ac)_2 \cdot 2H_2O$, $Fe(NO_3)3 \cdot 9H_2O$ and $AgNO_3$ salts with electrospinning method. Then, they produced carbon nanofibers containing $ZnFe_2O_4$, Fe_3O_4, and Ag particles obtained by carbonization of these nanofibers. They showed that these carbon nanotubes containing metal oxide could be used as catalysts in the treatment of wastewater and environmental fields [110].

Kim and his colleagues prepared TiO_2 nanofibers containing Pt by calcination PEO nanofibers at 773 K which were prepared from PEO aqueous

solutions containing Ti(OH) n and Pt nanoparticles. The obtained nanofibers had the rougher surface than PEO/Ti(OH)n/Pt nanofibers because of the oxidation of Ti(OH)n to TiO_2 and PEO degradation. Diameter of Pt loaded TiO_2 nanotubes was 200-900 nm range. The catalytic activity of Pt loaded TiO_2 nanotubes in water gas shift reactions was found to be 5-7 times better than bulk catalyst. This improvement in catalytic activity was related to the greater surface area of nanofiber catalyst than bulk catalyst [111]. Chen et al. have made the polyacrylonitrile nanofibers containing palladium acetate salt by electrospinning method and they have obtained Pd carrying carbon nanofibers by carbonization of these nanofibers. Researchers reported that this catalyst system had high catalytic efficiency in Sonogashira coupling reactions of phenylacetyl and iodobenzene in the liquid phase and could be reused in Sonogashira reactions [112].

2.4.3. Energy Transformation and Storage

The long-term exposure to electromagnetic waves are known to have adverse effects on human health like fatigue, insomnia, irritability and headache [113]. In addition, its impact on information security and sensitive electronic equipments is one of the issues that need to be focused as well. Therefore, the studies on electromagnetic interference (EMI) shielding are increasing every day. Metallic materials are used at conventional EMI shielding. Polymer composites or coatings comprising metallic powders and fibers use in EMI shielding applications but also have disadvantages especially in the aviation, aerospace and satellite systems due to their weights.

Wang and Jing stated that semiconductor materials such as polyaniline (PANI) and polypyrrole have a high importance at anti-radar and camouflage applications due to the lower density than the metal and not expose to corrosion [114]. Desai and Sung stated that electrospun poly(methyl methacrylate) nanofibers containing polyaniline have the potential to use for EMI shielding [115]. Sen et al. stated that carbon nanotubes due to the electrical conductivity when blended with the non-conductive polymer, the obtained composite materials developed their EMI shielding properties [116]. Im et al. prepared Fe_2O_3/$BaTiO_3$ and Fe_2O_3/$BaTiO_3$ /MWNT doped carbon fibers by carbonization of the doped Fe_2O_3/$BaTiO_3$ /MWNT (MWNT: multi-layer carbon nanotube) polyacrylonitrile

electrospun nanofibers. The researchers stated that added metal oxide after the heat treatment kept its original property and used dopant materials increased electrical conductivity and EMI shielding activity of the fibers. Furthermore, the best result in this study was obtained with Fe_2O_3/$BaTiO_3$ /MWNT doped carbon fibers [117]. Im et al. in their another study reported that MWNT contribution of MWNT doped PANI / PEO electrospun nanofibers has increased the electrical conductivity of the nanofibers and thus reached 42 dB EMI effectivity [118].

Park et al. have indicated that carbon nanotube / polymer composite materials could be used for electromagnetic shielding and antistatic materials, but carbon nanotubes due to their high surface area it is difficult to disperse homogeneously in composite material [119]. On the other hand, Gorur et al. (2011), Meuer et al. (2009), and Li et al. (2011) have reported that polymers with polyaromatic hydrocarbon groups such as pyrene got interaction with carbon nanotubes in a non-covalent way and carbon nanotubes ensured homogeneous dispersion in organic solvents [120-122].

2.4.4. Sensors

Sensors have found wide use in the detection of chemicals for environmental protection, industrial process control, medical diagnostics, security and defense applications. A good sensor should have small volume, low production cost, and also functionality, high sensitivity, selectivity and reliability. High sensitivity and fast response require that sensor material should have a high specific area and a porous surface. Several approaches were tried to gain the sensor feature to nanofibers. Electrospun nanofibers were prepared using polymers with the sensor feature, the sensor molecules were mixed into the polymer solution before making a nanofiber or the sensor material were applied to the surface of nanofibers with coating/grafting methods.

Wang et al. used electrospun poly(acrylic acid) nanofibers grafted with pyrene methanol with Fe^{+3} and Hg^{+2} metal ions to determine the presence of 2,4-dinitrotoluene (DNT) in water [123]. This type of sensor application is based on the suppression of the fluorescence properties of pyrene in proportion to the concentrations of the determined chemicals and nanofibers have high sensitivity due to their high surface area. Rathfon et al. have developed chemical sensors

which is sensitive to the neurotoxic chemical warfare agents such as sarin, soman and SAS-Cl using pyrene doped electrospun polystyrene nanofibers [124]. Chemosensors with chlorosarin neurotoxins could be detected in a shorter time than 1 second at 5 ppm. In a similar way, it was reported that pyrene methanol grafted poly(methyl methacrylate) electrospun nanofibers showed 10 times more sensitivity than the cast film due to their high surface area against the DNT analyte [125]. Vapor of 2,4,6-trinitrotoluene (TNT) explosive was determined higher precision than than the casting poly(triphenylamine-alt-biphenylenevinylene) (TPE-PBPV) films using poly(acrylonitrile) nanofibers coated with a thin layer of a TPE-PBPV conjugated polymer. This situation was connected to have extremely high surface area and porous structure of nanofibers [126].

In addition, Yang and colleagues reported that picric acid, TNT, DNT and 2,4-dinitrophenol explosives could be detected in a sensitive way using tetrakis (4-methoxyphenyl)porphyrin (TMOPP) charged nanofibers obtained as a result of the electrospinning of the polystyrene solution and TMOPP [127]. In addition to fluorescence characteristics, nanofibers containing a conjugated polymer polydiacetylene were also used to detect volatile organic compounds (VOCs) based on the optical absorption properties [128]. Ding et al. developed a gas sensor using specific adsorption interaction between ammonia and poly(acrylic acid) nanofibers. The difference in weight caused by gas adsorption was measured using a quartz crystal microbalance (QCM). This sensor was capable to detect ammonia in the air in the ppb level and its sensitivity was four-fold higher than the casting poly(acrylic acid) films [129]. Luoh and Hahn developed a gas sensor for detecting carbon dioxide using electrospun poly(acrylonitrile) nanofibers containing metal oxides such as Fe_2O_3 and ZnO. This sensor was based on the principle of the influence between FT-IR absorption and carbon dioxide adsorption. The addition of metal oxide nanoparticles enhanced gas adsorption and hence sensitivity [130].

2.4.5. Biomedical Applications

Electrospun nanofibers are very suitable candidates for wound dressing materials. It owes this to ensure pores for removal of the fluid from the wound,

suitable for input of oxygen and moisture, prevent microorganisms, and to be able to add drugs to the obtained fibers (Figure 2.9).

a) b)

Figure 2.9: An electrospun wound dressing: a) and b).

A wound dressing made with the electrospun polyurethane membrane, effectively threw out liquid in the wound without being stored under the membrane and also wound did not dry under the membrane. In a study, the collagen nanofiber membrane provided that wound showed faster front healing than a cotton gauze [131].

2.4.6. Other Applications

Carbon-based nanofibers are especially used in aerospace equipments and supplies extensively due to superior properties such as high strength, durability and low weight. The nanofiber surfaces are used in solar and light panels built in space. Another usage area is the protective clothes (Figure 2.10). Thus, it is planned to oppose against biological attacks [132].

Figure 2.10: Usage for protection purpose against biological attacks.

2.5. Electrospinning Equipment

Electrospinning unit at Istanbul Medeniyet University (IMU) consists of syringe pump, high voltage supply, and a collector (Figure 2.11). Syringe pump (Model: NE-1000) is situated horizontally, and electric field was comprised by the high voltage power supply (Nanoweb, Elektro-Spin 101). Mostly, electrospun nanofibers were deposited on a grounded stationary cylindrical metal collector covered by a piece of aluminum foil. The electrospinning was carried out in enclosed Plexiglas box. That box is suctioned by portative hood for protection from hazardous solvents.

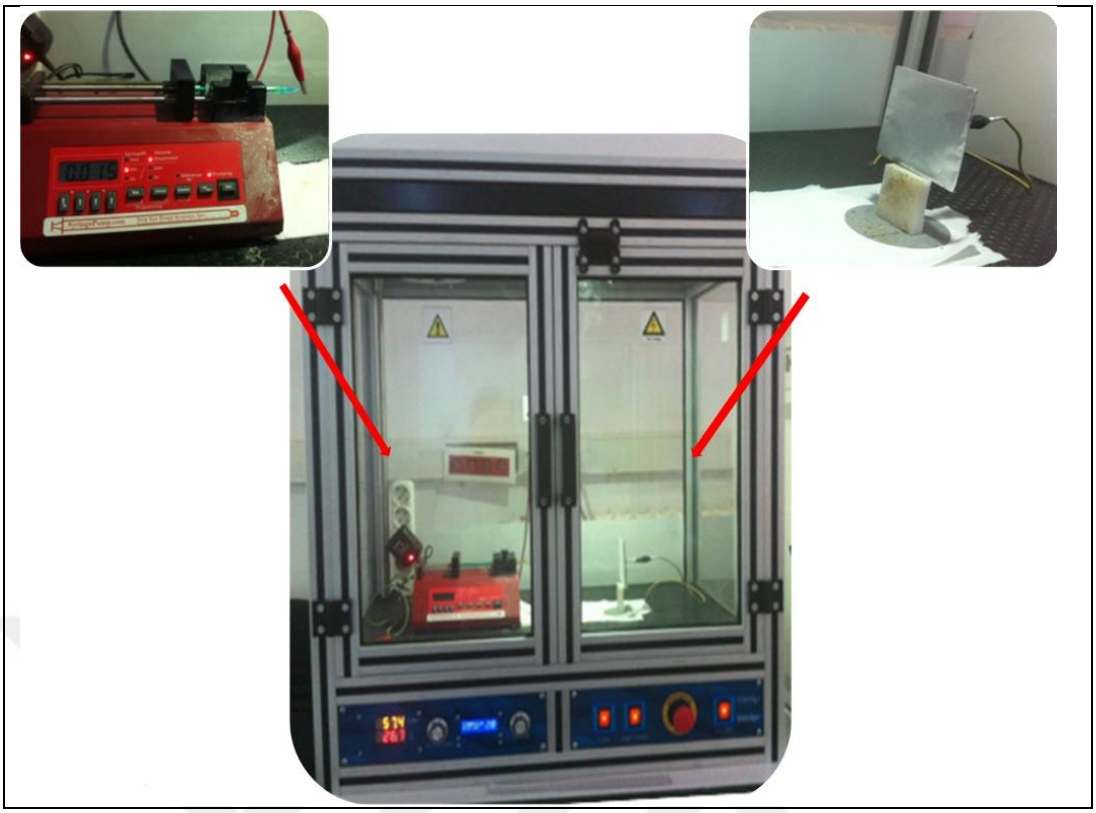

Figure 2.11: Electrospinning unit consists of syringe pump, high voltage power supply, and collector.

3. POLYMERIZATION METHODS AND CLICK CHEMISTRY

3.1 Nitroxide Mediated Radical Polymerization (NMP)

In this method, a free radical initiator and a stable nitroxy radical as (2,2,6,6-tetramethyl-1-piperidinyloxy) (TEMPO) are used. The TEMPO keeps polymer chain growth under control and acts as a catalyst. However, it does not start the reaction by itself. TEMPO is bound to the polymer end after added each monomer to radical in order to ensure a controlled growth. In this way, monodisperse polymers are obtained. The structure with the TEMPO end group undergoes homolytic fragmentation to give polymeric radical and stable free radical reversibly. The propagation step continues until monomer consumed in the medium. The chemical structure of TEMPO is shown in Figure 3.1.

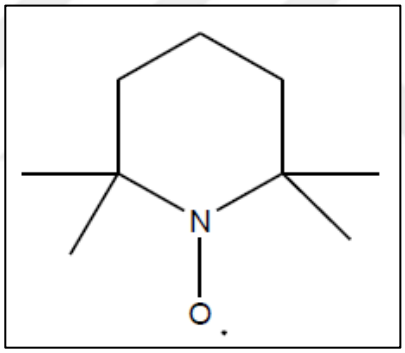

Figure 3.1: The chemical structure of TEMPO.

3.1.1. Basic Mechanism

TEMPO and its derivatives form a strong covalent bond in alkoxyamines. The equilibrium constant (kd (dissociation rate constant) / kc (cross-coupling/association rate constant)) is usually very small, in the presence of excess TEMPO. The equilibrium is strongly shifted towards the dormant species and dramatically reduces the polymerization rate. Living radical polymerization method with TEMPO is successful at controlling the polymerization of styrene monomers but not successful for acrylate and methacrylate monomers for this

reason. A general mechanism for the nitroxide mediated radical polymerization (NMP) is shown in Figure 3.2 [133].

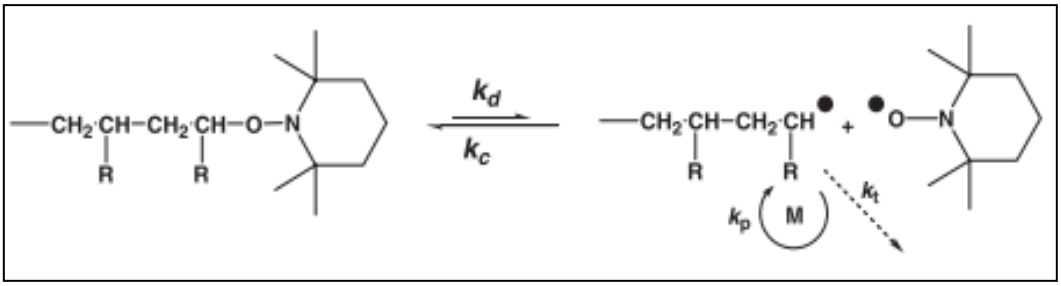

Figure 3.2: Dynamic equilibration for nitroxide mediated radical polymerization (NMP)

Nitroxide-mediated radical polymerization (NMP) reactions can be carried out under homogeneous conditions (bulk or solution polymerization) and under heterogeneous conditions (suspension and emulsion polymerization). The viscosity of the medium is low and the purification of the obtained products is quite easy [134].

3.2. Copper(I)-catalyzed Azide-Alkyne Cycloaddition Click Chemistry

It is important to be converted of functional groups in high yield after completion of the polymer reaction successfully. In this regard, "click" chemistry technique is used, due to its high efficiency and ease of reaction conditions [135].

1,3-dipolar cycloaddition reaction, which is performed applying heat from alkyne and azide groups found by Huisgen, is the precursor reaction of the "click chemistry". Additionally, Huisgen type cycloaddition reactions generally give 1,4- and 1,5-triazole isomers (about 1:1) [136]. This method was developed by Sharpless and the non-activated reaction between azide and alkyne groups is carried out in very high yield using Cu(I) salt catalyst under mild conditions and 1,4-triazole formation was performed with high selectivity (Figure 3.3) [137]. Also, Sharpless type "click reactions" have high tolerance for many different functional groups and are carried out in many solvents and solvent mixtures without compromising yield [135].

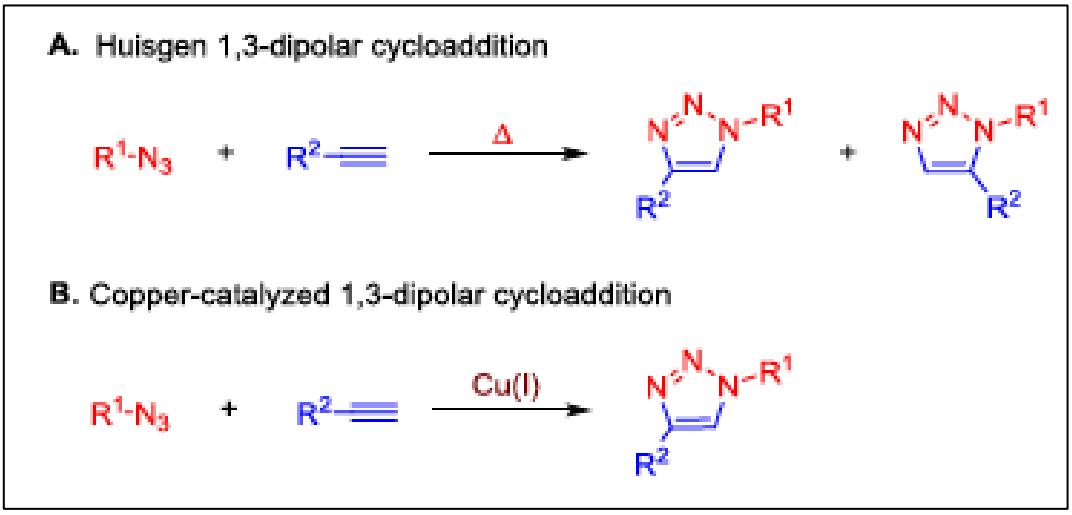

Figure 3.3: Synthesis of 1,2,3-triazoles via 1,3-dipolar cycloaddition of azides and terminal alkynes; a) Huisgen and b) Copper-catalyzed cycloaddition reactions.

4. MATERIAL AND METHOD

The chemicals and their properties used in this study are listed in Table 4.1.

Table 4.1: The chemicals used in synthesis, separation and purification processes.

Name	Company	CAS Number	Assay
Cupper(I) bromide (CuBr)	Sigma-Aldrich	7787-70-4	98%
Dichloromethane (DCM)	Sigma-Aldrich	75-09-2	99.8%
Methanol	Sigma-Aldrich	67-56-1	99.8%
Magnesium sulfate ($MgSO_4$)	Sigma-Aldrich	7487-88-9	99.5%
N,N,N′,N″,N″-Pentamethyldiethylenetriamine (PMDETA)	Aldrich	3030-47-5	99%
N,*N*-Dimetilformamide (DMF)	Sigma-Aldrich	68-12-2	99.8%
Sodium azide (NaN_3)	Aldrich	26628-22-8	≥ 99%
Sodium bicarbonate ($NaHCO_3$)	Sigma-Aldrich	144-55-8	≥ 99.7%
Sodium chloride	Alfa-Aesar	7647-14-5	99%
Styrene	Aldrich	100-42-5	≥ 99%
Triethylamine (TEA)	Sigma-Aldrich	121-44-8	≥ 99%
4-Vinylbenzyl chloride	Sigma-Aldrich	1592-20-7	90%
1-ethynylpyrene	Sigma-Aldrich	34993-56-1	96%
Dansyl chloride	Sigma-Aldrich	605-65-2	98%
3-butyn-1-ol	Aldrich	927-74-2	97%
2,2,6,6- Tetramethyl-1-piperidinyloxy (TEMPO)	Aldrich	2564-83-2	98%
BPO (Benzoyl peroxide)	Aldrich	94-36-0	70%
Propionic acid	Sigma-Aldrich	79-09-4	≥99.5%
4-Hydroxybenzaldehyde	Alfa-Aesar	123-08-0	98%
4-tert-butylbenzaldehyde	Aldrich	939-97-9	97%
Pyrrole	Aldrich	109-97-7	98%
Chloroform	Sigma-Aldrich	67-66-3	≥99.9%
Zinc acetate	Aldrich	557-34-6	99.99%

Table 4.1: Continuation of the table.

Sodium sulfate (Na_2SO_4)	Sigma-Aldrich	7757-82-6	≥99%
Potassium carbonate (K_2CO_3)	Sigma-Aldrich	584-08-7	≥99%
Propargyl bromide	Aldrich	106-96-7	80%
Sodium ascorbate	Sigma	134-03-2	≥98%
Cupper(II) sulphate pentahydrate	Sigma-Aldrich	7758-99-8	≥98%
7-hydroxycoumarin	Aldrich	93-35-6	99%
N′,N″-dimethylacetamide (DMAc)	Sigma-Aldrich	127-19-5	99.8%

The devices used in this study are listed in Table 4.2.

Table 4.2: The devices used in the characterization studies.

Name	Conditions
Differential Scanning Calorimetry (DSC)	DSC 8500 (Perkin Elmer) instrument under a nitrogen flow of 10 mL/min. The samples were first heated from 25°C to 160 °C, then cooled to 25 °C, and finally heated to 160 °C at a scan rate of 10 °C min^{-1}.
Thermal Gravimetric Analysis (TGA)	TGA/SDTA 851 (Mettler Toledo) thermogravimetric analyzer from room temperature up to 700 °C at a heating rate of 10 °C min^{-1} under nitrogen atmosphere
Fourier-transform Infrared Spectroscopy (FTIR)	Perkin Elmer Spectrum Two™ spectrometer equipped with UATR accessory.
Gel Permeation Chromatography (GPC)	Agilent 1260 Infinity GPC/SEC instrument consisting of a pump, a refractive index detector and two Agilent PLgel columns (Mixed-C, 5 μm, 7.5 × 300 mm) at 40 °C which was calibrated with linear polystyrene standards. THF was used as the eluent at a flow rate of 1 mL/min.

Table 4.2: Continuation of the table.

Mass Spectrometry	Bruker MicroTOF LC–MS (ESI)
Mass Spectrometry	Bruker microflex LT MALDI-TOF MS
Nuclear Magnetic Resonance Spectroscopy (NMR)	Varian ^{UNITY} INOVA 500 spectrometer at 25 °C in $CDCl_3$ solutions relative to the non-deuterated solvent traces as the internal reference.
Scanning Electron Microscope (SEM)	Philips XL 30 SFEG
Scanning Electron Microscope (SEM)	FEI Quanta 200 FEG
Ultraviolet–visible (UV-vis) Spectroscopy	Shimadzu UV 2600
Fluorescence Spectroscopy	Agilent Carry Eclipse Bundle A time resolved fluorescence spectrophotometer (FL-1057 TCSPC).
Electrospinning Device	Mavi Teknik, consists of syringe pump (Model: NE-1000), high voltage supply(Nanoweb, Elektro-Spin 101), and a cylindrical metal collector.

5. EXPERIMENTAL

5.1. General Procedure

The reactions were performed in inert atmosphere (dry argon atmosphere) in order to prevent chemicals from influence of oxygen and moisture in the air. The glassware used in the reactions were dried in the burner flame, argon was passed through them and used after filling with argon by cooling.

5.1.1. Preperation of Dry Styrene and Vinyl Benzyl Chloride Monomers

Styrene and vinyl benzyl chloride monomers were dried by passing neutral Al_2O_3 under argon atmosphere. The dried products were stored in the refrigerator.

5.1.2. Preperation of Dry *N,N*-Dimetilformamide (DMF)

DMF was stirred overnight by adding CaH_2 and then distilled under vacuum. Dry DMF, was kept under argon in the presence of molecular sieves (4A°).

5.1.3. Preperation of Dry K_2CO_3

K_2CO_3 was dried under reduced pressure heating at 60 °C for 20 hours. Dry K_2CO_3 was stored in the desiccator under vacuum.

5.1.4. Drying of the Synthesized Polymers

The synthesized polymers were precipitated in appropriate solvents (methanol or hexane), filtered through a G4 sintered filter and weighed on a precision balance. Polymers were allowed to dry at room temperature under reduced pressure by recording the weighing results. Then, weight of the polymer was measured periodically and the same value of the last three measurements showed that polymer was dry.

5.1.5. Gravimetric Determination of the Monomer Conversion

The ratio of the dry polymer weight to the total weight of initiator and the monomer was used for gravimetric monomer conversion.

The average molecular weights of the styrene copolymers (P1-P6) were measured by GPC. The polydispersity values ranged between 1.23 and 2.35. Whereas, the average molecular weights from GPC experiments are estimated values based on non-functional polystyrene calibration standards. The hydrodynamic volumes of the functional styrene copolymers (P1-P6) were different, to some extent, from the calibration standards. Thus, average molecular weight values from GPC experiments are accepted to be less reliable than those obtained from ^{1}H NMR calculations. In the ^{1}H NMR spectra of the styrene copolymers (P1-P6), the signals of BPO and TEMPO residues were overlapped by those of the repeating units or were very weak due to dilution of terminal units in long polymer chains. Fortunately, the ratio between monomeric residues (m/n) in the styrene copolymers, could be calculated from the integral ratios of aromatic phenyl proton signals (C_6H_5 plus C_6H_4-CH_2-) and methylene protons next to the benzene ring (C_6H_4-CH_2). Therefore, the molar mass of the fragments containing single functional unit (-Cl or -N_3) were calculated using the equation: (m/n) x MW of styrene + MW of chloride or azide functional repeating units.

5.2. Experiments

This study includes three stages: i) polystyrene synthesis having different side groups, ii) characterization of the products, and iii) the usage of the polymers for electrospun nanofiber production. Parameters such as ratios between the repeating polymers units (styrene/4-vinylbenzyl chloride) and the polymer molecular weights were tried to optimize in order to achieve uniform beadless nanofibers. Therefore, some polymers have been synthesized more than once. Especiallly, polymers with chloride and azide side groups have been synthesized many times because they are also the starting material of the other polymers.

Different codes were given to the polymers having chloride and azide groups in order to avoid confusion in the interpretation of data. For example, P1-a represents P1 polymer having chloride side groups in this coding system. The

codes were used such as P1-a and P1-b to distinguish P1 polymers at different reaction conditions (such as different monomer/initiator ratio or styrene/4-vinylbenzyl chloride ratio) (Table 5.1).

Table 5.1: Encodings used in the synthesis of polymers.

Side Group	**Chlorinated Polymer**	**Azide Polymer**	**Final Product**
Pyrene	P1-a	P2-a	P3
Dansyl	P1-b	P2-b	P4-a
	P1-c	P2-c	P4-b
Porphyrin	P1-d	P2-d	P5
Coumarin	P1-e	-	P6

The thesis includes the synthesis of functional styrene polymers with flurescence properties and preparation of electrospun nanofibers. The work in this thesis can be divided into main four sections with regards to the functional groups of the targeted polymers.

In each section, different styrene polymers with different functional groups were synthesized and employed in the preparation of electrospun nanofibers. These sections are:

i) Synthesis of pyrene functional styrene copolymer (P3) and its use in electrospun nanofibers,
ii) Synthesis of dansyl functional styrene copolymer (P4) and its use in electrospun nanofibers,
iii) Synthesis of porphyrin functional styrene copolymer (P5) and its use in electrospun nanofibers,
iv) Synthesis of coumarin functional styrene copolymer (P6) and its use in electrospun nanofibers.

In the preperation of polymers, NMP method, which is a controlled polymerization method, was used. Pyrene, dansyl, and porphyrin functional styrene copolymers were synthesized using CuAAC click chemistry technique,

which is a very effective functionalization method, and also coumarin functional styrene copolymer was synthesized using etherification reaction.

For this purpose, chloromethylated polystyrene (P1) was synthesized via NMP of styrene and 4-vinylbenzyl chloride as monomers using BPO as the radical initiator and TEMPO as the stable radical (Figure 5.1). Vinylbenzyl chloride is preferred for its chloride group that can be modified chemically. Then, chloride side-groups were converted into azide by reacting P1 with sodium azide in DMF, yielding azide-functional styrene copolymer (P2) (Figure 5.2).

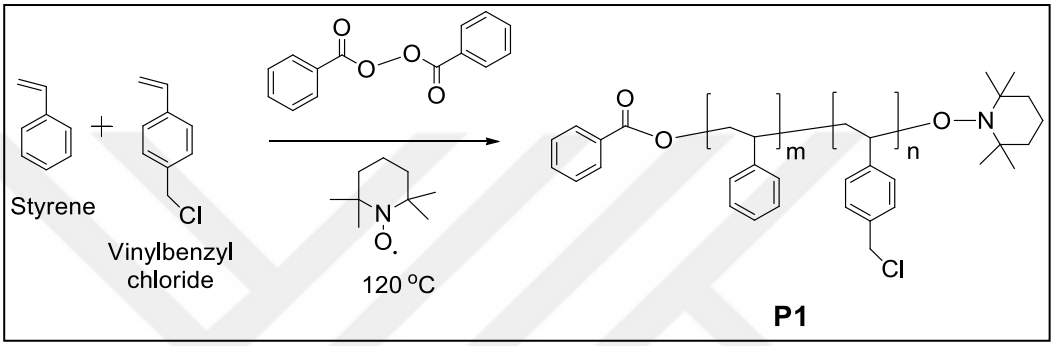

Figure 5.1: General reaction scheme for the synthesis of polystyrene (P1)

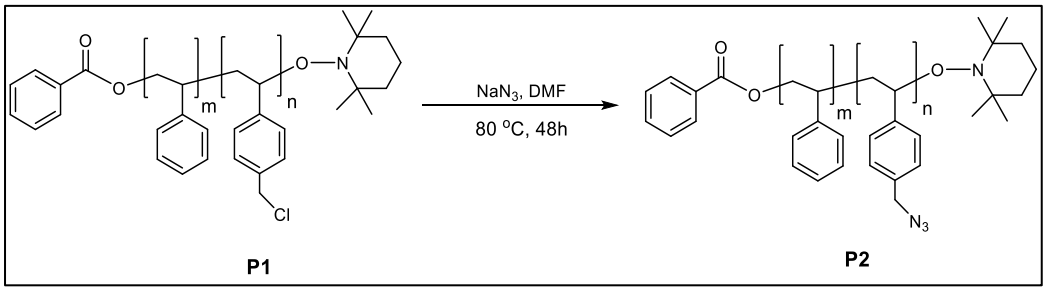

Figure 5.2: General reaction scheme for the synthesis of azide functional styrene copolymer (P2)

After P2 step, pyrene, dansyl, and porphyrin-functional styrene copolymers were synthesized quantitatively through 1,3-dipolar cycloaddition using P2 polymer. After P1 step, coumarin-functional styrene copolymers were synthesized quantitatively using P1 polymer.

The obtained styrene polymers with different functional groups were employed in the production of nanofibers via electrospinning method. So that, it requires optimization of electrospinning parameters separately for each polymer to

obtain a smooth nanofiber structure. The priority target is to produce homogenous and bead-free nanofibers from these polymers. For this purpose, different solvents (DMF, chloroform, dichloromethane, etc.) were used to obtain bead-free and smooth shape nanofibers. Moreover, solution parameters (solvent type, viscosity and conductivity of the solution) and method parameters (applied voltage, collection distance of the fibers, flow rate of the polymer solution, diameter of the syringe tip) were optimized.

5.2.1. Synthesis of Pyrene Functional Styrene Copolymer (P3)

Pyrene-functional polystyrene copolymer (P3) was prepared in a three-step synthetic procedure. Firstly, chloride-functional styrene copolymer (P1-a) was synthesized via nitroxy-mediated stable free radical polymerization (NMP) of styrene and 4-vinylbenzyl chloride as monomers using BPO as the radical initiator and TEMPO as the co-radical (Figure 5.1). Secondly, chloride side-groups were converted into azide by reacting P1-a with sodium azide in DMF, yielding azide-functional styrene copolymer (P2-a) (Figure 5.2). Lastly, pyrene-functional polystyrene copolymer (P3) was prepared via 1,3-dipolar cycloaddition reaction (Sharpless-type click reaction) between azide-functional styrene copolymer (P2-a) and 1-ethynylpyrene (Figure 5.3). Subsequently, P3 was made into nanofibers by using electrospinning method.

5.2.1.1. Synthesis of Chloromethylated Polystyrene (P1-a)

Styrene (6.97 g, 66.92 mmol), 4-vinylbenzyl chloride (1.13 g, 7.43 mmol), and TEMPO (0.009 g, 0.06 mmol) were put into a one-necked round-bottom flask and stirred for 10 min under gentle argon purge. BPO (0.010 g, 0.031 mmol) was added, and the flask was tightly closed and then immersed in a thermostated oil bath at 120 °C; the mixture continued stirring for 48 h. After the reaction mixture was cooled to room temperature, the crude polymerization product was dissolved in DCM (15 mL) and purified by precipitating in cold methanol. P1-a was recovered by vacuum filtration through a sintered glass filter (G4) and dried under reduced pressure at 35 °C for 48 h.

Yield: 5.75 g (69.5%). $M_{n,GPC}$: 90500 g/mol; M_w/M_n: 1.23.. FT-IR (cm^{-1}): 3027−3063 (CH stretching, aromatic); 2848−2921 (CH stretching, aliphatic). ^1H NMR (500 MHz, $CDCl_3$, δ, ppm): 6.46−7.09 (C_6H_4 and C_6H_5); 4.51 ($C_6H_4CH_2Cl$); 1.42−2.04 (polymer). Composition (m/n): 8.4.

5.2.1.2. Synthesis of Azide-Functional Polystyrene (P2-a)

P1-a (4.5 g, contains 4.38 mmol Cl) was dissolved in DMF (50 mL) under argon atmosphere. NaN_3 (2.63 g, 40.46 mol) was then added, and the reaction mixture was degassed with a slow stream of argon for 10 min and placed in an oil bath thermostated at 80 °C with stirring for 48 h. After the mixture was allowed to cool to ambient temperature, it was transferred to a separatory flask with DCM (100 mL) and then washed with water (2 × 100 mL). The organic phases were then combined, dried over $MgSO_4$, concentrated to ∼10 mL with rotary evaporation, and precipitated into cold methanol. P2-a was recovered by vacuum filtration through a sintered glass filter (G4) and dried under reduced pressure at 35 °C for 48h.

Yield: 3.62 g (80.0%). $M_{n,GPC}$: 90800 g/mol; M_w/M_n: 1.25. FT-IR (cm^{-1}): 3027−3063 (CH stretching, aromatic); 2848−2921 (CH stretching, aliphatic); 2095 (N3). ^1H NMR (500 MHz, $CDCl_3$, δ, ppm): 6.46−7.09 (C_6H_4 and C_6H_5); 4.22 ($C_6H_4CH_2N_3$); 1.42−2.04 (polymer backbone). Composition (m/n): 8.4.

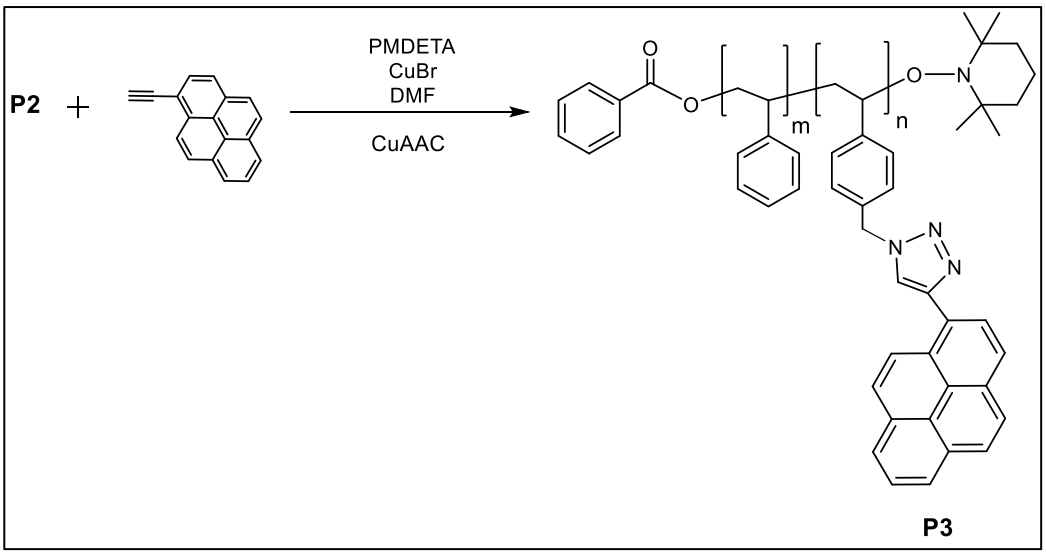

Figure 5.3: General reaction scheme for the synthesis of styrene copolymer, containing pyrene side-groups.

5.2.1.3. Synthesis of Pyrene-Functional Polystyrene (P3)

P2-a (4.0 g, contains 3.87 mmol N_3) and 1-ethynylpyrene (1.05 g, 4.64 mmol) were dissolved in DMF (50 mL) under an argon atmosphere. PMDETA (2.01 g, 11.60 mmol) was added, and the reaction mixture was degassed by gently purging with oxygen-free argon for 5 min. Subsequently, CuBr (1.66 g, 11.60 mmol) was added to the solution, and the solution was degassed again. After the reaction mixture was stirred at room temperature for 48 h, it was transferred to an extraction funnel, diluted with DCM (100 mL), and washed successively with and water (2 × 100 mL). The collected organic phases were dried over $MgSO_4$, concentrated to ∼10 mL by a rotary evaporator, and P3 was isolated by precipitation from cold methanol. The obtained polymer was collected by vacuum filtration through a sintered glass filter (G4) and dried under reduced pressure at 35 °C for 48 h.

Yield. 3.89 g (79.9%). $M_{n,GPC}$: 91 300 g/mol; M_w/M_n: 1.28. FT-IR (cm^{-1}): 3027−3063 (CH stretching, aromatic); 2848−2921 (CH stretching, aliphatic). ^1H NMR (500 MHz, $CDCl_3$, δ, ppm): 7.68−8.68 (CH, pyrene); 6.46−7.09 (C_6H_4 and C_6H_5); 5.22 ($C_6H_4CH_2$-C_2HN_3); 1.42−2.04 (polymer backbone). Composition (m/n): 8.4.

5.2.1.4. Electrospinning of the Fluorescence Nanofibers (P3)

The homogeneous clear solution of pyrene functional polystyrene copolymer (P3) was placed in a 1 mL syringe fitted with metallic needles of 0.4 mm inner diameter. This was followed by the horizontal fixing of the syringe on the syringe pump (model SP 101IZ, WPI). The polymer solution was pumped with a feed rate of 0.5 mL/h during electrospinning. By using a high voltage supply, the applied voltage to the metal needle tip (Spellman, SL Series) was 15 kV and the tip-to-collector distance was set at 15 cm for electrospinning of the prepared solution. Collectively, electrospun fluorescence P3 nanofibers were deposited on the aluminum foil covering the plate-type collector. The electrospinning process was performed at 20 °C and 20% relative humidity in an enclosed Plexiglas box.

5.2.2. Synthesis of Dansyl Functional Styrene Copolymer (P4)

Dansyl-functional styrene copolymer (P4) was prepared in a four-step synthetic procedure. In the first step, compound 1 having acetylene functional groups was obtained via condensation reactions between dansyl chloride and 3-butyn-1-ol (Figure 5.4). In the second step, chloride-functional styrene copolymer (P1) was synthesized via nitroxy-mediated stable free radical polymerization (NMP) of styrene and 4-vinylbenzyl chloride as monomers using BPO as the radical initiator and TEMPO as the co-radical. Then, chloride side-groups were converted into azide by reacting P1-b with sodium azide in DMF, yielding azide-functional styrene copolymer (P2-b). In the last step, a dansyl-functional polystyrene copolymer (P4) was prepared via 1,3-dipolar cycloaddition reaction (Sharpless-type click reaction) between azide-functional styrene copolymer (P2-b) and compound 1 (Figure 5.5).

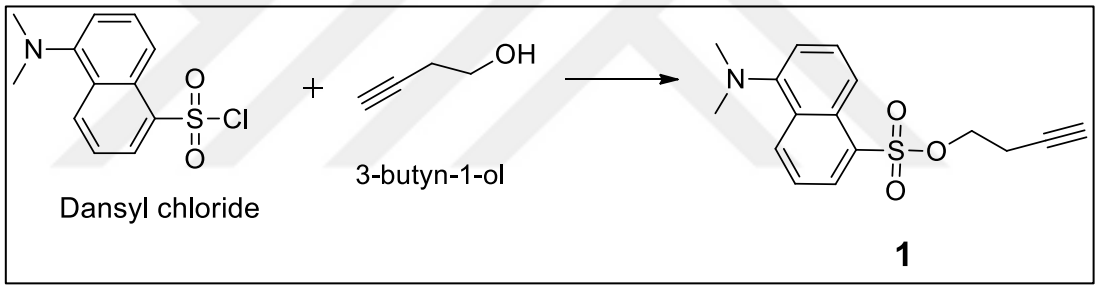

Figure 5.4: General reaction scheme for the synthesis of compound 1, having acetylene functional groups.

5.2.2.1. Synthesis of Compound 1 (But-3-ynyl 5- dimethylamino) naphthalene -1-sulfonate (dansyl alkyne)

This compound (Compound 1) was synthesized following a procedure described in the literature [138]**.** Dansyl chloride (4.00 g, 14.83 mmol) was dissolved in dry dichloromethane (30 ml) under argon atmosphere. 3-butyn-1-ol (1.25 g, 17.79 mmol) and then triethylamine (3.00 g, 29.66 mmol) were added. The reaction mixture was stirred at room temperature overnight and subsequently heated to 40°C for 4 h. After cooling the mixture to ambient temperature, it was transferred to a separatory flask with dichloromethane (100 mL), washed with $NaHCO_3$ solution (aq, 5 wt%) and then with water (2x100 mL). The organic phases

were then combined, dried over $MgSO_4$ and the solvent was removed with rotary evaporation. The crude product was purified by silica gel chromathography (solvent: DCM).

Yield: 3.18 g (61%). MS (MALDI-TOF, m/z): 303.476 $[M+H]^+$ (Figure B1.1). ^1H NMR (500 MHz, $CDCl_3$, δ, ppm): 8.72 (1H, f), 8.41 – 8.21 (2H, e,g), 7.66 – 7.50 (2H, h), 4.08 (2H, c), 2.96 (d), 2.53 (2H, a), 1.87 (1H, b).

5.2.2.2. Synthesis of Chloromethylated Polystyrene (P1-b)

Styrene (18.06 g, 0.17 mol), 4-vinylbenzyl chloride 2.65 g, 0.017 mol), and TEMPO (0.04g, 0.17 mmol) were put into a one-necked round-bottom flask and stirred for 10 min under gentle argon purge. BPO (0.08 g, 0.52 mmol) was added, the flask was tightly closed and then immersed in a thermostated oil bath at 120 ^oC and continued stirring for 48 hours. After the reaction mixture was cooled to room temperature, the crude polymerization product was dissolved in DCM (15 mL) and purified by precipitating in cold methanol. P1-b was recuperated by vacuum filtration through a sintered glass filter (G4) and dried under reduced pressure at 35 °C for 48 hours.

Yield: 15.52 g (75%). $M_{n,GPC}$: 36100 g/mol; M_w/M_n: 1.59.

5.2.2.3. Synthesis of Azide-Functional Polystyrene (P2-b)

P1-b (14.72 g, contains 12.28 mmol Cl) was dissolved in DMF (50 mL) under argon atmosphere. NaN_3 (6.39 g, 98.22 m mol) was then added, reaction mixture was degassed with a slow stream of argon for 10 min. and placed in an oil bath thermostated at 80 °C with stirring for 48 h. After the mixture was allowed to cool to ambient temperature, it was transferred to a separatory flask with DCM (100 mL) and then washed with water (2x100 mL). The organic phases were then combined, dried over $MgSO_4$, concentrated to around 10 mL with rotary evaporation, and precipitated into cold methanol. P2-b was recuperated by vacuum filtration through a sintered glass filter (G4) and dried under reduced pressure at 35 °C for 48 hours.

Yield: 13.06 g (89%). $M_{n,GPC}$: 44600 g/mol; M_w/M_n: 1.48.

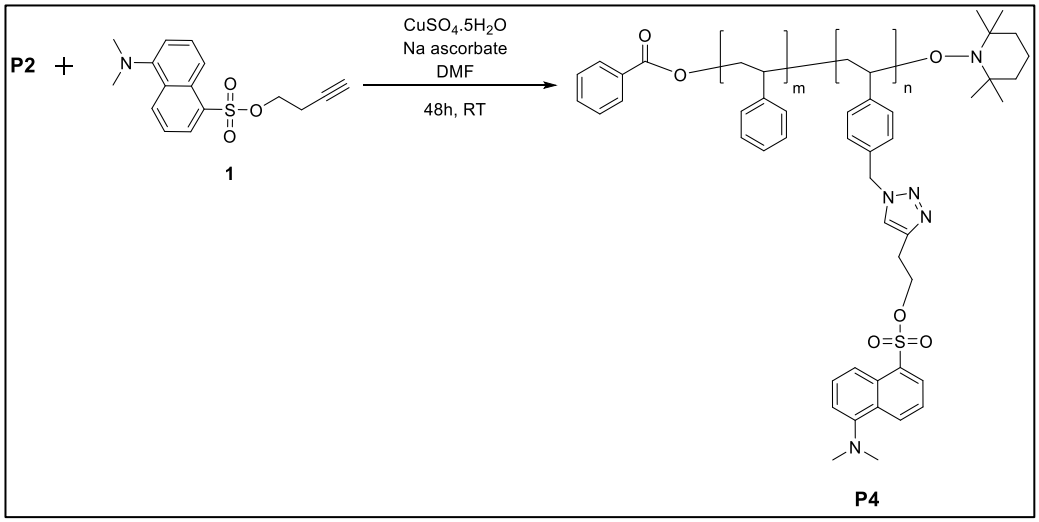

Figure 5.5: General reaction scheme for the synthesis of styrene copolymer, containing dansyl side-groups.

5.2.2.4. Synthesis of Dansyl-Functional Polystyrene (P4-a)

P2-b (2.2 g, 1.83 mmol) and compound 1 (1.11 g, 3.66 mmol) were dissolved in DMF (50 mL) in an inert atmosphere. Sodium ascorbate (0.73 g, 3.66 mmol) was added and the reaction mixture was degassed by gently purging with oxygen-free argon for 5 minutes. Subsequently, a solution of copper(II) sulfate (0.46 g, 1.83 mmol) in water (10 ml) was added dropwise and the solution was degassed again. After the reaction mixture was stirred at room temperature for 48 h, it was transferred to an extraction funnel, diluted with DCM (100 mL), and washed successively with and water (2x100 mL). The collected organic phases were dried over $MgSO_4$, concentrated to about 10 mL by a rotary evaporator and isolated by precipitation from cold hexane. The obtained polymer was collected by vacuum filtration through a sintered glass filter (G4) and dried under reduced pressure at 35 °C for 48 h.

Yield: 1.374 g (62%). $M_{n,GPC}$: 30866 g/mol; M_w/M_n: 1.64.

5.2.2.5. Electrospinning of the Fluorescence Nanofibers (P4-a)

The electrospinning solution of dansyl functional polystyrene copolymer (P4-a) was obtained by dissolving in different solvent mixtures at different 5%, 10%, and 20% (w/v, with respect to solvent) concentrations. The homogeneous clear solution was placed in a 1 mL syringe fitted with metallic needles of 0.4 mm

inner diameter. This was followed by the horizontal fixing of the syringe on the syringe pump (model SP 101IZ, WPI). The polymer solution was pumped with a feed rate of 0.5 mL/h during electrospinning. By using a high voltage supply, the applied voltage to the metal needle tip (Spellman, SL Series) was 17.5 kV and the tip-to-collector distance was set at 10 cm for electrospinning of the prepared solution. Collectively, electrospun fluorescence P4-a nanofibers were deposited on the aluminum foil covering the plate-type collector. The electrospinning process was performed at 20 °C and 20% relative humidity in an enclosed Plexiglas box.

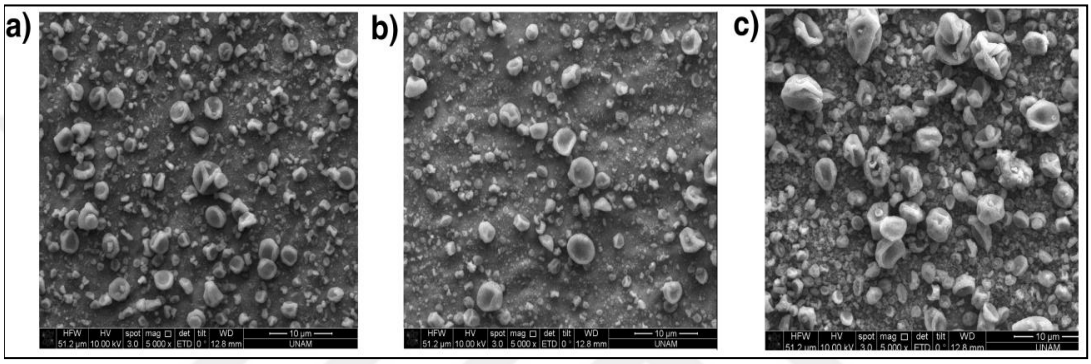

Figure 5.6: SEM micrographs of electrospun nanofibers of P4-a polymer having dansyl side groups using a) 5% (w/v) in DCM/DMF (3/2- v/v), b) 10% (w/v) in DCM/DMF (3/2- v/v), and c) 20% (w/v) in DCM/DMF (3/2- v/v) solvent systems.

As shown in Figure 5.6, the best resolution was provided at DCM/DMF (3/2) (v/v) mixture and it could be dissolved until 20% (w/v) polymer concentration. Only bead structures were obtained although the concentration was increased. Because of all this negativity, the electrospinning process of polymer P4-a was terminated. Then, P1-c, P2-c and P4-b polymers were synthesized respectively and used in electrospinning studies for the synthesis of styrene polymers having dansyl side groups at lower rate (Section 5.2.2.6 - 5.2.2.9).

5.2.2.6. Synthesis of Chloromethylated Polystyrene (P1-c)

Styrene (12.38 g, 0.12 mol), 4-vinylbenzyl chloride (0.91 g, 0.006 mol), and TEMPO (0.02g, 0.08 mmol) were put into a one-necked round-bottom flask and stirred for 10 min under gentle argon purge. BPO (0.04 g, 0.25 mmol) was added, the flask was tightly closed and then immersed in a thermostated oil bath at 120 ^{o}C and continued stirring for 48 hours. After the reaction mixture was cooled to

room temperature, the crude polymerization product was dissolved in DCM (15 mL) and purified by precipitating in cold methanol. P1-c was recuperated by vacuum filtration through a sintered glass filter (G4) and dried under reduced pressure at 35 °C for 48 hours.

Yield: 9.218 g (69%). $M_{n,GPC}$: 36000 g/mol; M_w/M_n: 2.35. FT-IR (cm^{-1}): 2890-3077 (CH stretching, aromatic); 2840-2886 (CH stretching, aliphatic). ^1H NMR (500 MHz, $CDCl_3$, δ, ppm): 6.12-7.3 (C_6H_4 and C_6H_5); 4.50 ($C_6H_4CH_2Cl$); 1.1-2.1 (polymer backbone). Composition (m/n): 18.2.

5.2.2.7. Synthesis of Azide-Functional Polystyrene (P2-c)

P1-c (9.07 g, contains 4.04 mmol Cl) was dissolved in DMF (40 mL) under argon atmosphere. NaN_3 (2.10 g, 32.36 mmol) was then added, reaction mixture was degassed with a slow stream of argon for 10 min. and placed in an oil bath thermostated at 80 °C with stirring for 48 h. After the mixture was allowed to cool to ambient temperature, it was transferred to a separatory flask with DCM (100 mL) and then washed with water (2x100 mL). The organic phases were then combined, dried over $MgSO_4$, concentrated to around 10 mL with rotary evaporation, and precipitated into cold methanol. P2-c was recuperated by vacuum filtration through a sintered glass filter (G4) and dried under reduced pressure at 35 °C for 48 hours.

Yield: 8.4 g (93%). $M_{n,GPC}$: 39000 g/mol; M_w/M_n: 2.19. FT-IR (cm^{-1}): 2890-3077 (CH stretching, aromatic); 2840-2886 (CH stretching, aliphatic); 2095 (N_3). ^1H NMR (500 MHz, $CDCl_3$, δ, ppm): 6.12-7.3 (C_6H_4 and C_6H_5); 4.22 ($C_6H_4CH_2N_3$); 1.1-2.1 (polymer backbone). Composition (m/n): 18.2.

5.2.2.8. Synthesis of Dansyl-Functional Polystyrene (P4-b)

PS-Dansyl (P4-b) was prepared as follows: P2-c (3.00 g, 1.34 mmol) and compound 1 (0.81 g, 2.68 mmol) were dissolved in DMF (35 mL) in an inert atmosphere. Sodium ascorbate (0.53 g, 2.68 mmol) was added and the reaction mixture was degassed by gently purging with oxygen-free argon for 5 minutes. Subsequently, dropwise of copper(II) sulfate (0.33 g, 1.34 mmol) in water (5ml) solution was added and the solution was degassed again. After the reaction mixture

was stirred at room temperature for 48 h, it was transferred to an extraction funnel, diluted with DCM (100 mL), and washed successively with and water (2x100 mL). The collected organic phases were dried over $MgSO_4$, concentrated to about 10 mL by a rotary evaporator and isolated by precipitation from cold methanol. The obtained polymer was collected by vacuum filtration through a sintered glass filter (G4) and dried under reduced pressure at 35 °C for 48 h.

Yield: 1.798 g (59%). $M_{n,GPC}$: 42000 g/mol; M_w/M_n: 1.87. FT-IR (cm^{-1}): 2890-3077 (CH stretching, aromatic); 2840-2886 (CH stretching, aliphatic). ^1H NMR (500 MHz, $CDCl_3$, d, ppm): 7.4-8.3 (dansyl group protons);6.1-7.3 (phenyl group protons); 4.27 (CH_2N); 1.1-2.1 (polymer backbone). Composition (m/n): 18.2.

5.2.2.9. Electrospinning of the Fluorescence Nanofibers (P4-b)

The homogeneous clear solution of dansyl functional polystyrene copolymer (P4-b) was contained in a 1 mL syringe with a plane tip of metallic needle witth an inner diameter of 0.4 mm. The feeding rate of the polymer solution into the tip was controlled at 0.5 ml/h using the syringe pump (model SP 101IZ, WPI). The applied high voltage to the metal needle tip (Spellman, SL Series) and the tip-to-collector distance were fixed at 17.5 kV and 15 cm, respectively. The electrospun fluorescence P4-b nanofibers were collected horizontally on an aluminum foil covering a plate-type collector. The electrospinning process was conducted at 20 °C and 20% relative humidity in an enclosed Plexiglas box. The obtained fiber mats were observed with a scanning electron microscope (SEM).

5.2.3. Synthesis of Porphyrin Functional Styrene Copolymer (P5)

Porphyrin-functional polystyrene copolymer (P5) was synthesized in a four-step procedure. In the first step, asymmetric porphyrin derivative (compound 2) was prepared through a reaction between 4-hydroxybenzaldehyde and 4-tert-butylbenzaldehyde in the presence of pyrrole (Figure 5.7). In the second step, asymmetric zinc-porphyrin compound (compound 3) was obtained via a reaction between compound 2 and zinc acetate (Figure 5.8) [139]. Then, acetylene-

functional asymmetric porphyrin compound (compound 4) was produced through a reaction between compound 3 and propargyl bromide (Figure 5.9). In the last step, porphyrin-functional styrene copolymer was synthesized via click reaction between azide-functional styrene copolymer (P2-d) and compound 4 (Figure 5.10).

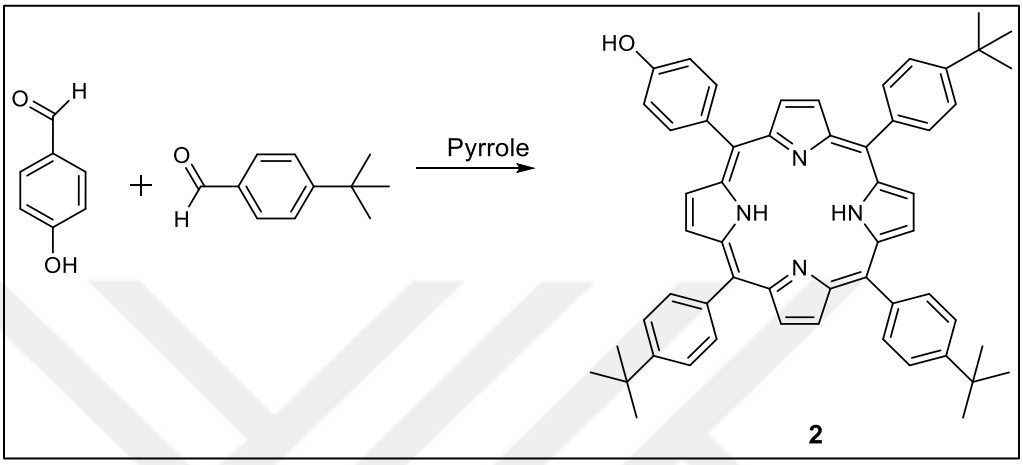

Figure 5.7: General reaction scheme for the synthesis of compound 2.

5.2.3.1. Synthesis of Compound 2

To a refluxing propionic acid solution (100 ml) of 4-hydroxybenzaldehyde (0.5 g, 4.09 mmol) and 4-tert-butylbenzaldehyde (6.64 g, 40.94 mmol), pyrrole (3.02 g, 45.04 mmol) was added dropwise. The mixture was stirred for 3 hours under refluxing and then cooled to room temperature. The solutionwas concentrated to 100 mL and methanol (200 mL) was added. The precipitate was filtered and washed with water and methanol. The residue was then purified by column chromatography on silica using chloroform as eluent. A large amount of symmetrical porphyrin, was collected as the first fraction, then the second fraction containing the target purple compound was collected [140].

Purple crystals: 0.36 g (Yield: 9.98%). MS (MALDI-TOF, m/z): 799.360 [M^+]. (Figure B1.2)

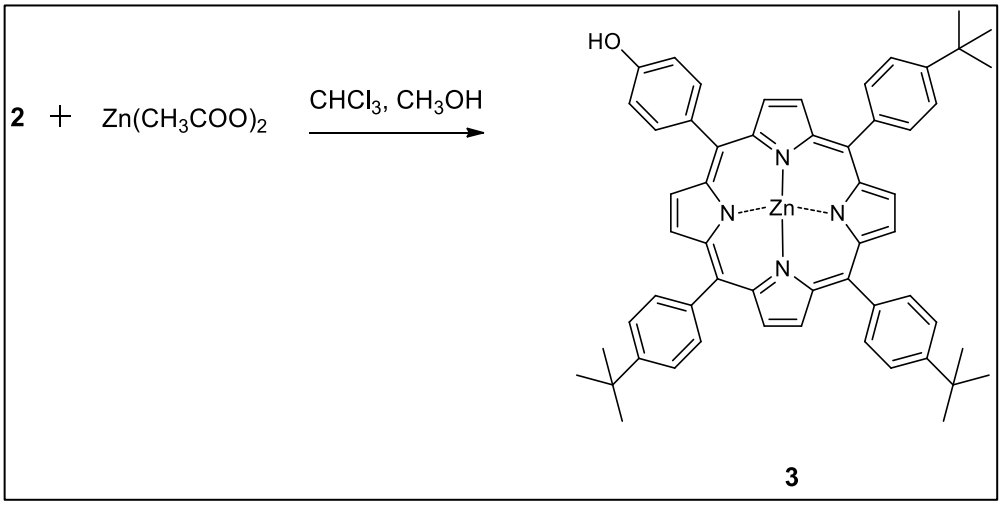

Figure 5.8: General reaction scheme for the synthesis of zinc-porphyrin compound 3.

5.2.3.2. Synthesis of Compound 3

Saturated zinc acetate (1.24g, 6.75 mmol) - methanol (30 mL) solution was added to a solution of compound 2 (0.3 g, 0.38 mmol) in chloroform (70 mL). The mixture was stirred at room temperature for 3 h and then was transferred to an extraction funnel and washed with water (2x100 mL). The collected organic phases were dried over anhydrous Na_2SO_4. The solvent was removed in vacuo [141].

Yield: 0.27 g (90%). MS (MALDI-TOF, m/z): 878.464 [M-2H+H_2O]. (Figure B1.3)

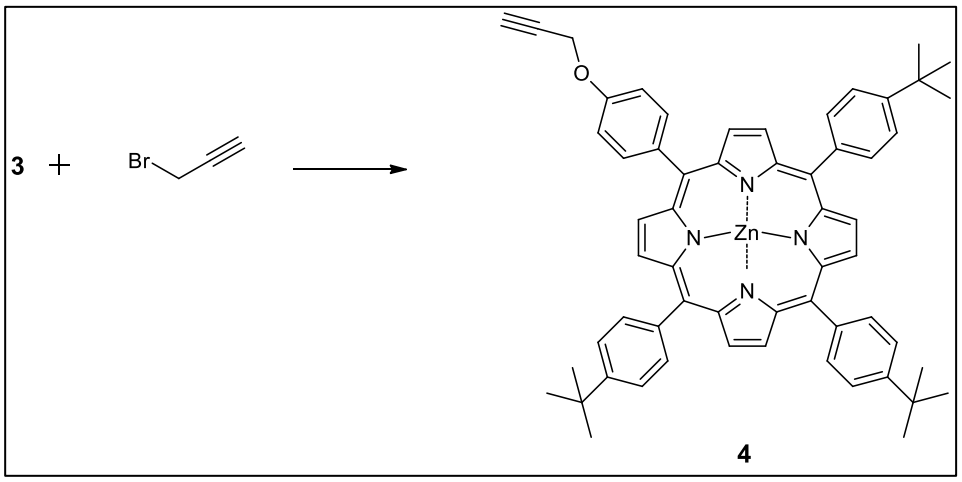

Figure 5.9: General reaction scheme for the synthesis of acetylene-functional asymmetric porphyrin compound 4.

5.2.3.3. Synthesis of Compound 4

Under argon, compound 3 (0.26 g, 0.30 mmol) was dissolved in anhydrous DMF (32 mL), then anhydrous K_2CO_3 (1.10 g, 0.74 mmol) and propargyl bromide (76.54 μL, 0.89 mmol) was slowly added under argon, and the reaction mixture was stirred and maintained reflux for 10 h. After cooling to room temperature, the mixture was concentrated. Water (2x100 mL) and dichloromethane (100 mL) were added, the layers were dried (MgSO4). Solvent was evaporated under reduced pressure and the residue was then purified by column chromatography on silica gel with chloroform as eluent [141].

Yield: 0.13 g (36%). MS (MALDI-TOF, m/z): 916.157 [M-H+H_2O]. (Figure B1.4)

5.2.3.4. Synthesis of Chloromethylated Polystyrene (P1-d)

Styrene (14.09 g, 0.13 mol), 4-vinylbenzyl chloride (0.17 g, 1.13 mmol), and TEMPO (0.04 g, 0.26 mmol) were put into a one-necked round-bottom flask and stirred for 10 min under gentle argon purge. BPO (0.02g, 0.09 mmol) was added, the flask was tightly closed and then immersed in a thermostated oil bath at 120 ^oC and continued stirring for 48 hours. After the reaction mixture was cooled to room temperature, the crude polymerization product was dissolved in DCM (30 mL) and purified by precipitating in cold methanol. P1-d was recuperated by vacuum filtration through a sintered glass filter (G4) and dried under reduced pressure at 35 °C for 48 hours.

Yield:11.24 g (79%). $M_{n,GPC}$: 65300 g/mol; M_w/M_n: 1.91. FT-IR (cm^{-1}): 3027−3063 (CH stretching, aromatic); 2848-2921 (CH stretching, aliphatic). ^1H NMR (500 MHz, $CDCl_3$, δ, ppm): 6.3-7.24 (C_6H_4 and C_6H_5); 4.48 ($C_6H_4CH_2Cl$); 1.2-2.1 (polymer backbone). Composition (m/n): 98.2.

5.2.3.5. Synthesis of Azide-Functional Polystyrene (P2-d)

P1-d (11.0 g, 0.87 mmol Cl) was dissolved in DMF (75 mL) under argon atmosphere. NaN_3 (0.45 g, 6.94 mmol) was then added, reaction mixture was degassed with a slow stream of argon for 10 min. and placed in an oil bath

thermostated at 80 °C with stirring for 48 h. After the mixture was allowed to cool to ambient temperature, it was transferred to a separatory flask with DCM (100 mL) and then washed with water (2x100 mL). The organic phases were then combined, dried over $MgSO_4$, concentrated to around 10 mL with rotary evaporation, and precipitated into cold methanol. P2-d was recuperated by vacuum filtration through a sintered glass filter (G4) and dried under reduced pressure at 35 °C for 48 hours

Yield: 10.273 g (93.39%). $M_{n,GPC}$: 61900 g/mol; *Mw/Mn*: 1.96 FT-IR (cm-1): 3027−3063 (CH stretching, aromatic); 2848−2921 (CH stretching, aliphatic); 2096 (N_3). ^{1}H NMR (500 MHz, $CDCl_3$, δ, ppm): 6.3-7.24 (C_6H_4 and C_6H_5); 4.22 ($C_6H_4CH_2N_3$); 1.2-2.1 (polymer backbone). Composition (m/n): 98.2.

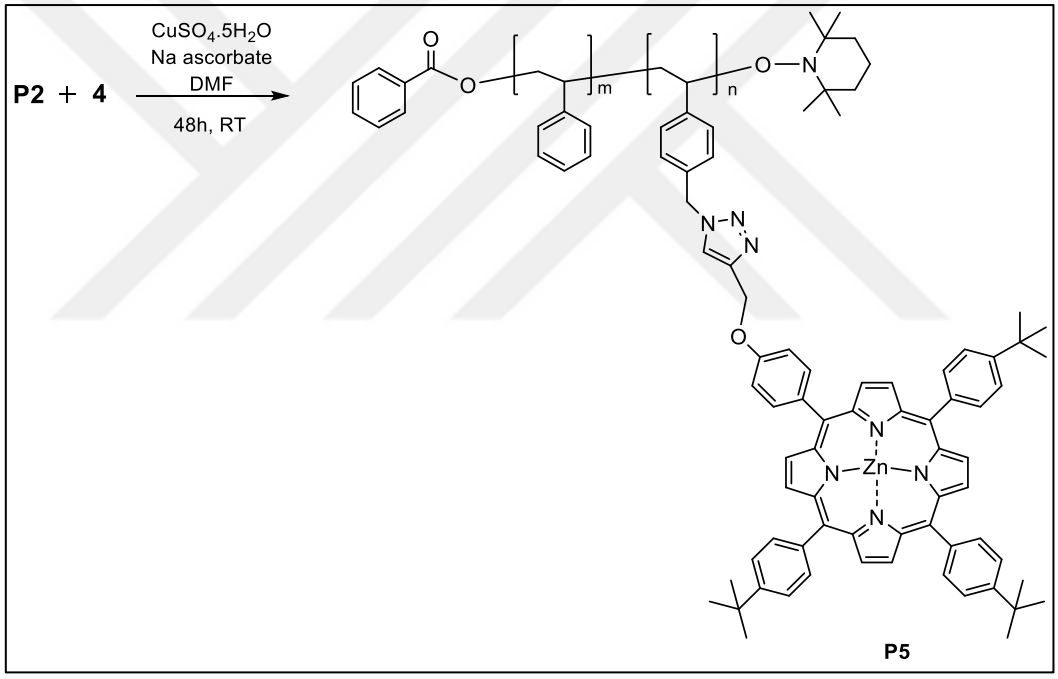

Figure 5.10: General reaction scheme for the synthesis of styrene copolymer, containing porphyrin side-groups.

5.2.3.6. Synthesis of Porphyrin-Functional Polystyrene (P5)

PS-Porphyrin (P5) was prepared as follows: P2-d (2.2 g, 0.21 mmol) and compound 4 (0.29 g, 0.31 mmol) were dissolved in DMF (40mL) in an inert atmosphere. Sodium ascorbate (0.19 g, 0.94 mmol) was added and the reaction mixture was degassed by gently purging with oxygen-free argon for 5 minutes. Subsequently, dropwise of copper(II) sulfate (0.12 g, 0.47 mmol) in water (5ml)

solution was added and the solution was degassed again. After the reaction mixture was stirred at room temperature for 48 h, it was transferred to an extraction funnel, diluted with DCM (100 mL), and washed successively with and water (2x100 mL). The collected organic phases were dried over $MgSO_4$, concentrated to about 10 mL by a rotary evaporator and isolated by precipitation from cold methanol. The obtained polymer was collected by vacuum filtration through a sintered glass filter (G4) and dried under reduced pressure at 35 °C for 48 h.

Yield: 2.24g (90%). $M_{n,GPC}$: 112200 g/mol; M_w/M_n: 2.4. FT-IR (cm^{-1}): 3027−3063 (CH stretching, aromatic); 2848−2921 (CH stretching, aliphatic). ^1H NMR (500 MHz, $CDCl_3$, d, ppm): 7.75-8.16 (porphyrin group protons); 6.1-7.3 (phenyl group protons); 4.21 (CH_2N); 1.2-2.1 (polymer backbone). Composition (m/n): 98.2.

5.2.3.7. Electrospinning of the Fluorescence Nanofibers (P5)

The homogeneous clear solution of porphyrin functional polystyrene copolymer (P5) was contained in a 1 mL syringe with a plane tip of metallic needle with an inner diameter of 0.4 mm. The feeding rate of the polymer solution into the tip was controlled at 1ml/h using the syringe pump (Model: NE-1000). The applied high voltage to the metal needle tip (Spellman, SL Series) and the tip-to-collector distance were fixed at 17.2 kV and 15 cm, respectively. The electrospun fluorescence P5 nanofibers were collected horizontally on an aluminum foil covering a plate-type collector. The electrospinning process was conducted at 20 °C and 20% relative humidity in an enclosed Plexiglas box. The obtained fiber on the aluminum plate was observed with a scanning electron microscope (SEM).

5.2.4. Synthesis of Coumarin Functional Styrene Copolymer (P6)

Coumarin-functional polystyrene copolymer (P6) was prepared in a two-step synthetic procedure. In the first step, chloride-functional styrene copolymer (P1-e) was synthesized via nitroxy-mediated stable free radical polymerization (NMP) of styrene and 4-vinylbenzyl chloride as monomers. Then, a coumarin-

functional polystyrene copolymer (P6) was prepared between chloride-functional styrene copolymer (P1-e) and 7-hydroxycoumarin via etherification reaction (Figure 5.11).

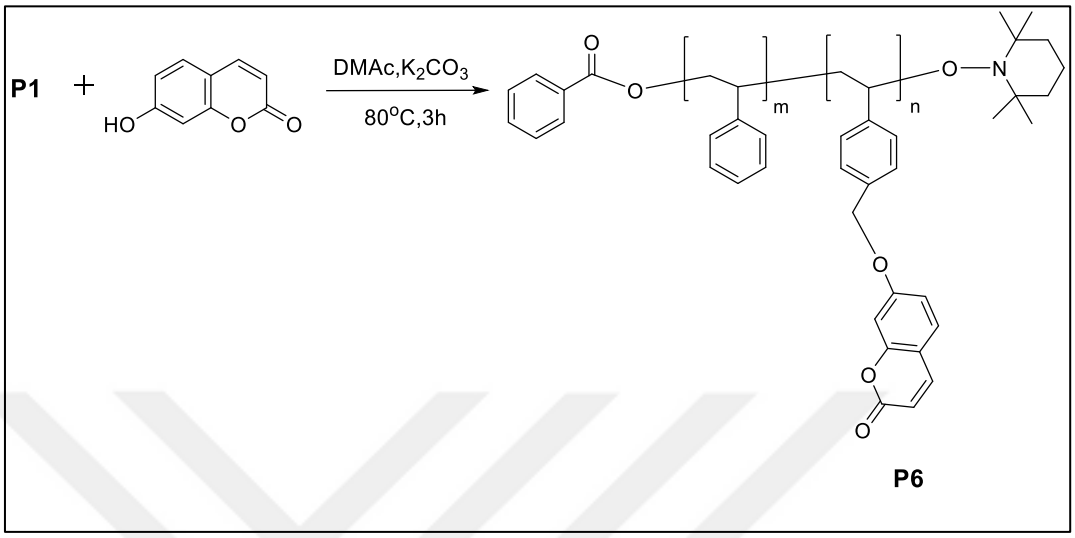

Figure 5.11: General reaction scheme for the synthesis of styrene copolymer, containing coumarin side-groups.

5.2.4.1. Synthesis of Chloromethylated Polystyrene (P1-e)

Styrene (12.64 g, 0.12 mol), 4-vinylbenzyl chloride (2.65 g, 0.017 mol), and TEMPO (0.04 g, 0.26 mmol) were put into a one-necked round-bottom flask and stirred for 10 min under gentle argon purge. BPO (0.02 g, 0.09 mmol) was added, the flask was tightly closed and then immersed in a thermostated oil bath at 120 ^{o}C and continued stirring for 48 hours. After the reaction mixture was cooled to room temperature, the crude polymerization product was dissolved in DCM (10 mL) and purified by precipitating in cold methanol. P1-e was recuperated by vacuum filtration through a sintered glass filter (G4) and dried under reduced pressure at 35 °C for 48 hours.

Yield: 1.467 g (10%). $M_{n,GPC}$: 45220 g/mol; M_w/M_n: 2.25. FT-IR (cm^{-1}): 3027-3063 (CH stretching, aromatic); 2848-2932 (CH stretching, aliphatic). ^{1}H NMR (500 MHz, $CDCl_3$, δ, ppm): 6.2-7.2 (C_6H_4 and C_6H_5); 4.50 ($C_6H_4CH_2Cl$); 1.1-2.1 (polymer backbone). Composition (m/n): 7.2.

5.2.4.2. Synthesis of Coumarin-Functional Polystyrene (P6)

A mixture of 7-hydroxycoumarin (0.58 g, 3.55 mmol) and potassium carbonate (0.56 g, 4.06 mmol) in N',N''-dimethylacetamide (DMAc, 35 mL) was heated to 80 °C. P1-e (0.5 g, 0.51 mmol) solution in DMAc (15 mL) was added to the mixture and then magnetically stirred at 80 °C for 3 h under a nitrogen atmosphere. The solution mixture was cooled to room temperature and then poured into methanol to obtain a white precipitate. The precipitate was further purified by several reprecipitations from the DMAc solution into methanol and then washed with water to remove potassium carbonate and any remaining salts. The product was obtained after drying overnight in a vacuum [142].

Yield: 0.53 g (50%). $M_{n,GPC}$: 50000 g/mol; M_w/M_n: 2.35. FT-IR (cm^{-1}): 1739 (C—O), 1613 (C—C in benzene ring), 1120 (C(C—O)–O). ^1H NMR (500 MHz, $CDCl_3$, δ, ppm): 1.6–2.2 (m, 3H, –CH_2–CPhH–), 4.8–5.1 (s, 2H, Ph–CH_2–O–), 6.1–6.2 (d, 1H, –OCOCH—CH–), 6.2–6.3 (m, 1H, –OPhH–), 6.4–7.4 (m, 6H, PhHCH_2–, –OPhH–), 7.5–7.7 (d, 1H, –OCOCH—CH–). Composition (m/n): 7.2.

5.2.4.3. Electrospinning of the Fluorescence Nanofibers (P6)

The homogeneous clear solution of coumarin functional polystyrene copolymer (P6) was contained in a 1 mL syringe with a plane tip of metallic needle witth an inner diameter of 0.6 mm. The feeding rate of the polymer solution into the tip was controlled at 1 ml/h using the syringe pump (Model: NE-1000). The applied high voltage to the metal needle tip (Spellman, SL Series) and the tip-to-collector distance were fixed at 17.2 kV and 15 cm, respectively. The electrospun fluorescence P6 nanofibers were collected horizontally on an aluminum foil covering a plate-type collector. The electrospinning process was conducted at 20 °C and 20% relative humidity in an enclosed Plexiglas box. The obtained fiber on the aluminum plate was observed with a scanning electron microscope (SEM).

6. RESULTS AND DISCUSSION

6.1. Characterization of Pyrene Functional Styrene Copolymer (P3)

The chemical structures of the synthesized copolymers (P1-a, P2-a, P3) were supported via FT-IR and ^{1}H NMR spectral analysis. In their FT-IR spectra given in Figure 6.1, aromatic and aliphatic C-H stretching bands are observed around 3027−3063 and 2848−2921 cm^{-1}, respectively. In the FT-IR spectrum of P2-a, the signal observed at 2095 cm^{-1} clearly indicates the presence of azide functional groups in the chemical structure of P2-a. Upon CuAAC click reaction between P2-a and 1-ethynylpyrene, the complete disappearence of azide signal, which was observed in the FT-IR spectrum of the precursor, proves that pyrene side groups were attached quantitatively, yielding P3.

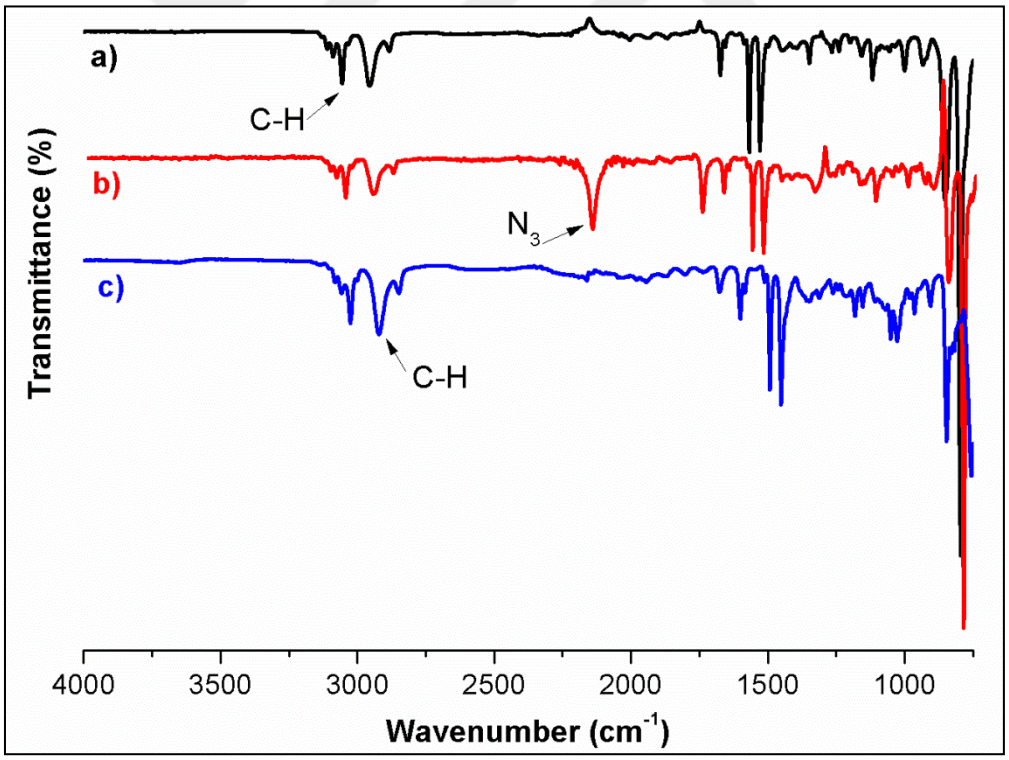

Figure 6.1: FT-IR spectra of the functional styrene copolymers: a) P1-a, b) P2-a and c) P3.

In the ^{1}H NMR spectra of the copolymers (Figure 6.2), the backbone protons (H_a) gave signals between 1.42 and 2.04 ppm, while aromatic CH protons

(H_c) in styrene and vinylbenzyl repeating units resonanced between 6.46 and 7.09 ppm. In the ^{1}H NMR spectrum of P1-a, the signal of the methylene protons (H_b) next to the benzene ring was observed at 4.51 ppm and it was shifted to higher magnetic field (4.22 ppm) in the ^{1}H NMR spectrum of P2 upon azidification. After click reaction of P2-a with 1-ethynylpyrene, the chemical environment of these protons (H_b) changed, and they gave resonances at 5.52 ppm. The clear shift of H_b protons on azidification and click reactions, explicitly proves the success of the reactions. Copolymer composition of the polymers (P1-a, P2-a, P3) was calculated by comparing the integral ratios of H_b and H_c and found as 8.4. Besides, pyrene proton signals and triazole proton signal were observed between 7.68 and 8.68 ppm in the ^{1}H NMR spectrum of P3.

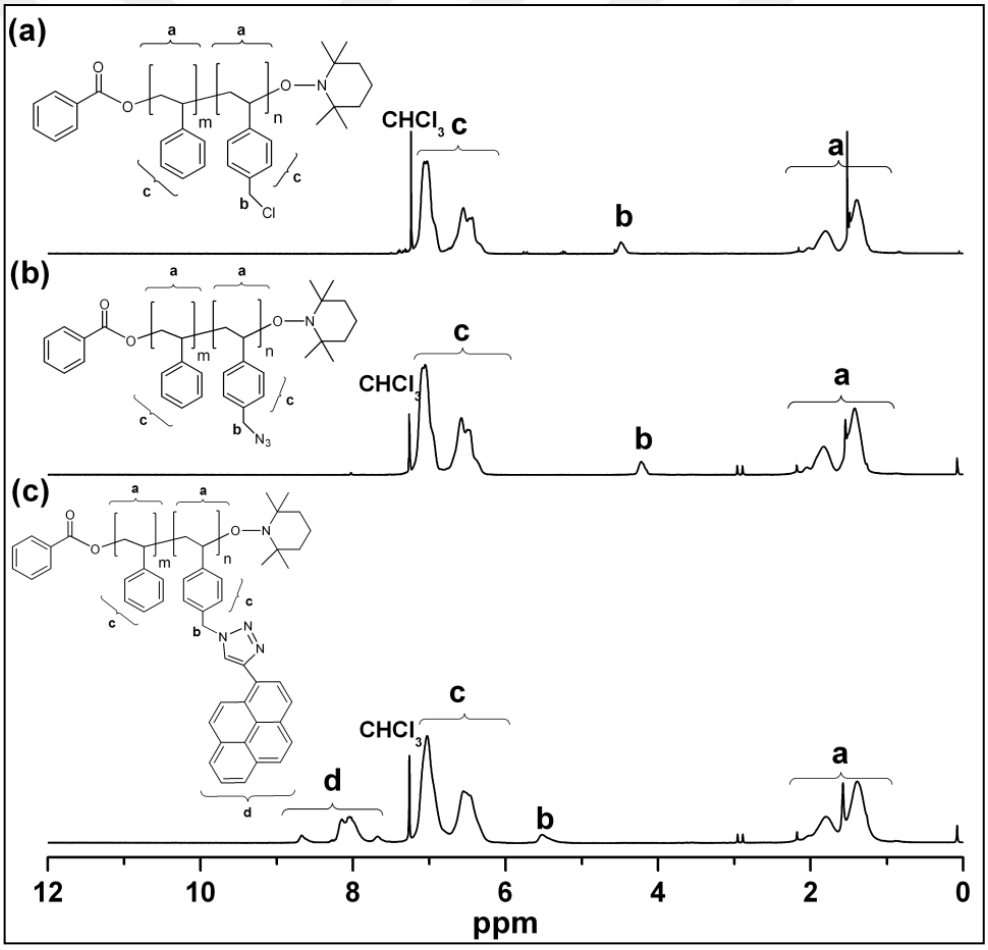

Figure 6.2: ^{1}H NMR spectra of the functional styrene copolymers, a) P1-a, b) P2-a and c) P3.

Differential scanning calorimetry (DSC) technique was used in order to determine thermal transitions (e.g. Tg) of the synthesized polymers with different

side-functional groups. Figure 6.3 shows the DSC curves of the styrene copolymers in the second heating run. Tg values of the chloride functional styrene copolymer (P1-a) was measured as ~104 °C. Upon azidification, Tg of the styrene copolymer (P2-a) decreased slightly to ~99 °C. However, attachment of pyrene side groups considerably increased Tg (~126 °C) of the resultant fluorescent styrene copolymer (P3), due to rigid structure and π-stacking of pyrene side-units.

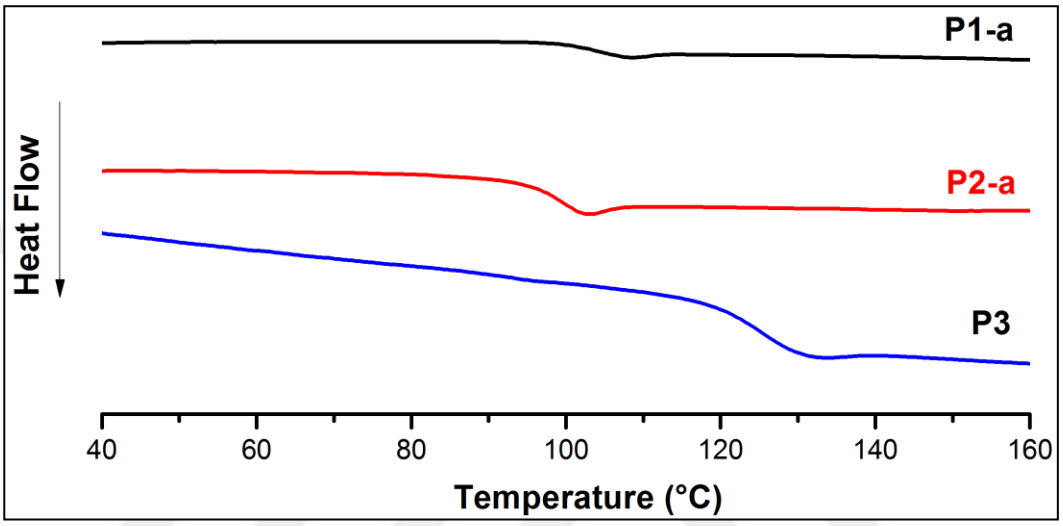

Figure 6.3: DSC thermograms of the functional styrene copolymers, P1-a, P2-a, and P3.

As for the thermogravimetric properties of the copolymers, their maximum decomposition temperatures (T_{Max}) of the styrene copolymers were very close to each other as seen from Figure 6.4, indicating that their thermal stabilities were almost similar. Besides, the percent char yield of the pyrene functional styrene copolymer was remarkably greater than the others.

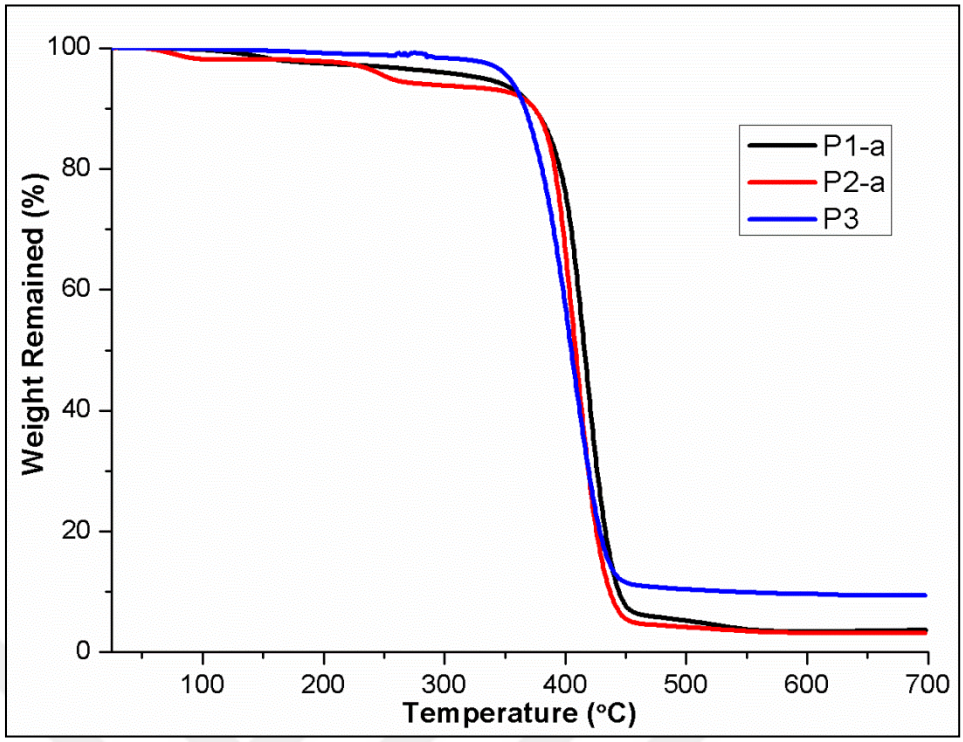

Figure 6.4: TGA thermograms of the functional styrene copolymers, P1-a, P2-a and P3.

Different solvent systems were tried for electrospinning of pyrene-functional polystyrene copolymer (P3). Heavily nanofibers with beaded structures were obtained as the solution prepared with the DMF solvent that could be observed from Figure 6.5-a. Firstly, polymer solution at 10% (w/v) concentration in DMF\chloroform (4/1-v/v) solvent system was prepared and tried to obtain nanofiber structure using the above-mentioned electrospinning conditions (Figure 6.5-b). When the polymer concentration was increased to 12% (w/v) beadless nanofibers could not be obtained (Figure 6.5-c). In DMF/ chloroform (4/1-v/v) solvent mixture, beadless structure could not be obtained although increasing concentration and therefore viscosity to 12% and the polymer solution solidified at the syringe tip. Therefore, solvent system changed to DMF/DCM (7/3-v/v) and at 12% (w/v) concentration uniform beadless nanofibers could be obtained (Figure 6.5-d).

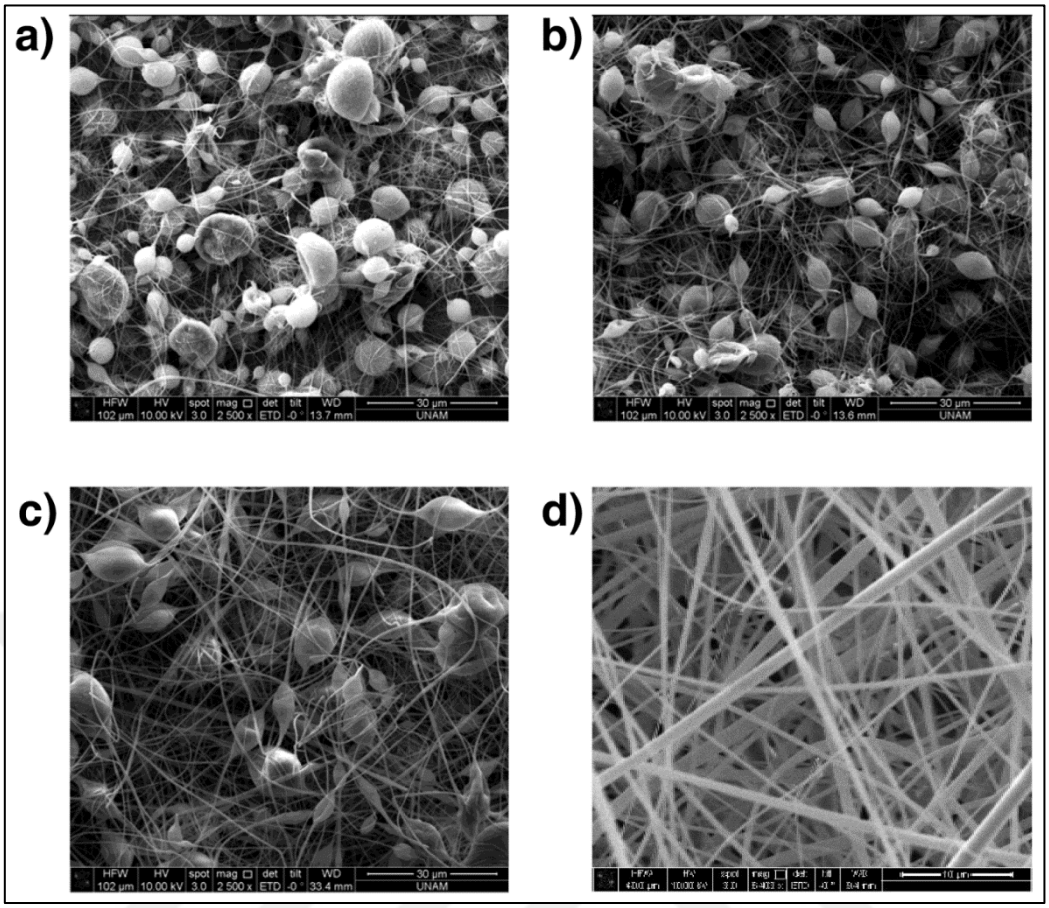

Figure 6.5: SEM micrographs of electrospun nanofibers of P3 polymer having pyrene side groups using a) 10% (w/v) in DMF, b) 10% (w/v) in DMF/chloroform (4/1- v/v), c) 12% (w/v) in DMF/chloroform (4/1- v/v), and d) 12% (w/v) in DMF/DCM (7/3- v/v) solvent systems.

The SEM image of electrospun pyrene-functional styrene copolymer (P3) depicts a uniform defect-free porous structure with average fiber diameter of 400 ± 140 nm as illustrated in Figure 6.6. The of pores is clearly seen on surface of the nanofibers with an average pore size of 30−40 nm. And also cross-sectional view of the fiber confirms the occurrence of porous structure inside the fiber. Additionally, the fluorescent nanofibrous membrane (FNFM) exhibited bright bluish green emission, visually observed under UV light (λext-254 nm) as shown in Figure. 6.6b and their depiction under normal light conditions is displayed in Figure. 6.6c.

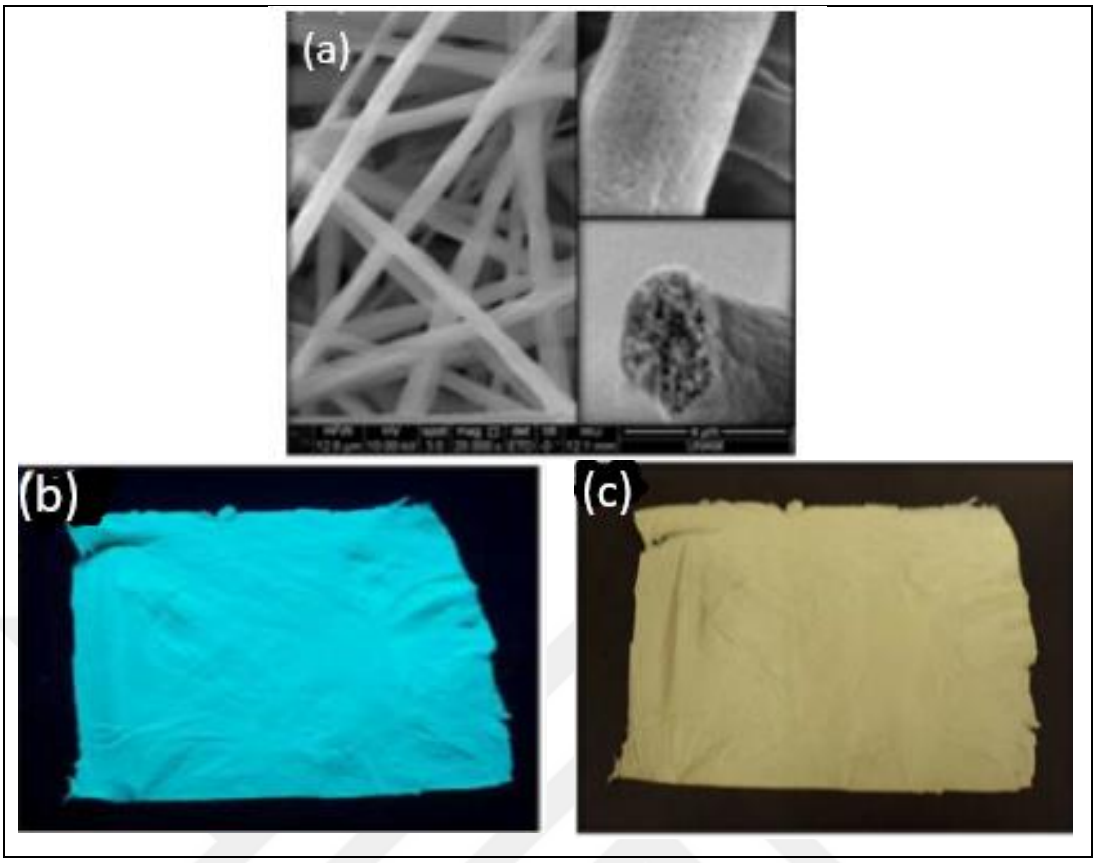

Figure 6.6: a) SEM image of the pyrene functional polystyrene copolymer nanofibers. (inset) Porous nature and cross-sectional view of the nanofiber. b) Photograph of FNFM under UV light (λ_{ext}-254 nm) and c) Day light.

The fluorescent polymer (P3) demonstrated excimer emissions mainly due to increased local concentration of pyrene moieties on the polymer backbone as shown in Figure 6.7.

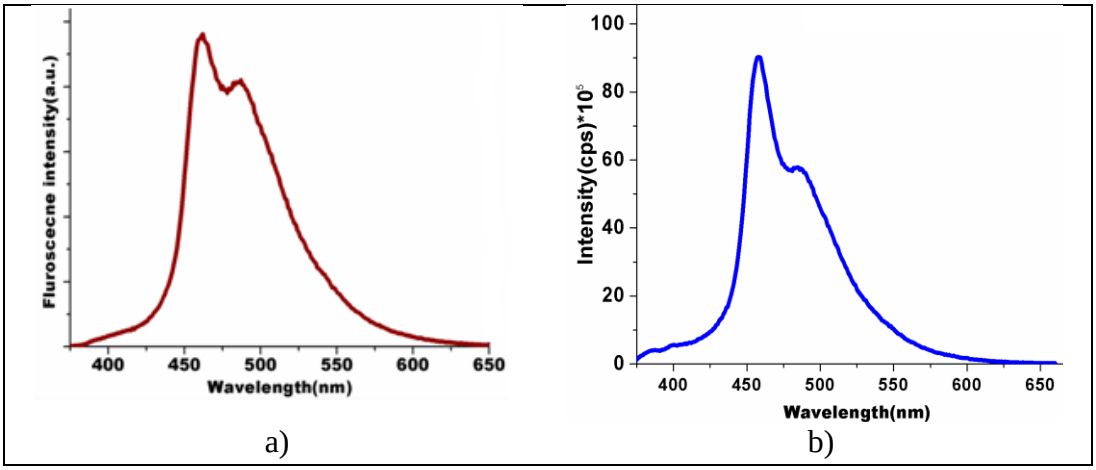

a) b)

Figure 6.7: Fluorescence emission spectra of pyrene-functional polystyrene copolymer (a) nanofiber (λext-340 nm) and b) in solution phase.

6.2. Characterization of Dansyl Functional Styrene Copolymer (P4)

FT-IR and ^{1}H NMR analysis techniques were used to confirm the chemical structures of the synthesized copolymers (P1-c, P2-c, P4). In their FT-IR spectra (Figure 6.8), aromatic and aliphatic C-H stretching bands are observed around 2890-3077 and 2840-2886 cm^{-1}, respectively. In the FT-IR spectrum of P2-c, the signal observed at 2095 cm^{-1} clearly indicates the presence of azide functional groups in the chemical structure of P2-c. The disappearence of azide signal, which was observed in the FT-IR spectrum of P4-b, proves the attaching of dansyl side-groups.

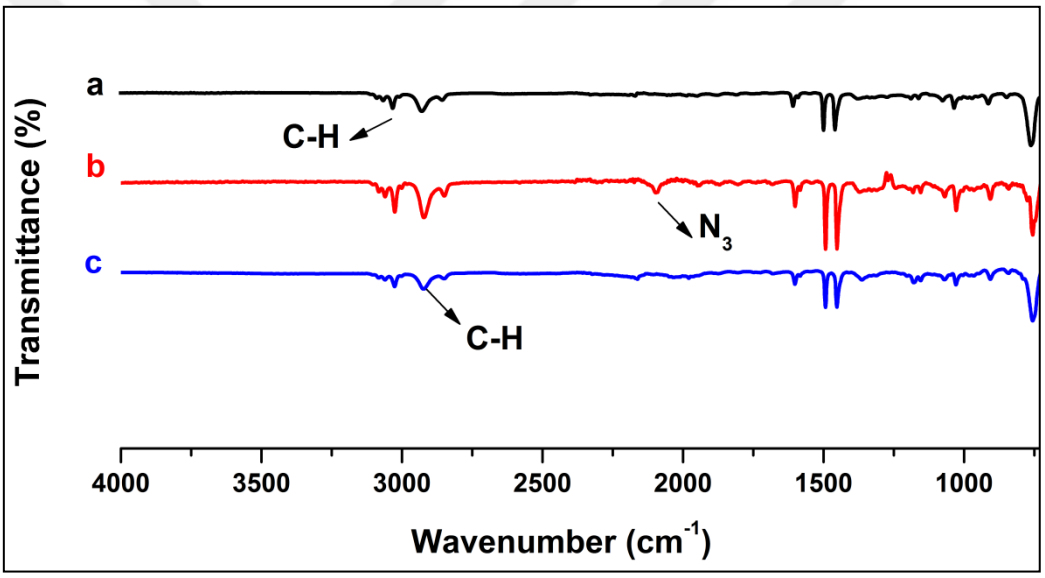

Figure 6.8: FT-IR spectra of the functional styrene copolymers: a) P1-c, b) P2-c and c) P4-b.

To attach the dansyl functionality to the P2-c, acetylene functional dansyl compound (compound 1) was prepared. In the ^{1}H NMR spectrum of compound 1, characteristic peaks at 8.72 (f), 8.41-8.21 (e, g), 7.66-7.50 (h), 4.08 (c), 2.96 (d), 2.53 (a), and 1.87 (b) ppms show compatibility with with its structure. This data show that compound 1 was successfully synthesized (Figure 6.9).

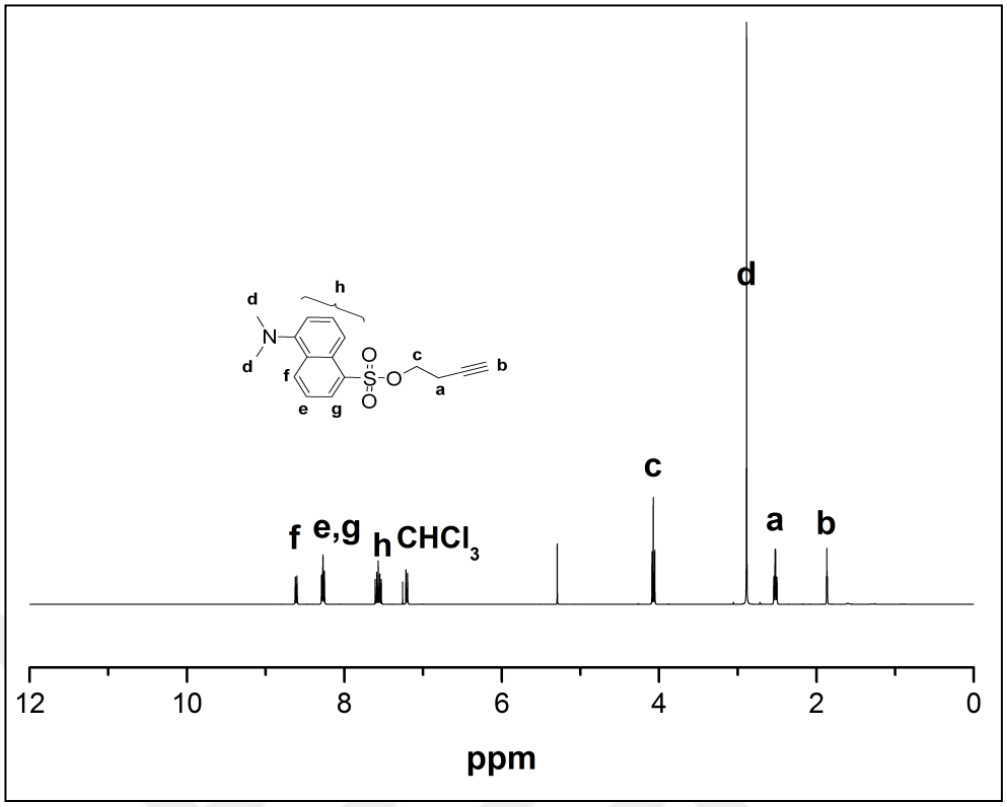

Figure 6.9: ^{1}H NMR spectrum of Compound 1.

In the ^{1}H NMR spectra of the copolymers (Figure 6.10), the backbone protons (H_a) gave signals between 1.1 and 2.1 ppms, while aromatic CH protons (H_c) in styrene and vinylbenzyl repeating units gave resonances between 6.12 and 7.3 ppms. In the ^{1}H NMR spectrum of P1-c, the signal of the methylene protons (H_b) next to the benzene ring was observed at 4.50 ppm. Upon azidification of P2-c, the signal H_b moved to higher magnetic field (4.22 ppm) in the ^{1}H NMR spectrum.

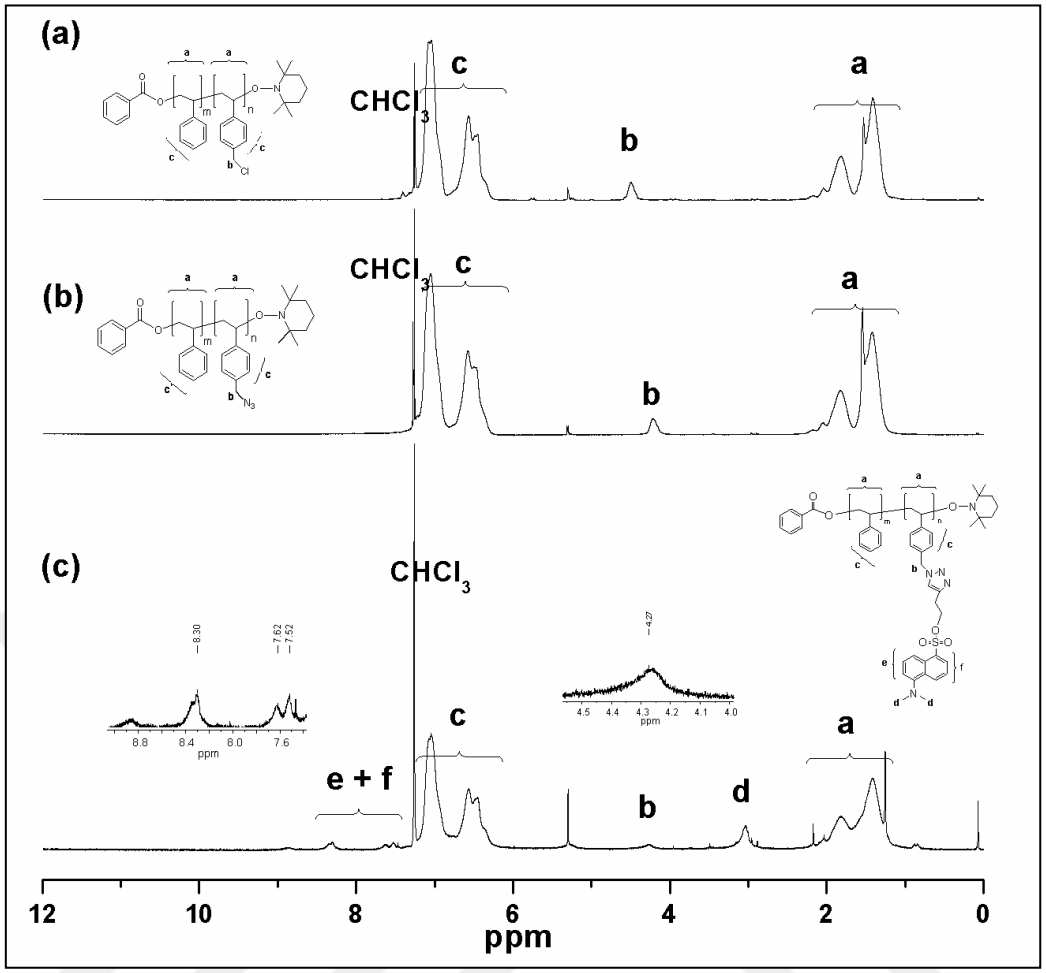

Figure 6.10: ^{1}H NMR spectra of the functional styrene copolymers, a) P1-c, b) P2-c and c) P4-b.

After click reaction of P2-c with compound 1, the chemical environment of these protons (H_b) changed and they gave rosonces at 4.27 ppm. The clear shift of H_b protons on azidification and click reactions, clearly confirms the success of the reactions. Copolymer composition of the polymers (P1-c, P2-c, P4-b) was calculated by comparing the integral ratios of Hb and Hc and found as 18.2. Besides, dansyl proton signals were observed between 7.4 and 8.3 ppms and triazole proton signal was observed at 8.9 ppm in the ^{1}H NMR spectrum of P4-b.

The thermal transitions such as T_g of the synthesized polymers with different side-functional groups were determined by DSC. The DSC curves of the styrene copolymers in the second heating run were shown in Figure 6.11. T_g values value of the chloride functional styrene copolymer (P1-c) was measured as 105.4. Upon azidification, T_g of the styrene copolymer (P2-c) decreased slightly to 104.9. Then, attachment of dansyl side groups considerably increased T_g of the

resultant fluorescent styrene copolymer (P4-b), due to the structure of dansyl side-units.

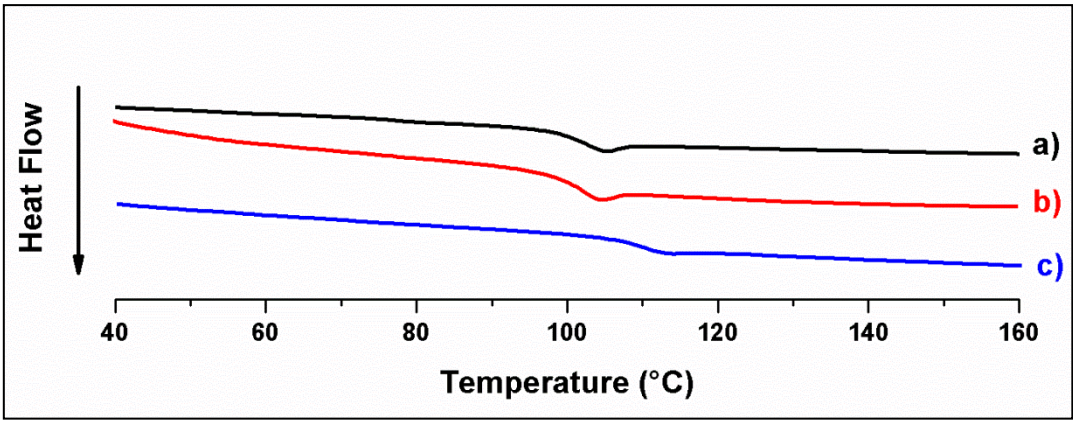

Figure 6.11: DSC thermograms of the functional styrene copolymers, a) P1-c, b) P2-c and c) P4-b.

Thermal properties of the copolymers were measured via TGA experiments. Their maximum decomposition temperatures (T_{Max}) of the styrene copolymers were very close to each other as seen from Figure 6.11. Also, the percent char yield of the dansyl-functional styrene copolymer was greater than the others.

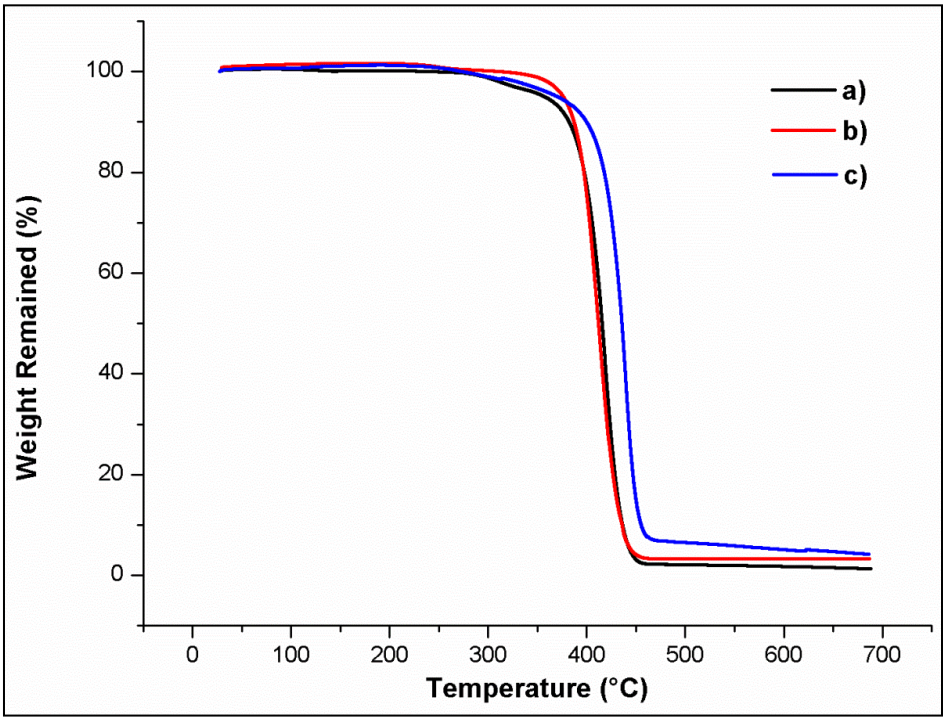

Figure 6.12: TGA thermograms of the functional styrene copolymers, a) P1-c, b) P2-c, and c) P4-b.

Different solvent systems were tried for electrospinning of dansyl-functional polystyrene copolymer. P4-a polymer was prepared at 5% (w/v), 10% (w/v) and 20% (w/v) concentrations in DCM/DMF (3/2-v/v), only bead structures were obtained (Figure 5.1). Because of all this negativity, P4-b polymer was used with lower dansyl percentage for electrospinning works. Then, concentration increased to 30% (w/v). Homogeneous electrospinning solution was prepared at 30% (w/v) concentration and it was tried to collect horizontally on an aluminum foil covering a plate-type collector at 15 cm tip-to-collector distance. Consequently, optimum yield and morphology for P4-b polymer in the system is DMF /DCM (7/3-v/v) solution and 30% (w/v) concentration. Beadless and uniform nanofibers were obtained clearly with these conditions. The strip-shape structure of the nanofibers is shown in Figure 6.13a.

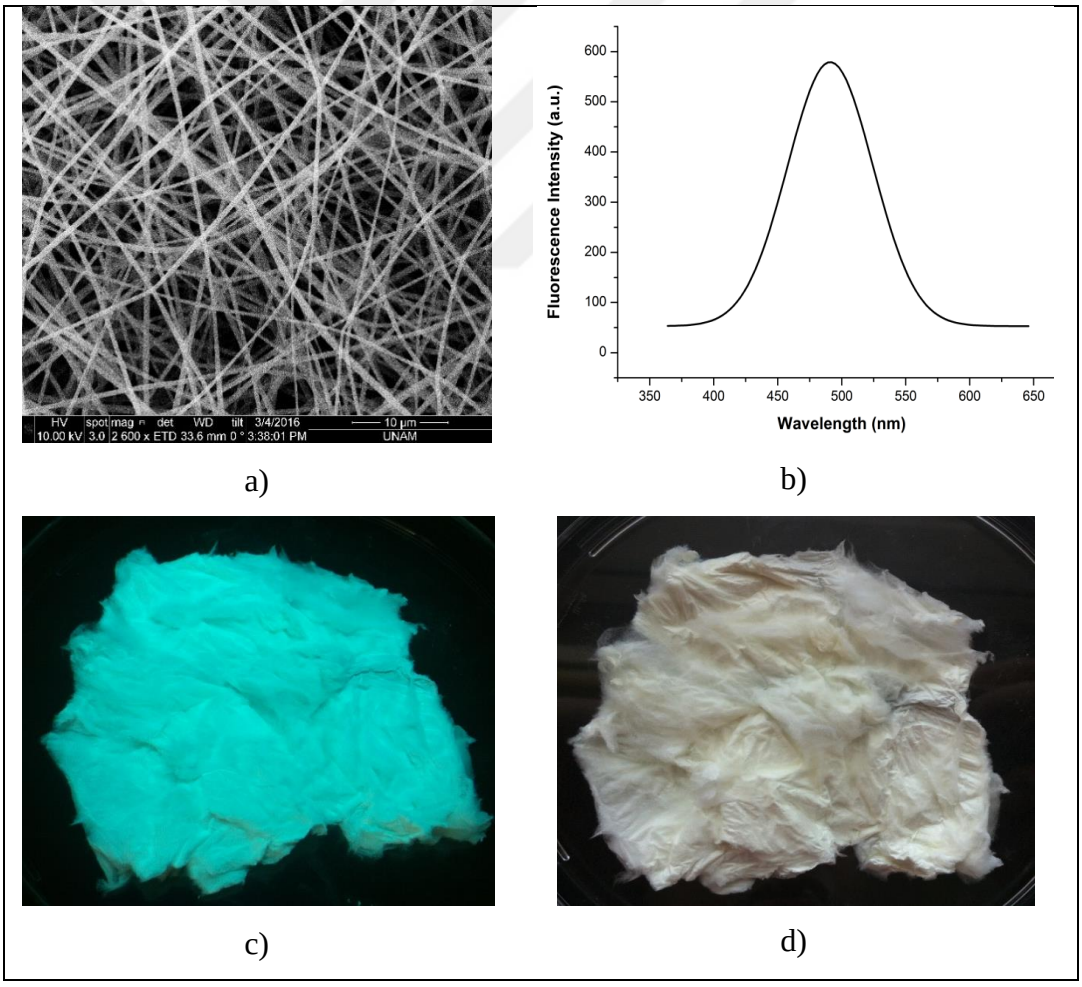

Figure 6.13: a) SEM image of the dansyl functional polystyrene copolymer nanofibers. b) Fluorescence emission spectrum (λext-350 nm). c) Photograph of FNFM under UV light (λext-254 nm) and d) daylight.

The procedure for the electrospinning process of nanofibers from dansyl functional polystyrene copolymer (P4-b) was used according to the literature [86]. The SEM image of electrospun dansyl functional styrene copolymer (P4-b) shows a uniform defect-free porous structure as illustrated in Figure 6.13a. The fluorescent polymer demonstrated emission mainly due to increased local concentration of dansyl moieties on the polymer backbone as shown in Figure 6.13b. Further, the fluorescent nanofibrous membrane (FNFM) exhibited bright blue emission, visually observed under UV light (λext-254 nm) as shown in Figure 6.13c, and their depiction under normal light conditions is displayed in Figure 6.13d.

6.3. Characterization of Porphyrin Functional Styrene Copolymer (P5)

FT-IR spectra of Compound 2-4 were given in Figure 6.14. In the FT-IR spectra of asymmetric porphyrin derivative (Compound 2) and asymmetric zinc-porphyrin (Compound 3), the wide signals observed at 3500 cm^{-1} clearly indicate the presence of OH groups in their chemical structures (Figure 6.14.a and b). Upon reaction between Compound 3 and propargyl bromide, the disappearence of OH signal, which was observed in the FT-IR spectrum of the Figure 6.14.c, proves that acetylene group was attached successively, yielding acetylene-functional asymmetric porphyrin (Compound 4).

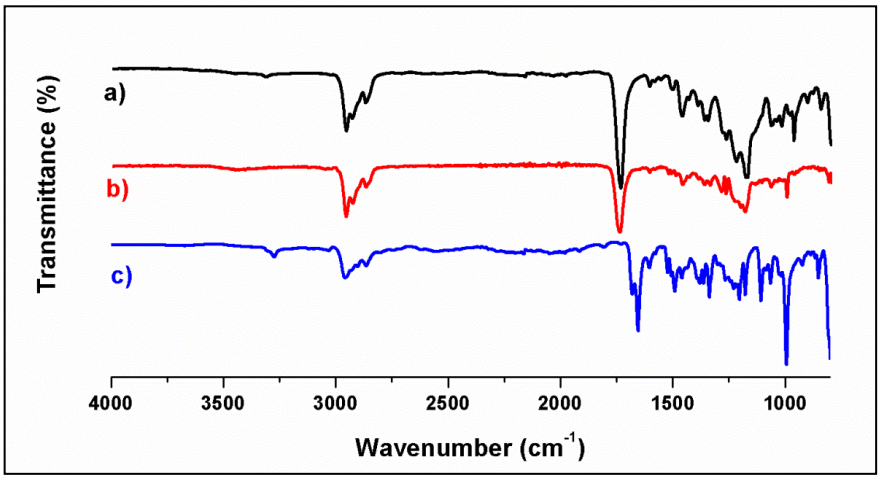

Figure 6.14: FT-IR spectra of a) Compound 2, b) Compound 3, and c) Compound 4.

FT-IR spectra of P1-d, P2-d and P5 were given in Figure 6.15. In their FT-IR spectra, aromatic and aliphatic C-H stretching bands are observed around 3027−3063 and 2848−2921 cm^{-1}, respectively. In the FT-IR spectrum of P2-d, the signal observed at 2096 cm^{-1} clearly indicates the presence of azide functional groups in the chemical structure of P2-d. Upon click reaction between P2-d and Compound 4, the complete disappearence of azide signal, which was observed in the FT-IR spectrum of the precursor, proves that porphyrin side groups were attached quantitatively, yielding P5.

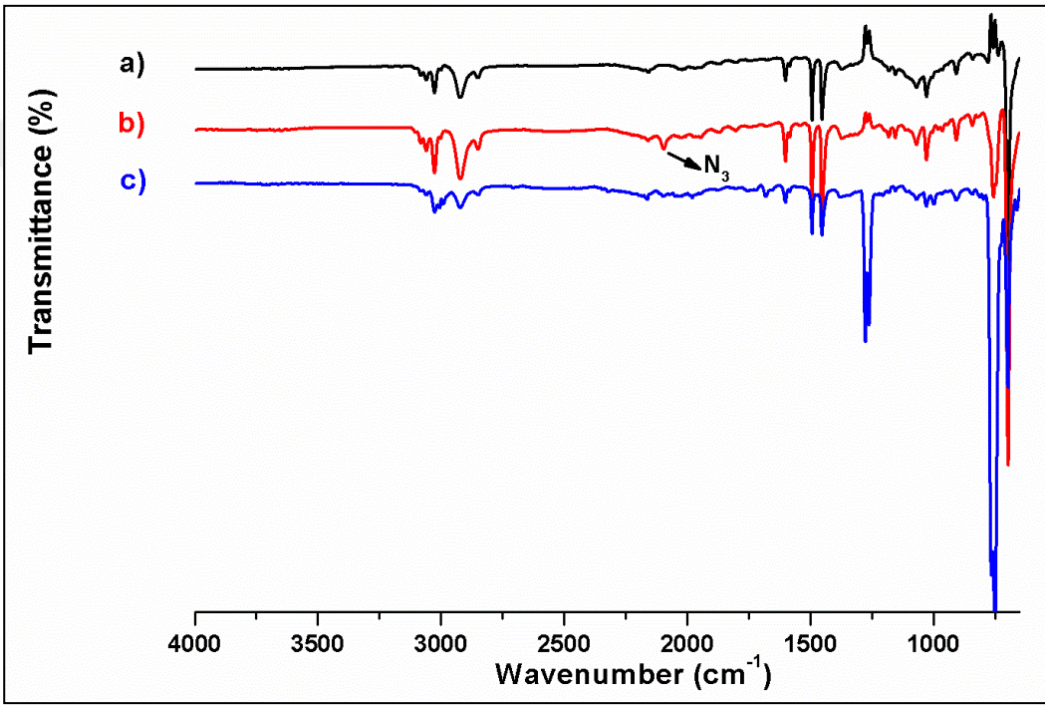

Figure 6.15: FT-IR spectra of the functional styrene copolymers: a) P1-d, b) P2-d, and c) P5.

In the ^{1}H NMR spectra of the compounds 2, 3, and 4 (Figure 6.16), the aromatic CH protons gave signals between 7.15 - 9.00 ppms and methyl group protons gave signals at 1.61ppm. In the ^{1}H NMR spectrum of compound 2 (Figure 6.16.a), the signal of the internal NH protons was observed at -2.76 ppm. Upon zincification of compound 2, this signal was disappeared in the ^{1}H NMR spectrum, clearly confirms that compound 3 synthesized successively. The CH acetylene proton of compound 4 gave signal at 2.70 ppm (Figure 6.16.c).

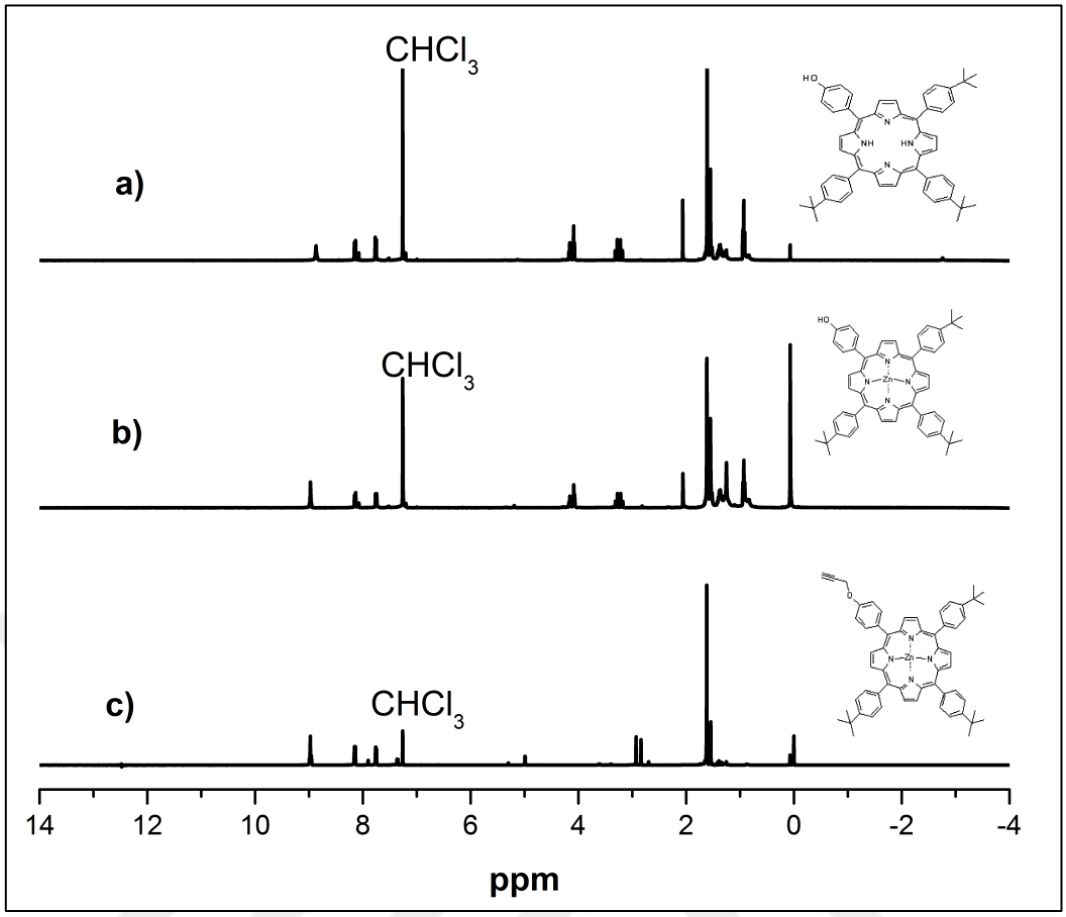

Figure 6.16: ^{1}H NMR spectra of the functional styrene copolymers: a) Compound 2, b) Compound 3, and c) Compound 4.

In the ^{1}H NMR spectra of the copolymers (Figure 6.17), the backbone protons (H_a) gave signals between 1.2 and 2.1 ppms, while aromatic CH protons (H_c) in styrene and vinylbenzyl repeating units gave resonances between 6.3 and 7.24 ppms. In the ^{1}H NMR spectrum of P1-d, the signal of the methylene protons (H_b) next to the benzene ring was observed at 4.48 ppm. Upon azidification of P2-d, the signal H_b moved to higher magnetic field (4.22 ppm) in the ^{1}H NMR spectrum. After click reaction of P2-d with compound 4, the chemical environment of these protons (H_b) changed and they gave rosonces at 5.30 ppm. The shift of H_b protons on azidification and click reactions, clearly confirms the success of the reactions. Copolymer composition of the polymers (P1-d, P2-d, P5) was calculated by comparing the integral ratios of H_b and H_c and found as 98.2. Besides, aromatic CH protons of porphyrin group were observed at 7.75 and 8.16 ppms and triazole proton signal was observed at 8.98 ppm in the ^{1}H NMR spectrum of P5 (Figure 6.17.c).

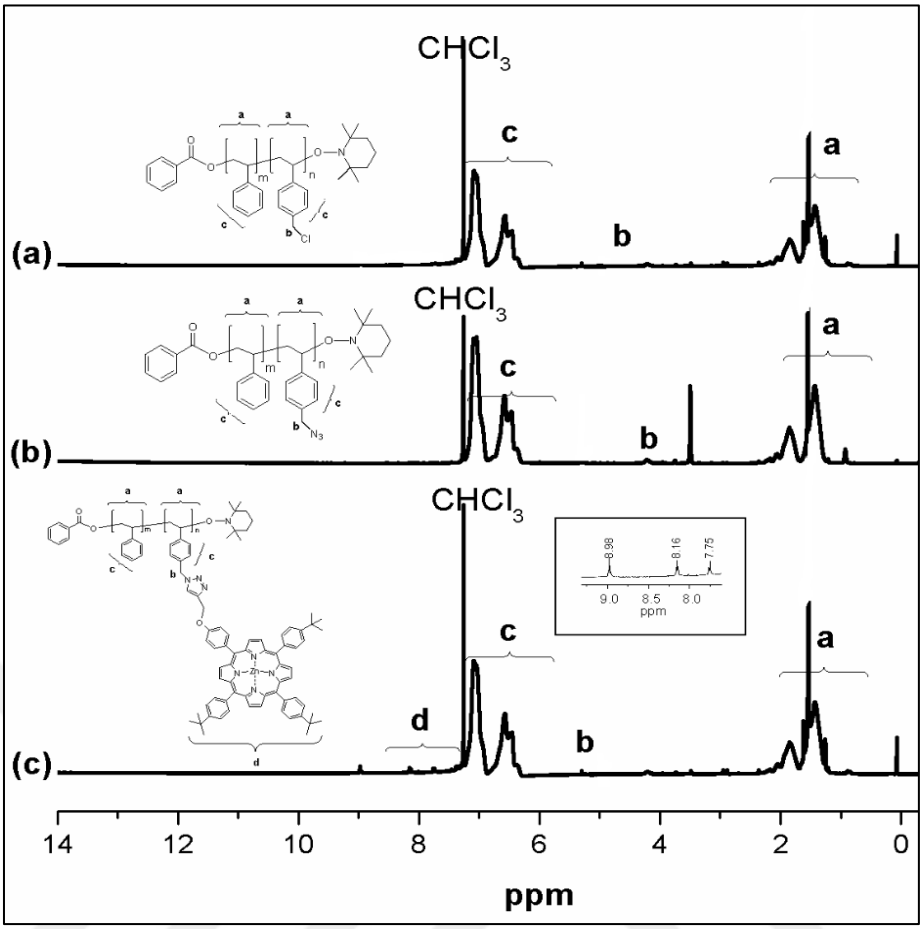

Figure 6.17: ^{1}H NMR spectra of the functional styrene copolymers:
a) P1-d, b) P2-d, and c) P5.

The thermal transitions of P1-d, P2-d, and P5 polymers with different side-functional groups were determined by DSC. The DSC curves of the styrene copolymers in the second heating run were shown in Figure 6.18. T_g values value of the chloride functional styrene copolymer (P1-d) was measured as 104. Upon azidification, T_g of the styrene copolymer (P2-d) decreased slightly to 103. Then, attachment of porphyrin side groups considerably increased T_g (127.9) of the resultant fluorescent styrene copolymer (P5), due to the structure of porphyrin side-units.

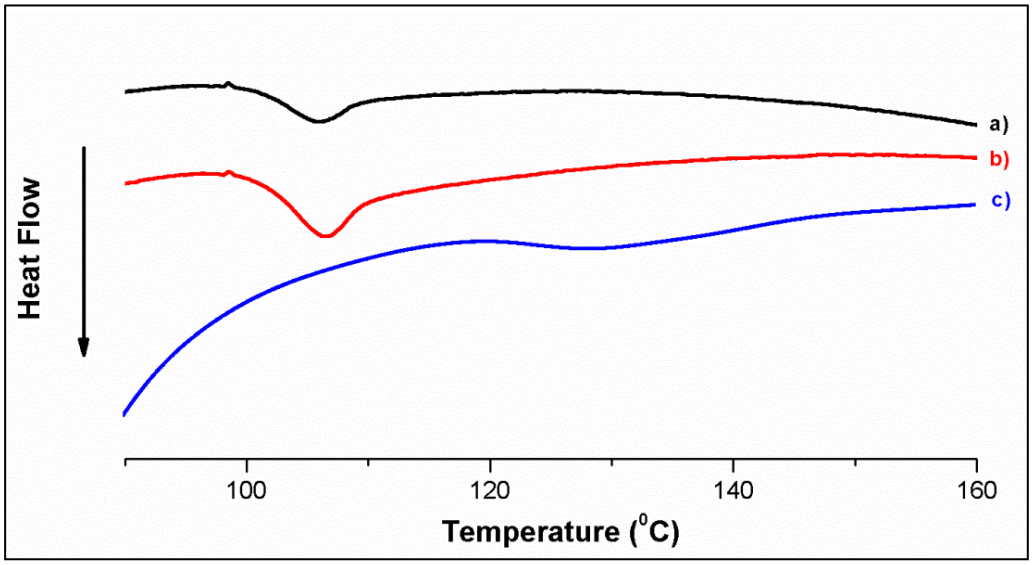

Figure 6.18: DSC thermograms of the functional styrene copolymers, a) P1-d, b) P2-d, and c) P5.

Thermal properties of the synthesized copolymers were measured via TGA experiments. Their maximum decomposition temperatures (T_{Max}) of the styrene copolymers were very close to each other as seen from Figure 6.19. The percent char yields of the chloride (P1-d) and azide (P2-d) functional polymers were found 4.2% and 0.40%, respectively at 700 °C. Also, the percent char yield of the porphyrin-functional styrene copolymer (P5) was remarkably (8.87%) greater than the others.

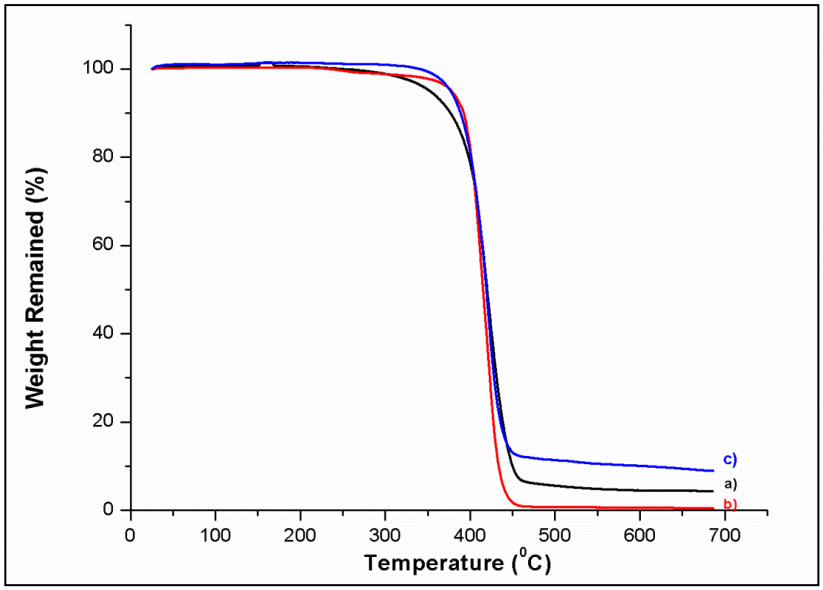

Figure 6.19: TGA thermograms of the functional styrene copolymers, a) P1-d, b) P2-d, and c) P5.

UV-vis spectra of Compound 2, compound 3, compound 4, P2-d, and P5 in DMF solvent (0.2 mg/ml) is shown in Figure 6.20. The UV-vis spectrum of P5 shows that characteristic Soret band peak of porphyrin molecules is observed at 428 nm and Q-band peaks are observed at 518, 562 and 602 nm. These results indicate the presence of porphyrin side groups in P5 polymer structure.

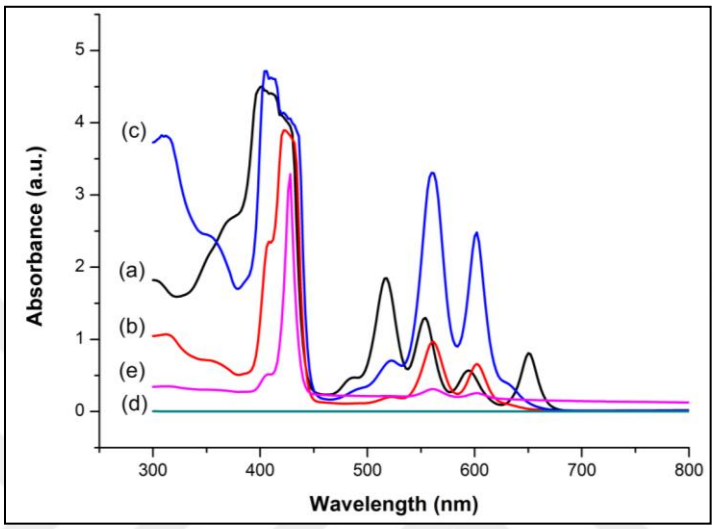

Figure 6.20: UV-vis spectra of a) Compound 2, b) Compound 3, c) Compound 4, d) P2-d, and e) P5.

The fluorescent polymer P5 in DMF solvent (0.2 mg/ml) demonstrated excimer emissions mainly due to increased local concentration of porphyrin moieties on the polymer backbone as shown in Figure 6.21.

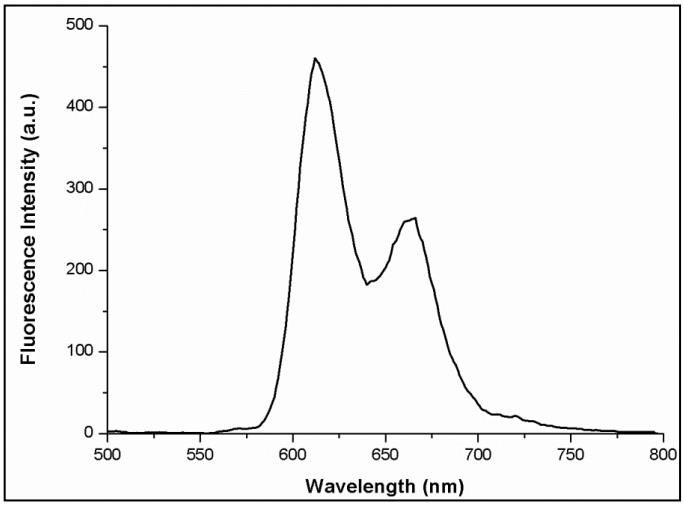

Figure 6.21: Fluorescence emission spectrum of the porphyrin functional polystyrene copolymer (λext-420 nm).

Different solvent systems were tried for electrospinning of porphyrin-functional polystyrene copolymer (P5). Firstly, polymer solution in 10% (w/v) DMF solvent system was prepared. Heavily nanofibers with beaded structures were obtained (Figure 6.22-a). When the polymer concentration was increased to 13% in DMF, nanofibers were obtained beside the bead structures (Figure 6.22-b). Therefore, changes were made in the solvent system. Nanofibers of polymer solution at 10% (w/v) concentration in DMF\DCM (7/1-v/v) have shown improvement, but beadless structure could not be formed (Figure 6.22-c). Then, electrospinning using 10% (w/v) concentration in DMF\DCM (7/3-v/v) solvent mixture showed significant improvements in fiber quality although beadless structure could not be produced (Figure 6.22-d). After that, increasing DCM ratio in the solvent mixture (DMF/DCM, 7/5, v/v) at the same concentration (10%, w/v) beadless structure could not be obtained in the electrospining of the polymer solution (Figure 6.22-e). Thereupon, beadless structures were tried to be achieved by increasing the solution concentration and therefore the viscosity. Bead structures were decreased and significant improvements were observed in fiber homogenity in the electrospinning experiment at 13% (w/v) concentration in DMF\DCM (7/1-v/v) solvent system (Figure 6.22-f).

After all this, electrospinning studies of polymer solution were performed in DMF/DCM (7/3, v/v) solvent system at the same concentration (13%). In this trial, beadless uniform nanofiber structures were obtained (Figure 6.22-g,h). The SEM image of electrospun porphyrin-functional styrene copolymer (P5) depicts a uniform defect-free structure as illustrated in Figure 6.22-g,h.

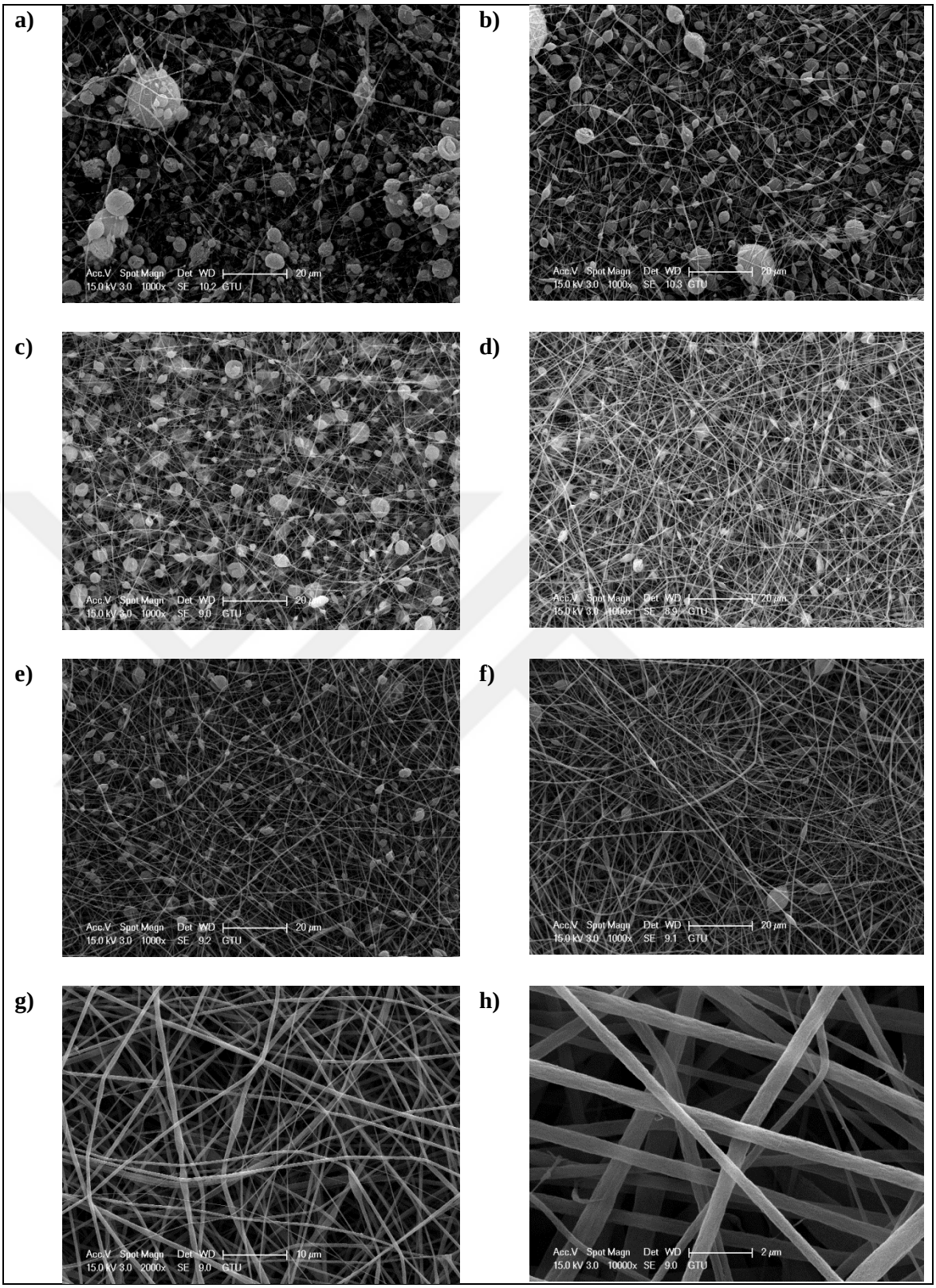

Figure 6.22: SEM micrographs of electrospun nanofibers of P5 polymer having porphyrin side groups using a) 10% (w/v) in DMF, b) 13% (w/v) in DMF, c) 10% (w/v) in DMF/DCM (7/1- v/v), d) 10% (w/v) in DMF/DCM (7/3- v/v), e) 10% (w/v) in DMF/DCM (7/5- v/v), f) 13% (w/v) in DMF/DCM (7/1- v/v), g), and h) 13% (w/v) in DMF/DCM (7/3- v/v) solvent systems. The magnification ratio was applied 1000X for a, b, c, d, e and f, 2000X for g, and h for 10000X.

6.4. Characterization of Coumarin Functional Styrene Copolymer (P6)

FT-IR spectra of chloride-functional styrene copolymer (P1-e) and coumarin-functional polystyrene copolymer (P6) were given in Figure 6.23. In their FT-IR spectra, aromatic and aliphatic C-H stretching bands are observed around 3027−3063 and 2848−2932 cm^{-1}, respectively. Upon etherification reaction between P1-e and 7-hydroxycoumarin, the complete disappearence of chloride signal (1260 cm^{-1}), proves that coumarin side groups were attached quantitatively, yielding P6.

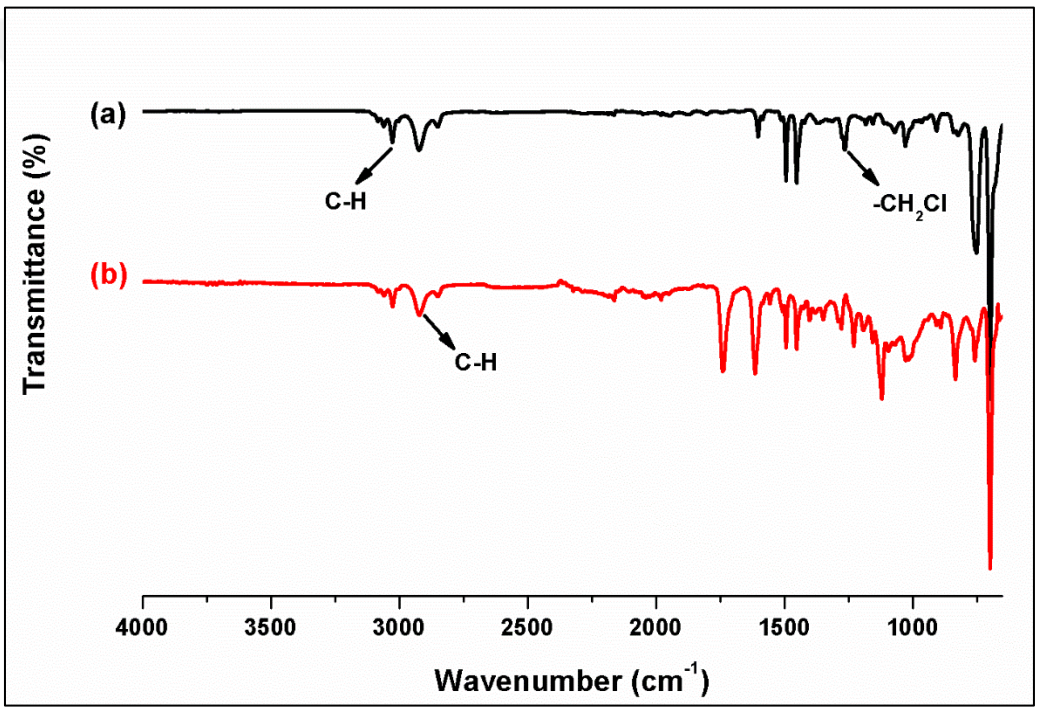

Figure 6.23: FT-IR spectra of the functional styrene copolymers: a) P1-e and b) P6.

In the ^1H NMR spectra of the copolymers (Figure 6.24), the backbone protons (H_a) gave signals between 1.1 and 2.1 ppms, while aromatic CH protons (H_c) in styrene and vinylbenzyl repeating units gave resonances between 6.2 and 7.2 ppms. In the ^1H NMR spectrum of P1-e, the signal of the methylene protons (H_b) next to the benzene ring was observed at 4.50 ppm. After reaction of P1-e with 7-hydroxycoumarin, the chemical environment of these protons (H_b) changed and they gave rosonces at 4.97 ppm. The clear shift of H_b protons, clearly

confirms the success of the reaction. Copolymer composition of the polymers (P1-e, P6) was calculated by comparing the integral ratios of H_b and H_c and found as 7.2. Besides, coumarin proton signals were observed between 7.5 and 7.7 ppms in the ^{1}H NMR spectrum of P6.

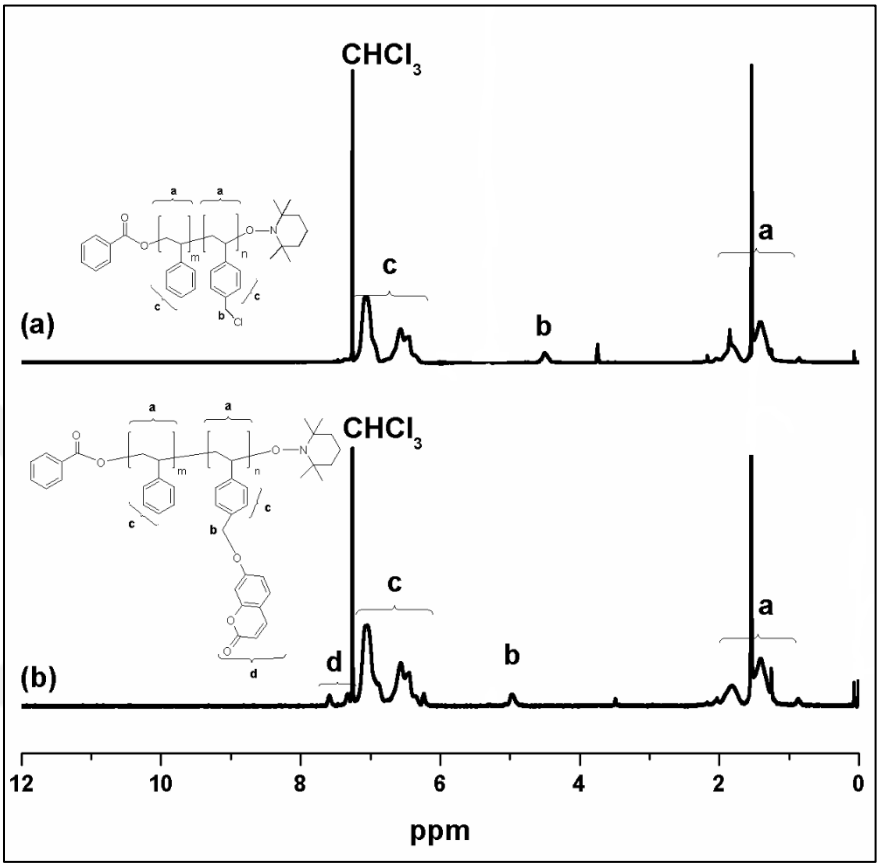

Figure 6.24: ^{1}H NMR spectra of the functional styrene copolymers: a) P1-e and b) P6.

The thermal transitions, of P1-e and P6 polymers with different side-functional groups were determined by differential scanning calometry (DSC). The DSC curves of the styrene copolymers in the second heating run were shown in Figure 6.25. Tg values value of the chloride functional styrene copolymer (P1-e) was measured as 108.9. Then, attachment of coumarin side groups increased (115.9) T_g of the resultant fluorescent styrene copolymer (P6), due to the structure of coumarin side-units.

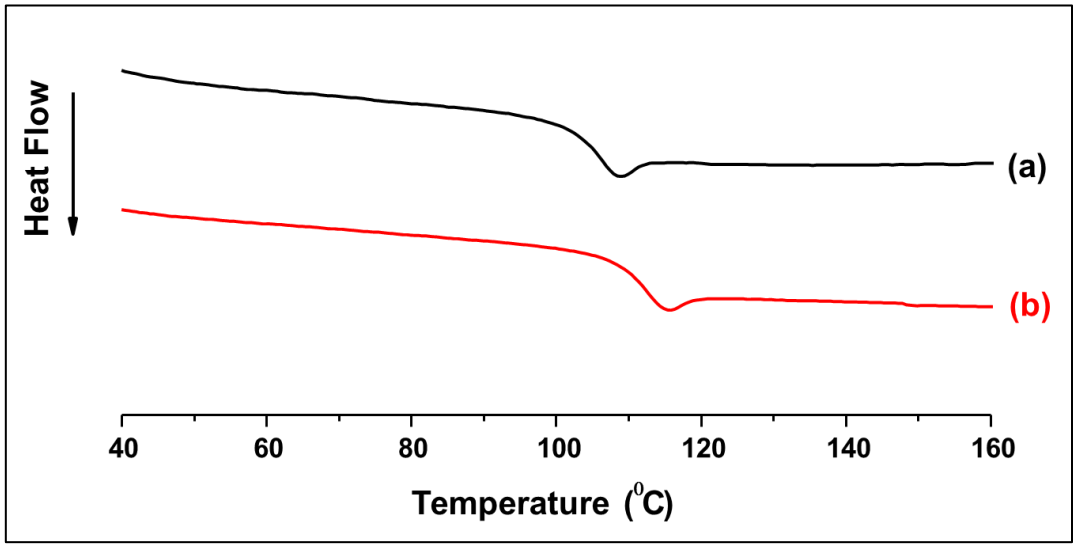

Figure 6.25: DSC thermograms of the functional styrene copolymers, a) P1-e and b) P6.

Thermal properties of the P1-e and P6 copolymers were measured via TGA experiments. Their maximum decomposition temperatures (T_{Max}) of the styrene copolymers were close to each other as seen from Figure 6.26. Also, the percent char yield of the coumarin-functional styrene copolymer was greater than chloride functional polymer.

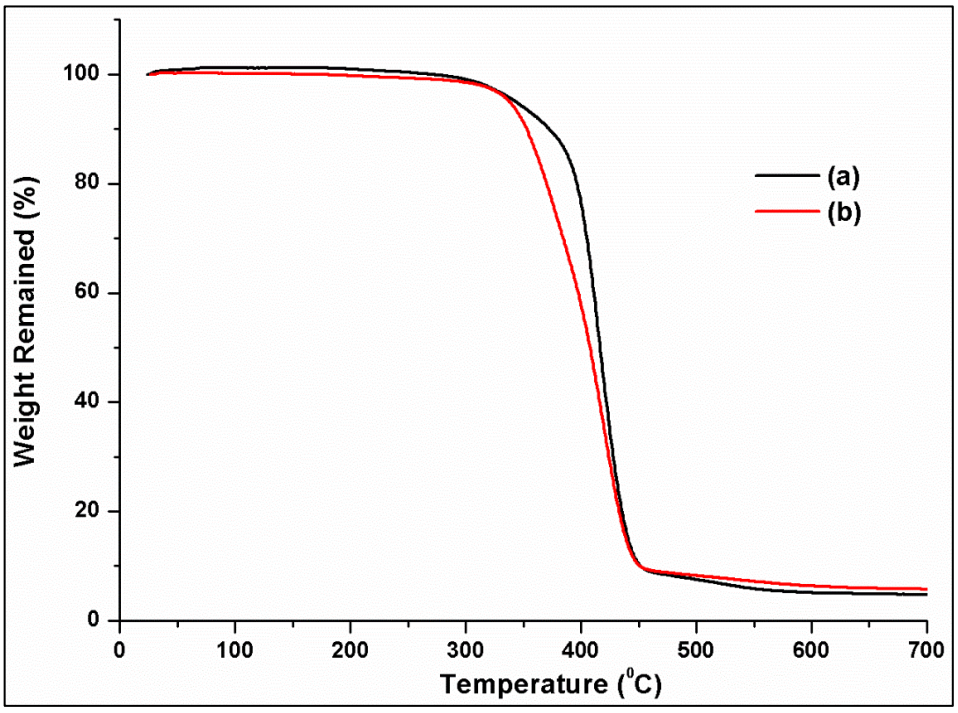

Figure 6.26: TGA thermograms of the functional styrene copolymers, a) P1-e and b) P6.

The fluorescent polymer demonstrated emission mainly due to increased local concentration of coumarin moieties on the polymer backbone as shown in Figure 6.27.

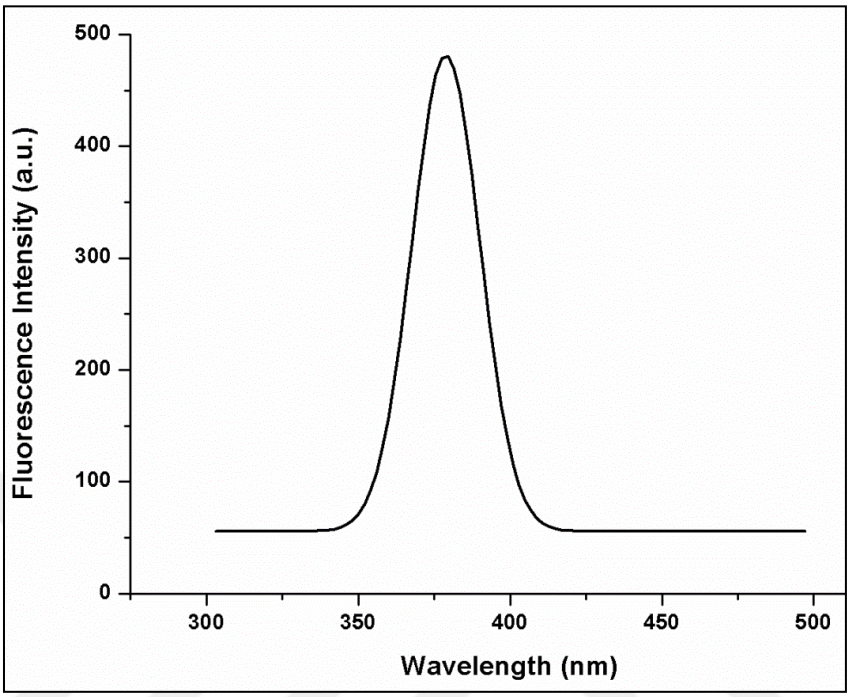

Figure 6.27: Fluorescence emission spectrum of the coumarin functional polystyrene copolymer (λext-300 nm).

Different solvent systems were tried for electrospinning of coumarin-functional polystyrene copolymer (P6). Firstly, polymer solution in 5% (w/v) DMF solvent system was prepared. Heavily nanofibers with beaded structures were obtained (Figure 6.28a-b). Therefore, various solvent mixtures were tried to improve this system. P6 polymer was prepared at 10% (w/v) concentration in DMF\DCM (7/1-v/v), DMF/DCM (7/3-v/v), and DMF/DCM (7/5-v/v) solvent systems. The SEM images of electrospun coumarin-functional styrene copolymer (P6) depict that bead structures were decreased. And, the nanofiber structure having less beads was obtained at 10% (w/v) concentration in DMF/DCM (7/3-v/v) solvent system (Figure 6.28-e,f).

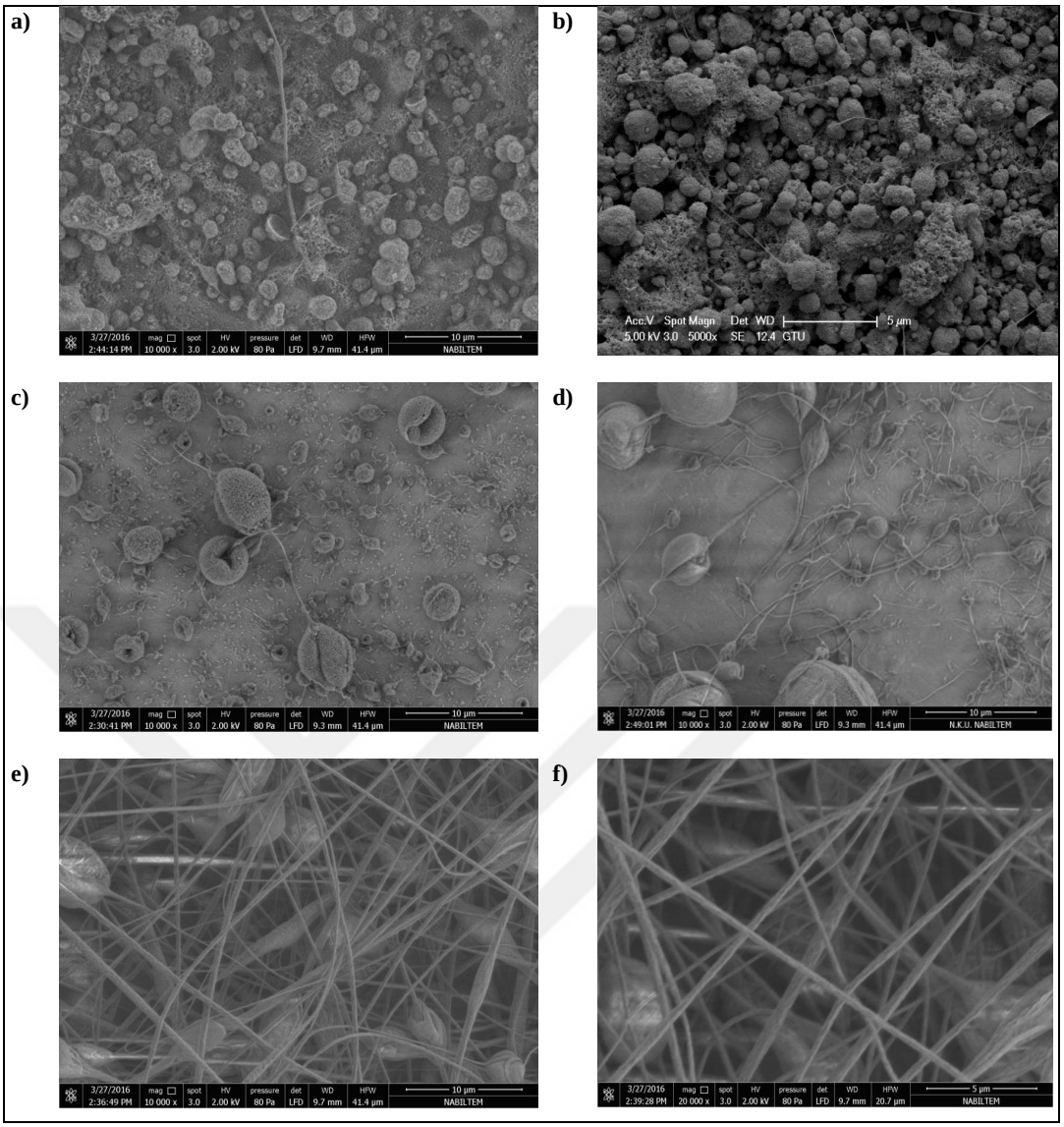

Figure 6.28: SEM micrographs of electrospun nanofibers of P6 polymer having coumarin side groups using a) and b) 5% (w/v) in DMF, c) 10% (w/v) in DMF/DCM (7/1- v/v), d) 10% (w/v) in DMF/DCM (7/5- v/v), e) and f) 10% (w/v) in DMF/DCM (7/3- v/v) solvent systems.

6.5. Sensing Applications of Electrospun Pyrene Functional Styrene Copolymer

The fluorescence quenching experiments were done similar to the literature papers. At a concentration of 10^{-2} M, stock solutions of nitro explosives and metal ions were prepared by dissolving in ACN/H_2O (1:1) mixture. The nanofiber mat was put into the cuvette with 2 mL of ACN/H_2O (1:1) and then the solution of nitroaromatics and metal ions were injected and allowed to reach equilibrium.

This is followed by diluting different concentrations of quenchers from the stock solution [84].

Metal ion and nitroaromatic sensing experiments of P3 fluorescent nanofibrous membrane (FNFM) were performed in ACN : water (1:1) solvent mixtures at room temperature for 10 min dipping the membrane. The detailed measurements of concentration changes were made for TNT. The corresponding fluorescence spectra before and after the treatment of TNT, with a concentration ranging from 5 mM to 5 nM is illustrated in Figure 6.29a. This spectrum clearly shows that fluorescence nature of the fiber changes as a function of the concentration of TNT. The quenching efficiency rises with increasing concentration of TNT, shown in Figure 6.29b.

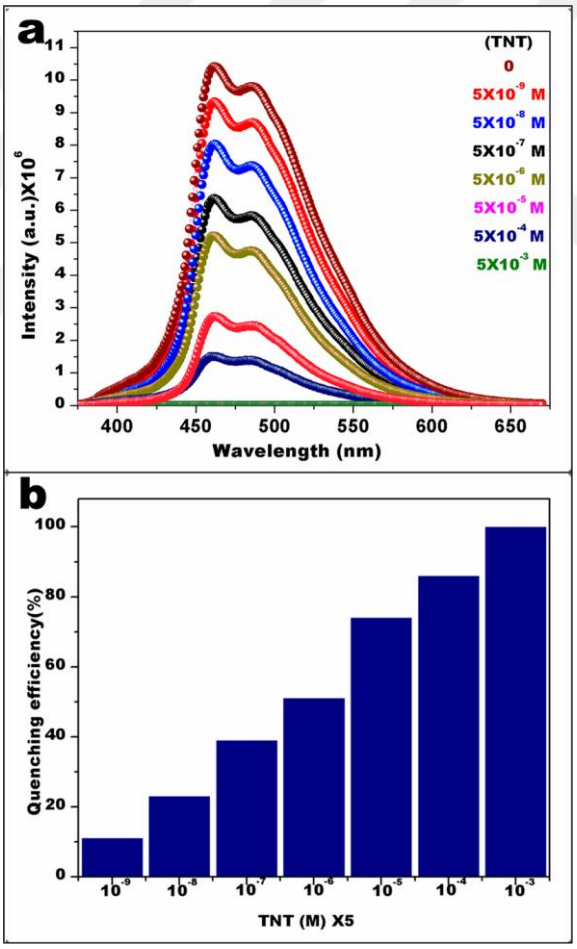

Figure 6.29: a) Fluorescence emission spectra of FNFM upon exposure to various concentrations of TNT and their b) quenching efficiency.

Further, visual colorimetric detection was performed for different concentrations of TNT from 5 mM to 5 nM. Obviously, the visual colorimetric

sensing performance of FNFM is easily identifiable under UV light (λ_{ext} -254 nm), since the color of the membrane changes from bright bluish-green to blue at selected concentrations. Further, maintaining the same and normal light conditions, their photographs were taken, demonstrated in Figure 6.30. It is apparent that color changed from light sandal to dark sandal at higher concentration under normal light conditions.

Figure 6.30: Visual colorimetric detection of TNT. Photograph of the fluorescence quenching of FNFM treated with different concentrations of TNT in aqueous phase when viewed under UV (λext-254 nm) a) and daylight b). The tested TNT concentrations are $5x10^{-3}$, $5x10^{-4}$, $5x10^{-5}$, $5x10^{-6}$, and $5x10^{-7}$M from left to right.

The importance of selective response was investigated from other nitro aromatic compounds and commonly found toxic metals in water. Significantly, the results showed that the presence of 2,4-dinitrotoluene at a concentration of 1 mM decreases the fluorescence intensity considerably, and 4-nitrophenol also slightly decreases the fluorescence intensity. Excitingly, at this concentration, the highest quenching efficiency was obtained in the presence of TNT indicating their enhanced sensing response. Besides this, no significant change in fluorescence emission was noticed in the presence of toxic metal ions visually and spectroscopically, presented in Figure 6.31.

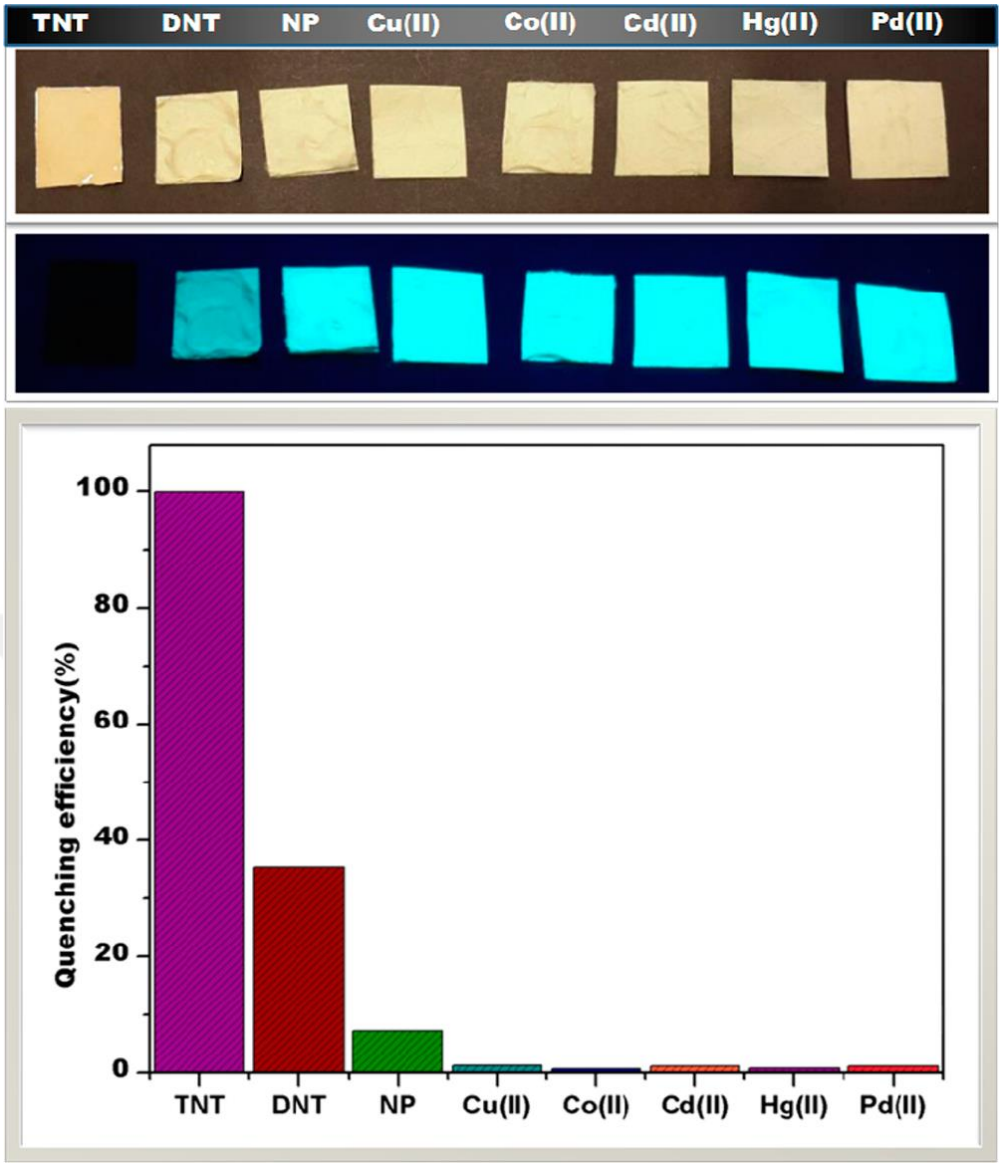

Figure 6.31: Selective sensing performance of FNFM upon exposure to other nitro aromatic compounds and toxic metal ions.

7. CONCLUSION

In this thesis, styrene based copolymers bearing different fluorescence active functional groups were synthesized and employed in the preparation of nanofibers via electrospinning method. The effects of polymer molecular weight, polymer solution concentration, solvent, and solvent systems to nanofiber formation were examined by SEM analysis. We divide it into four main parts and the significant results are given below.

In the first part, pyrene-functional polystyrene copolymer (P3) was synthesized and employed in the preparation of electrospun nanofibers. Different solvent systems were tried for electrospinning of pyrene-functional polystyrene copolymer (P3). Firstly, polymer solution in 10% (w/v) DMF solvent system was prepared. Nanofibers with beaded structures were obtained, then changes were made in the solvent system. In DMF/ chloroform (4/1-v/v) solvent mixture at 10% (w/v) concentration, beadless structure could not be obtained although increasing concentration and therefore viscosity to 12%. When the concentration was increased more, the polymer solution solidified at the syringe tip. Therefore, DMF/DCM (7/3-v/v) solvent system was tried and at 12% (w/v) concentration uniform beadless nanofibers could be obtained without any problems. The obtained nanofibers were used as the fluorescence active sensing material against trinitrotoluene (TNT) [84].

In the second part, dansyl-functional polystyrene copolymer (P4) was synthesized and employed in the preparation of electrospun nanofibers. Different solvent systems were tried for electrospinning of dansyl-functional polystyrene copolymer (P4). The best resolution was achieved at DCM/DMF (3/2) (v/v) for electrospinning of dansyl-functional styrene polymer (P4-a) and could be dissolved until 20% (w/v) polymer concentration. Despite the concentration was increased, only bead structures were obtained. Because of all these difficulties, P4-b polymer having lower dansyl percentage was used in the electrospinning studies. In DCM/DMF (3/7-v/v) solvent system and increasing concentration to 30% (w/v), uniform beadless nanofibers could be obtained without any problems.

In the third part, porphyrin-functional polystyrene copolymer (P5) was synthesized and employed in the preparation of electrospun nanofibers. Different solvent systems were tried for electrospinning of porphyrin-functional polystyrene

copolymer (P5). Firstly, polymer solution in 10% (w/v) DMF solvent system was used and heavily beaded nanofiber structures were obtained. Then, the polymer concentration was increased to 13%, nanofibers were obtained beside the bead structures. Therefore, the solvent system was changed and DMF\DCM (7/1-v/v), DMF/DCM (7/3-v/v), and DMF/DCM (7/5-v/v) solvent systems at 10% (w/v) concentration were tried. Beadless structure could not be produced although significant improvements were observed in fiber quality. Then, the solution concentration and therefore viscosity value was increased. At 13% (w/v) concentration in DMF\DCM (7/1-v/v) solvent system, bead structures were decreased and significant improvements were observed in fiber homogenity. After that, at the same concentration (13% (w/v)) in DMF/DCM (7/3, v/v) solvent system uniform beadless nanofibers could be obtained.

In the last part, coumarin-functional polystyrene copolymer (P6) was synthesized via etherification reaction and employed in the preparation of electrospun nanofibers. Different solvent systems were tried for electrospinning of coumarin-functional polystyrene copolymer (P6). Firstly, polymer solution in 5% (w/v) DMF solvent system was used and only beaded nanofiber structures were obtained. Then, the polymer concentration was increased to 10% and DMF\DCM (7/1-v/v), DMF/DCM (7/3-v/v), and DMF/DCM (7/5-v/v) solvent systems were tried. Nanofibers were obtained beside the bead structures at this concentration. The uniform and less bead nanofiber structure could be obtained at 10% (w/v) concentration in DMF/DCM (7/3-v/v) solvent system.

7.1. Benefits that are expected from thesis and its transfer to application

Electrospun nanofibers due to the magnitude of their surface area, are used in a wide range of applications, such as catalysis, nanofiltration, biosensor applications, and artificial tissue studies. The obtained nanofiber mats which are produced from styrene polymers with different functional groups (pyrene, dansyl, porphyrin and coumarin) are thought to have potential to be used in fluorescent chemical sensors towards various analytes.

REFERENCES

[1] Huang Z. M., Zhang Y. Z., Kotaki M., Ramakrishna S., (2003), "A review on polymer nanofibers by electrospinning and their applications in nanocomposites", Composites Science and Technology, 63, 2223-2253.

[2] Liang W. B, Martin C. R., (1990), "Template-synthesized polyacetylene fibrils show enhanced supermolecular order", J Am Chem Soc, 112 (26), 9666–9668.

[3] Cai Z. H., Lei J. T., Liang W. B., Menon V., Martin C. R., (1991), "Molecular and supermolecular origins of enhanced electric conductivity in template-synthesized polyheterocyclic fibrils. 1. Supermolecular effects", Chem Mater, 3 (5), 960–967.

[4] Cui T. Y., Cui F., Zhang J. H., Wang J. Y., Huang J., (2006), "From Monomeric Nanofibers to PbS Nanoparticles/Polymer Composite Nanofibers through the Combined Use of γ-Irradiation and Gas/Solid Reaction", J Am Chem Soc, 128 (19), 6298–6299.

[5] Noy A., Miller A. E., Klare J. E., Weeks B. L., Woods B. W., (2002), "Fabrication of Luminescent Nanostructures and Polymer Nanowires Using Dip-Pen Nanolithography", Nano Letters, 2 (2), 109–112.

[6] Marco C. D., Mele E., Camposeo A., Stabile R., Cingolani R., (2008), "Organic Light-Emitting Nanofibers by Solvent-Resistant Nanofluidics", Advanced Materials, 20 (21), 4158–4162.

[7] Li D., Xia Y. N., (2004), "Electrospinning of Nanofibers: Reinventing the Wheel?", Advanced Materials, 16 (14), 1151–1170.

[8] Camposeo A., Benedetto F. D., Stabile R., Never A. A. R., Cingolani R., (2009), "Laser Emission from Electrospun Polymer Nanofibers", Small, 5 (5), 562–566.

[9] Liu H. Q., Edel J. B., Bellan L. M., Craighead H. G., (2006), "Electrospun Polymer Nanofibers as Subwavelength Optical Waveguides Incorporating Quantum Dots", Small, 2 (4), 495–499.

[10] Dzenis Y., (2004), "Material science. Spinning continuous fibers for nanotechnology", Science, 304 (5679), 1917–1919.

[11] Harfenist S. A., Cambron S. D., Nelson E. W., Berry S. M., Isham A. W., (2004), "Direct Drawing of Suspended Filamentary Micro- and Nanostructures from Liquid Polymers", Nano Letters, 4 (10), 1931–1937.

[12] Gu F. X., Zhang L., Yin X. F., Tong L. M., (2008), "Polymer Single-Nanowire Optical Sensors", Nano Letters, 8 (9), 2757–2761.

[13] Xing X. B., Zhu H., Wang Y. Q., Li B. J., (2008), "Ultracompact Photonic Coupling Splitters Twisted by PTT Nanowires", Nano Letters, 8 (9), 2839–2843.

[14] Meng C., Xiao Y., Wang P., Zhang L., Liu Y. X., (2011), "Quantum-Dot-Doped Polymer Nanofibers for Optical Sensing", Advanced Materials, 23 (33), 3770–3774.

[15] Wang P., Zhang L., Xia Y. N., Tong L. M., Xu X., (2012), "Polymer Nanofibers Embedded with Aligned Gold Nanorods: A New Platform for Plasmonic Studies and Optical Sensing", Nano Letters, 12 (6), 3145–3150.

[16] Gu F. X., Yu H. K., Fang W., Tong L. M., (2013), "Nanoimprinted Polymer Micro/Nanofiber Bragg Gratings for High-Sensitivity Strain Sensing", IEEE Photon Technol Lett, 25 (1), 22–24.

[17] Wang P., Li Z. Y., Zhang L., Tong L. M., (2013), "Electron-beam-activated light-emitting polymer nanofibers", Optics Letters, 38 (7), 1040–1042.

[18] Fery-Forgues S., Fournier-Noël C., (2010), "Organic Fluorescent Nanofibers and Sub-Micrometer Rods", Ashok Kumar (Ed.), ISBN: 978-953-7619-86-2, InTech.

[19] Wang P., Wang Y., Tong L., (2013), "Functionalized polymer nanofibers: a versatile platform for manipulating light at the nanoscale", Light: Science & Applications, 2, e102.

[20] Wang Y., Serrano S., Santiago-Aviles J.J., (2002), "Conductivity measurement of electrospun PAN-based carbon nanofiber", Journal of Materials Science Letters, 21 (13), 1055-1057.

[21] Gupta P., Elkins C., Long T. E, Wilkes G. L., (2005), "Electrospinning of linear homopolymers of poly(methyl methacrylate): exploring relationships between fiber formation, viscosity, molecular weight and concentration in a good solvent", Polymer, 46 (13), 4799-4810.

[22] Huang X. J., Yu A. G., Xu Z. K., (2008), "Covalent immobilization of lipase from Candida rugosa onto poly(acrylonitrile-co-2-hydroxyethyl methacrylate) electrospun fibrous membranes for potential bioreactor application", Bioresource Technology, 99 (13), 5459-5465.

[23] Shao C., Kim H. Y., Gong J., Ding B., Lee D. R., Park S. J., (2003), "Fiber mats of poly(vinyl alcohol)/silica composite via electrospinning", Materials Letters, 57 (9-10), 1579-1584.

[24] Lyoo W., Lee K., Lee Y., Kim H., (2007), "Experimental Analysis of Nano and Engineering Materials and Structures", in: E.E. Gdoutos (Ed.), Springer Netherlands, 47-48.

[25] Casper C. L., Stephens J. S., Tassi N. G., Chase D. B., Rabolt J. F., (2003), "Controlling Surface Morphology of Electrospun Polystyrene Fibers: Effect of Humidity and Molecular Weight in the Electrospinning Process", Macromolecules, 37 (2), 573-578.

[26] Stephens J. S., Chase D. B., Rabolt J. F., (2004), "Effect of the Electrospinning Process on Polymer Crystallization Chain Conformation in Nylon-6 and Nylon-12", Macromolecules, 37 (3), 877-881.

[27] Jeong J. S., Jeon S. Y., Lee T. Y, Park J. H., Shin J. H., Alegaonkar P. S., Berdinsky A. S., Yoo J. B., (2006), "Fabrication of MWNTs/nylon conductive composite nanofibers by electrospinning", Diamond and Related Materials, 15 (11-12), 1839-1843.

[28] Demir M. M., Yilgor I., Yilgor E., Erman B., (2002), "Electrospinning of polyurethane fibers", Polymer, 43 (11), 3303-3309.

[29] Khil M. S., Cha D. I., Kim H. Y., Kim I. S., Bhattarai N., (2003), "Electrospun nanofibrous polyurethane membrane as wound dressing", Journal of Biomedical Materials Research Part B: Applied Biomaterials, 67B (2), 675-679.

[30] Lee K. H., Kim H. Y., Khil M. S., Ra Y. M., Lee D. R., (2003), "Characterization of Nano-Structured Poly(ε-Caprolactone) Nonwoven Mats via Electrospinning", Polymer, 44 (4), 1287-1294.

[31] Yang F., Murugan R., Wang S., Ramakrishna S., (2005), "Electrospinning of nano/micro scale poly(L-lactic acid) aligned fibers and their potential in neural tissue engineering.", Biomaterials, 26 (15), 2603-2610.

[32] Ma Z., Kotaki M., Yong T., He W., Ramakrishna S., (2005), "Surface engineering of electrospun polyethylene terephthalate (PET) nanofibers towards development of a new material for blood vessel engineering", Biomaterials, 26 (15), 2527-2536.s

[33] Kim J. S., Reneker D. H., (1999), "Polybenzimidazole nanofiber produced by electrospinning", Polymer Engineering & Science, 39 (5), 849-854.

[34] Kim S. J., Nam Y. S., Rhee D. M., Park H. S., Park W. H., (2007), "Preparation and characterization of antimicrobial polycarbonate nanofibrous membrane", European Polymer Journal, 43 (8), 3146-3152.

[35] Chen C., Wang L., Huang Y., (2007), "Electrospinning of thermo-regulating ultrafine fibers based on polyethylene glycol/cellulose acetate composite", Polymer, 48 (18), 5202-5207.

[36] Spasova M., Stoilova O., Manolova N., Rashkov I., Altankov G., (2007), " Preparation of PLLA/PEG Nanofibers by Electrospinning and Potential Applications", Journal of Bioactive and Compatible Polymers, 22 (1), 62-76.

[37] Hong K. H., Kang T. J., (2006), "Polyaniline–nylon 6 composite nanowires prepared by emulsion polymerization and electrospinning process", Journal of Applied Polymer Science, 99 (3), 1277-1286.

[38] Geng X., Kwon O. H., Jang J., (2005), "Electrospinning of chitosan dissolved in concentrated acetic acid solution", Biomaterials, 26 (27), 5427-5432.

[39] Ohkawa K., Cha D., Kim H., Nishida A., Yamamoto H., (2004), "Electrospinning of Chitosan", Macromolecular Rapid Communications, 25 (18), 1600-1605.

[40] Min B. M., Lee G., Kim S. H., Nam Y. S., Lee T. S., Park W. H., (2004), "Electrospinning of silk fibroin nanofibers and its effect on the adhesion and spreading of normal human keratinocytes and fibroblasts in vitro", Biomaterials, 25 (7-8), 1289-1297.

[41] Frey M. W., (2008), "Electrospinning Cellulose and Cellulose Derivatives", Polymer Reviews, 48 (2), 378-391.

[42] Ohkawa K., Hayashi S., Nishida A., Yamamoto H., Ducreux J., (2009), "Preparation of Pure Cellulose Nanofiber via Electrospinning", Textile Research Journal, 79 (15), 1396-1401.

[43] Jin H. J., Fridrikh S. V., Rutledge G. C., Kaplan D. L., (2002), "Electrospinning Bombyx mori Silk with Poly(ethylene oxide)", Biomacromolecules, 3 (6), 1233-1239.

[44] Jung K. H., Huh M. W., Meng W., Yuan J., Hyun S. H., Bae J. S., Hudson S. M., Kang I. K., (2007), "Preparation and antibacterial activity of PET/chitosan nanofibrous mats using an electrospinning technique", Journal of Applied Polymer Science, 105 (5), 2816-2823.

[45] Agarwal S., Wendorff J. H., Greiner A., (2010), "Chemistry on Electrospun Polymeric Nanofibers: Merely Routine Chemistry or a Real Challenge?", Macromolecular Rapid Communications, 31 (15), 1317-1331.

[46] Hajara M. G, Mehta K., Chase G. G., (2003), "Effects of humidity, temperature, and nanofibers on drop coalescence in glass fiber media", Separation and Purification Technology, 30 (1), 79-88.

[47] Gibson P., Schreuder-Gibson H., Rivin D., (2001), "Transport properties of porous membranes based on electrospun nanofibers", Colloids and Surfaces A: Physicochemical and Engineering Aspects, 187–188, 469-481.

[48] Beregoi M., Busuioc C., Evanghelidis A., Matei E., Iordache F., Radu M., Dinischiotu A., Enculescu T., (2016), "Electrochromic properties of polyaniline-coated fiber webs for tissue engineering applications", International Journal of Pharmaceutics, 510 (2), 465-473.

[49] Lee S.H., Ku B.C., Wang X., Samuelson L.A., Kumar J., (2002), "Design, synthesis and electrospinning of a novel fluorescent polymer for optical sensor applications", Mater. Res. Soc. Symp. – Proc., 708, BB10.45.1–BB10.45.6.

[50] Tao S. Y., Li G. T., Yin J. X., (2007), "Fluorescent nanofibrous membranes for trace detection of TNT vapor", Journal of Materials Chemistry, 17, 2730 - 2736.

[51] Wang Y., La A., Ding Y., Liu Y., Lei Y., (2012), "Novel Signal-Amplifying Fluorescent Nanofibers for Naked-Eye-Based Ultrasensitive Detection of Buried Explosives and Explosive Vapors", Advanced Functional Materials, 22 (17), 3547-3555.

[52] Hua K. Y., Deng C. M., He C., Shi L. Q., Zhu D. F., He Q. G., Cheng J. G., (2013), "Organic semiconductors-coated polyacrylonitrile (PAN) electrospun nanofibrous mats for highly sensitive chemosensors via evanescent-wave guiding effect", Chinese Chemical Letters, 24 (7), 643-646.

[53] Web 1, (2016), http://www.engr.utk.edu/mse/Textiles/Nanofiber%20Nonwo-vens.htm , (Erişim Tarihi: 02/10/2016).

[54] Li T. B., Liang J., Xu B. S., Wang J., (2010), "Preparation and characteristic of one dimensional Magnesium Borate Nanomaterials", Journal of Inorganic Materials, 25, 947.

[55] Electrostatic spinning of Nanofibers spin Technologies, Chattanooga, TN.

[56] Ondarçuhu T., Joachim C., (1998), "Drawing a single nanofibre over hundreds of microns", Europhysics letters, 42, 215-220.

[57] Ramarkrishra S., Fujihara K., Teo W., Lim T., Ma Z., (2005), "An introduction to electrospinning and nanofibers", World Scientific.

[58] Xing X., Yu H., Zhu D., Zheng J., Chen H., Chen W., Cai J., (2012), "Subwavelength and nanometer diameter optical polymer fibers as building blocks for miniaturized photonics integration", InTech.

[59] Jayaraman K., Kotaki M., Zhang Y., Mo X., Ramakrishna S., (2004), "Recent advances in polymer nanofibers", Journal of Nanoscience and Nanotechnology, 4, 52–65.

[60] Zhang Y., Lim C. T., Ramakrishna S., Huang Z. M., (2005), "Recent development of polymer nanofibers for biomedical and biotechnological applications", Journal of Materials Science: Materials in Medicine, 16, 933–946.

[61] Percec V., Dulcey A. E., Peterca M., Ilies M., Nummelin S., Sienkowska M. J., Heiney P. A., (2006), "Principles of self-assembly of helical pores from dendritic dipeptides", 103, 2518–2523.

[62] Greiner A., J. H. Wendorff, (2007), “Electrospinning: A Fascinating Method for the Preparation of Ultrathin Fibers”, Angewandte Chemie International Edition, 46 (30), 5670-5703.

[63] Formhals A., (1934), “Process and Apparatus for Preparing Artificial Threads”, US Patent, 1, 975,504.

[64] Simm W., Gosling K., Bonart R., Falkai B. von G. B, (1972), 1346231.

[65] Doshi J., Srinivasan G., Reneker D., (1995), “A novel electrospinning process”, Polymer News, 20, 206-207.

[66] Koombhongse S., Liu W.X., Reneker D.H., (2001), “Flat polymer ribbons and other shapes by electrospinning”, J. Polymer Sci.: Part B: Polymer Physics, 39, 2598–2606.

[67] Megelski S., Stephens J.S., Rabolt J.F., Bruce C.D., (2002), “Micro-and nanostructured surface morphology on electrospun polymer fibers”, Macromolecules, 35 (22), 8456–8466.

[68] Lyoo W., Lee K, Lee Y., Kim H., (2007), "Preparation of High Molecular Weight Poly (Vinyl Carbazole) Web by Electrospinning", in: E.E. Gdoutos (Ed.) Experimental Analysis of Nano and Engineering Materials and Structures, Springer Netherlands, 47-48.

[69] Senador Jr. A.E., Shawa M.T., Mathera P.T., (2001), “Electrospinning of Polymeric Nanofibers: Analysis of Jet Formation”, Mat. Res. Soc. Symp. Proc., 661, KK5.9.1–KK5.9.6.

[70] Jeong J. S., Jeon S. Y., Lee T. Y., Park J. H., Shin J. H., Alegaonkar P. S., Berdinsky A. S., Yoo J. B., (2006), “Fabrication of MWNTs/nylon conductive composite nanofibers by electrospinning”, Diamond and Related Materials, 15 (11-12), 1839-1843.

[71] Schreuder-Gibson H. L., Gibson P., Senecal K., Sennett M., Walker J., Yeomans W., (2002), “Protective textile materials based on electrospun nanofibers”, Journal of Advanced Materials, 34 (3), 44–55.

[72] Kim J.-S., Lee D.-S., (2000), “Thermal properties of electrospun polyesters” Polymer J., 32 (7), 616–618.

[73] Kayaci F., Aytac Z., Uyar T., (2013) “Surface modification of electrospun polyester nanofibers with cyclodextrin polymer for the removal of phenanthrene from aqueous solution”, Journal of Hazardous Materials, 261, 286-294.

[74] Kalaycı E., Avinç O., Yavaş A., (2014), “Polibenzimidazol (PBI) Lifleri”, Tekstil ve Mühendis, 21 (96), 52-67.

[75] Krishnappa V.N., Sung C.M., Schreuder-Gibson H., (2002), "Electrospinning of Polycarbonates and their surface characterization using the SEM and TEM", Mat. Res. Soc. Symp. Proc., 702, U6.7.1–U6.7.6.

[76] González E.; Shepherd L. M.; Saunders L.; Frey M. W., (2016), "Surface Functional Poly(lactic Acid) Electrospun Nanofibers for Biosensor Applications", Materials, 9, 47.

[77] Norris I. D., Shaker M. M., Ko F. K., Macdiarmid A. G., (2000), "Electrostatic fabrication of ultrafine conducting fibers: polyaniline/polyethylene oxide blends", Synthetic Metals, 114 (2), 109–114.

[78] Frey M. W., (2008), "Electrospinning Cellulose and Cellulose Derivatives", Polymer Reviews", 48 (2), 378-391.

[79] Yeum J. H., Park S. M., Yang S. B., Sabina Y., Kim Y. H., Shin J. C., (2016). "Novel Natural Polymer/Medicinal Plant Extract Electrospun Nanofiber for Cosmeceutical Application", Nanofiber Research Reaching New Heights, Prof. Mohammed Rahman (Ed.), InTech.

[80] Fong H., Liu W.-D., Wang C.-S., Vaia R.A., (2002), "Generation of electrospun fibers of nylon 6 and nylon 6-montmorillonite nanocomposite", Polymer, 43 (3), 775–780.

[81] Wang C., Yuan J., Niu H., Yan E., Zhao H., (2009), "Investigation of fundamental parameters affecting electrospun PVA/CuS composite nanofibres", Pigment & Resin Technology, 38 (1), 25–32.

[82] Barnes C. P., Sell S. A., Boland E. D., Simpson D. G., Bowlin G. L., (2007), "Nanofiber technology: Designing the next generation of tissue engineering scaffolds", Advanced Drug Delivery Reviews, 59 (14), 1413–1433.

[83] Erisken C., (2008), "Functionally Graded Scaffolds for The Engineerıng of Interface Tissues Using Hybrid Twin Screw Extrusion/Electrospinning Technology", Doktora Tezi, Stevens Institute of Technology.

[84] Senthamizhan A., Celebioglu A., Bayir S., Gorur M., Doganci E., Yilmaz F., Uyar T., (2015), "Highly fluorescent pyrene-functional polystyrene copolymer nanofibers for enhanced sensing performance of TNT", ACS Applied Materials and Interfaces, 7 (38), 21038–21046.

[85] Zeng J., (2011), "Non-Linear Electrohydrodynamics in Microfluidic Devices", Int J Mol Sci, 12, 1633-1649.

[86] Deitzel J. M., Kleinmeyer J., Harris D., Tan N. C. B., (2001), "The effect of processing variables on the morphology of electrospun nanofibers and textiles", Polymer, 42, 261-272.

[87] Jia T. Y., Gong J., Gu H. X., Kim Y. H., Dong J., Shen Y. X., (2007), "Fabrication and characterization of poly(vinyl alcohol)/chitosan blend

nanowbers produced by electrospinning method", Carbohydrate Polymers, 67, 403–409.

[88] Yang Q., Li Z., Hong Y., Zhao Y., Qiu S., Wang C., Wei Y., (2004), "Influence of solvents on the formation of ultrathin uniform poly (vinyl pyrrolidone) nanofibers with electrospinning", Journal of Polymer Science Part B: Polymer Physics, 42 (20), 3721-3726.

[89] Li Z., Wang C., (2013), "Effects of Working Parameters on Electrospinning One-Dimensional Nanostructures", SpringerBriefs in Materials, 15-28.

[90] Baştürk E., (2012), "Çapraz Bağlı Pva/B Nanofiberlerin Elektrospin Yöntemi İle Hazırlanması Ve Karakterizasyonu", Yüksek Lisans Tezi, Marmara Üniversitesi.

[91] Subbiah T., (2004), "Development of Nanofiber Protective Substrates", Yüksek Lisans Tezi, Texas Tech Üniversitesi.

[92] Jarusuwannapoom T., Hangrojjanawiwat W., Jitjaicham S., Wannatong L., Nithitanakul M., Pattamaprom C., Koombhongse P., Rangkupan R., Supaphol P., (2005), "Effect of Solvents on Electrospinnability of Polystyrene Solutions and Morphological Appearance of Resulting Electrospun Polystyrene Fibers", European Poly. J., 41, 409-421.

[93] Kumar P., (2012), "Effect of colletor on electrospinning to fabricate aligned nanofiber", Bachelor of Technology, Deemed University, India.

[94] Baumgarten P. K., (1971), "Electrostatic Spinning of Acrylic Microfibers", Journal of Colloid and Interface Science, 36, 71-79.

[95] Yener F., (2010), "Klasik ve İğnesiz Elektrospinning Yöntemleriyle Elde Edilen Nano Liflerin Kıyaslanması ve Bu Yöntemlerdeki Sistem Parametrelerinin Lif Üzerindeki Etkileri", Yüksek Lisans Tezi, Kahramanmaraş Sütçü İmam Üniversitesi.

[96] Cai Q., Feng Q., H. Liu, Yang X., (2013), "Preparation of biomimetic hydroxyapatite by biomineralization and calcination using poly(l-lactide)/gelatin composite fibrous mat as template", Materials Letters, 91, 275-278.

[97] Hou H., Jun Z, Reuning A., Schaper A., Wendorff J. H., Greiner A., (2002), "Poly(p-xylylene) Nanotubes by Coating and Removal of Ultrathin Polymer Template Fibers", Macromolecules, 35 (7), 2429-2431.

[98] Caruso R. A., Schattka J. H., Greiner A., (2001), "Titanium Dioxide Tubes from Sol–Gel Coating of Electrospun Polymer Fibers", Advanced Materials, 13 (20), 1577-1579.

[99] Qin X. H., Wang S. Y., (2006), "Filtration properties of electrospinning nanofibers", Journal of Applied Polymer Science, 102 (2), 1285-1290.

[100] Shin C., Chase G. G, (2004), "Water-in-oil coalescence in micro-nanofiber composite filters", AIChE Journal, 50 (2), 343-350.

[101] Abdel G. M. S., Davies G. A, (1985), "Simulation of non-woven fibre mats and the application to coalescers", Chemical Engineering Science, 40 (1), 117-129.

[102] Shin C., Chase G. G., Reneker D. H, (2005), "Recycled expanded polystyrene nanofibers applied in filter media", Colloids and Surfaces A: Physicochemical and Engineering Aspects, 262 (1-3), 211-215.

[103] Shin C., Chase G. G, Reneker D. H., (2005), "The effect of nanofibers on liquid–liquid coalescence filter performance", AIChE Journal, 51 (12), 3109-3113.

[104] Barhate R. S., Ramakrishna S., (2007), "Nanofibrous filtering media: Filtration problems and solutions from tiny materials", Journal of Membrane Science, 296 (1-2), 1-8.

[105] Ahn Y. C., Park S. K., Kim G. T., Hwang Y. J., Lee C. G., Shin H. S., Lee J. K., (2006), "Development of high efficiency nanofilters made of nanofibers", Current Applied Physics, 6 (6), 1030-1035.

[106] Graham K., Ouyang M., Raether T., Grafe T., McDonald B., Knauf P., (2002), "Polymeric Nanofibers in Air Filtration Applications", Advances in Filtration and Separation Technology, 15, 500-524.

[107] Jeong E. H., Yang J., Youk J. H., (2007), "Preparation of polyurethane cationomer nanofiber mats for use in antimicrobial nanofilter applications", Materials Letters, 61 (18), 3991-3994.

[108] Son W. K., Youk J. H., Lee T. S., Park W. H., (2004), "Preparation of Antimicrobial Ultrafine Cellulose Acetate Fibers with Silver Nanoparticles", Macromolecular Rapid Communications, 25 (18), 1632-1637.

[109] Graeser M., Pippel E., Greiner A., Wendorff J. H., (2007), "Polymer Core−Shell Fibers with Metal Nanoparticles as Nanoreactor for Catalysis", Macromolecules, 40 (17), 6032-6039.

[110] Xie J., Wu Q., Zhao D., (2012), "Electrospinning synthesis of $ZnFe_2O_4/Fe_3O_4$/Ag nanoparticle-loaded mesoporous carbon fibers with magnetic and photocatalytic properties", Carbon, 50 (3), 800-807.

[111] Kim H., Choi Y., Kanuka N., Kinoshita H., Nishiyama T., Usami T., (2009), "Preparation of Pt-loaded TiO_2 nanofibers by electrospinning and their application for WGS reactions", Applied Catalysis A: General, 352 (1-2), 265-270.

[112] Chen L., Hong S., Zhou X., Zhou Z., Hou H., (2008), "Novel Pd-carrying composite carbon nanofibers based on polyacrylonitrile as a catalyst for Sonogashira coupling reaction", Catalysis Communications, 9 (13), 2221-2225.

[113] Jang J., Park J., (2002), "Coating material for shielding electromagnetic waves", US 6355707.

[114] Wang Y., Jing X., (2005), "Intrinsically conducting polymers for electromagnetic interference shielding", Polymers for Advanced Technologies, 16 (4), 344-351.

[115] Desai K., Sung C., (2002), "Electrospinning Nanofibers of PANI/PMMA Blends", MRS Online Proceedings Library, 736, D2.7.

[116] Sen R., Zhao B., Perea D., Itkis M. E., Hu H., Love J., Bekyarova E., Haddon R. C, (2004), "Preparation of Single-Walled Carbon Nanotube Reinforced Polystyrene and Polyurethane Nanofibers and Membranes by Electrospinning", Nano Letters, 4 (3), 459-464.

[117] Im J. S., Kim J. G., Lee S. H, Lee Y. S., (2010), "Effective electromagnetic interference shielding by electrospun carbon fibers involving Fe_2O_3/$BaTiO_3$/MWCNT additives", Materials Chemistry and Physics, 124 (1), 434-438.

[118] Im J. S., Kim J. G., Lee S. H., Lee Y. S., (2010), "Enhanced adhesion and dispersion of carbon nanotube in PANI/PEO electrospun fibers for shielding effectiveness of electromagnetic interference", Colloids and Surfaces A: Physicochemical and Engineering Aspects, 364 (1-3), 151-157.

[119] Park S. J., Cho M. S., Lim S. T., Choi H. J, Jhon M., (2005), "Electrorheology of Multiwalled Carbon Nanotube/Poly(methyl methacrylate) Nanocomposites", Macromolecular Rapid Communications, 26 (19), 1563-1566.

[120] Gorur M., Yilmaz F., Kilic A., Sahin Z. M., Demirci A., (2011), "Synthesis of pyrene end-capped A6 dendrimer and star polymer with phosphazene core via "click chemistry"", Journal of Polymer Science Part A: Polymer Chemistry, 49 (14), 3193-3206.

[121] Meuer S., Braun L., Zentel R., (2009), "Pyrene Containing Polymers for the Non-Covalent Functionalization of Carbon Nanotubes", Macromolecular Chemistry and Physics, 210 (18), 1528-1535.

[122] Li M., Xu P., Yang J., Ying H, Haubner K., Dunsch L., Yang S., (2011), "Synthesis of Pyrene-Substituted Poly(3-hexylthiophene) via Postpolymerization and Its Noncovalent Interactions with Single-Walled Carbon Nanotubes", Journal of Physical Chemistry C, 115 (11), 4584-4593.

[123] Wang X., Drew C., Lee S. H., Senecal K. J., Kumar J., Samuelson L. A., (2002), "Electrospun Nanofibrous Membranes for Highly Sensitive Optical Sensors", Nano Letters, 2 (11), 1273-1275.

[124] Rathfon J. M., Al-Badri Z. M., Shunmugam R., Berry S. M., Pabba S., Keynton R. S., Cohn R. W., Tew G. N., (2009), "Fluorimetric Nerve Gas Sensing Based on Pyrene Imines Incorporated into Films and Sub-Micrometer Fibers", Advanced Functional Materials, 19 (5), 689-695.

[125] Wang X., Lee S. H., Ku B. C., Samuelson L. A., Kumar J., (2002), "Synthesis and Electrospinning of A Novel Fluorescent Polymer PMMA-PM for Quenching-Based Optical Sensing", Journal of Macromolecular Science Part A, 39 (10), 1241-1249**.**

[126] Deng C., Gong P., He Q., Cheng J., He C., Shi L., Zhu D., Lin T., (2009), "Highly fluorescent TPA-PBPV nanofibers with amplified sensory response to TNT", Chemical Physics Letters, 483 (4-6), 219-223.

[127] Yang Y., Wang H., Su K., Long Y., Peng Z., Li N., Liu F., (2011), "A facile and sensitive fluorescent sensor using electrospun nanofibrous film for nitroaromatic explosive detection", Journal of Materials Chemistry, 21, 11895-11900.

[128] Yoon J., Chae S. K., Kim J. M, (2007), "Colorimetric Sensors for Volatile Organic Compounds (VOCs) Based on Conjugated Polymer-Embedded Electrospun Fibers", Journal of the American Chemical Society, 129 (11), 3038-3039.

[129] Ding B., Yamazaki M., Shiratori S., (2005), "Electrospun fibrous polyacrylic acid membrane-based gas sensors", Sensors and Actuators B: Chemical, 106 (1), 477-483.

[130] Luoh R., Hahn H. T., (2006), "Electrospun nanocomposite fiber mats as gas sensors", Composites Science and Technology, 66 (14), 2436-2441.

[131] Rho K. S., Jeong L., Lee G., Seo B. M., Park Y. J., Hong S. D., Roh S., Cho J. J., Park W. H., Min B. M., (2006), "Electrospinning of collagen nanofibers: Effects on the behavior of normal human keratinocytes and early-stage wound healing", Biomaterials, 27 (8), 1452-1461.

[132] Çakmakçı E., (2009), "Elektrospinning Yöntemi ile Yeni Polimerik Malzemelerin Sentezi ve Karakterizasyonu", Yüksek Lisans Tezi, Marmara Üniversitesi.

[133] Mishra V., Kumar R., (2012), "Living Radical Polymerization: A Review", Journal of Scientific Research, 56, 141-176.

[134] Ayaz H., (2011), "Pirazabol Merkezli İki Kollu Polimetilmetakrilat'ın Hazırlanması ve Termal Davranışının İncelenmesi", Yüksek lisans Tezi, Adıyaman Üniversitesi.

[135] Binder W. H., Sachsenhofer R., (2007), "'Click' Chemistry in Polymer and Materials Science", Macromolecular Rapid Communications, 28 (1), 15-54.

[136] Moses J. E., Moorhouse A. D., (2007), "The growing applications of click chemistry", Chemical Society Reviews, 36 (8), 1249-1262.

[137] Haldón E., Nicasio M. C., Pérez P. J., (2015), "Copper-catalysed azide–alkyne cycloadditions (CuAAC): an update", Organic Biomolecular Chemistry, 13, 9528-9550.

[138] Kaufmann T., Gokmen M. T., Rinnen S., Arlinghaus H. F., Prez F. D., Ravoo B. J., (2012), "Bifunctional Janus Beads Made by "Sandwich" Microcontact Printing and Click Chemistry", Journal of Materials Chemistry**,** 22**,** 6190-6199.

[139] Morozumi T., Sato N., Nakamura H., (2006), "Selective Pseudo-Rotaxane Type Complex Formation of Zinc(II) (t-butylatedtetraphenyl) porphyrin-Viologen Linked Compounds with tri-O-methyl-β-Cyclodextrin", Journal of Inclusion Phenomena and Macrocyclic Chemistry, 56 (1), 141-148.

[140] Li L., Zhang X., He X., Lu W., Yang L., Bian Y., Weng Y., Jiang J., (2014), "C60-modified mixed (phthalocyaninato)(porphyrinato) yttrium(III) double-decker complex: Synthesis, characterization, and photophysical properties", Dyes and Pigments, 102, 257-262.

[141] Wang F., Tang J., Liu J., Wang Y., Wang R., Niu L., Huang L., Huang Z., (2011), "Synthesis and photoinduced electron transfer characteristic of a bis (zinc porphyrin)-perylene bisimide array", Journal of Physical Organic Chemistry, 24, 1101–1109.

[142] Kang H., Kwon K. S., Kang D., Lee J. C., (2007), "Enhanced, Perpendicular Liquid-Crystal Alignment on Rubbed Films of a Coumarin-Containing Polystyrene", Macromolecular Chemistry and Physics, 208, 1853–1861.

BIOGRAPHY

Sümeyra BAYIR was born in 1986 in Bursa, Turkey. She obtained her B.S. degree in Chemistry from Izmir Institute of Technology (IZTECH) in 2010. Then, she obtained her master degree in Chemistry from Graduate School of Natural and Applied Sciences, Gebze Technical University (GTU) in 2013. She then continued her Ph.D. at the same university. Her current research interests include polymer chemistry, electrospinning of functional polymers and fluorescence-active nanofibers.

APPENDICES

Appendix A: Publications

Anitha Senthamizhan, Asli Celebioglu, Sumeyra Bayir, Mesut Gorur, Erdinc Doganci, Faruk Yilmaz, Tamer Uyar, “Highly fluorescent pyrene-functional polystyrene copolymer nanofibers for enhanced sensing performance of TNT”, ACS Applied Materials and Interfaces, 2015, 7(38), 21038–21046.

A. Senthamizhan, A. Celebioglu, S. Bayir, M. Gorur, E. Doganci, T. Uyar, F. Yilmaz, "Production and TNT sensing application of polystyrene nanofibers containing fluorescent functional groups", European Polymer Federation (EPF), Dresden, 2015.

Sümeyra Bayır, Aslı Çelebioğlu, Mesut Görür, Erdinç Doğancı, Tamer Uyar, Faruk Yılmaz, “Dansil Yan Gruplarına Sahip Stiren Polimerlerin Sentezi ve Elektroeğilmiş Nanofiberlerinin Üretilmesi”, 27. Ulusal Kimya Kongresi, 23-28 Ağustos, 2015, Çanakkale.

S. Bayir, M. Gorur, E. Doganci, T. Uyar, F. Yilmaz, "Highly fluorescent porphyrin-functional styrene copolymer nanofibers", 46th International Symposium on Macromolecules (MACRO 2016)-IUPAC World Polymer Congress, June 17-21, 2016, Istanbul.

Appendix B: Mass spectra of synthesized compounds

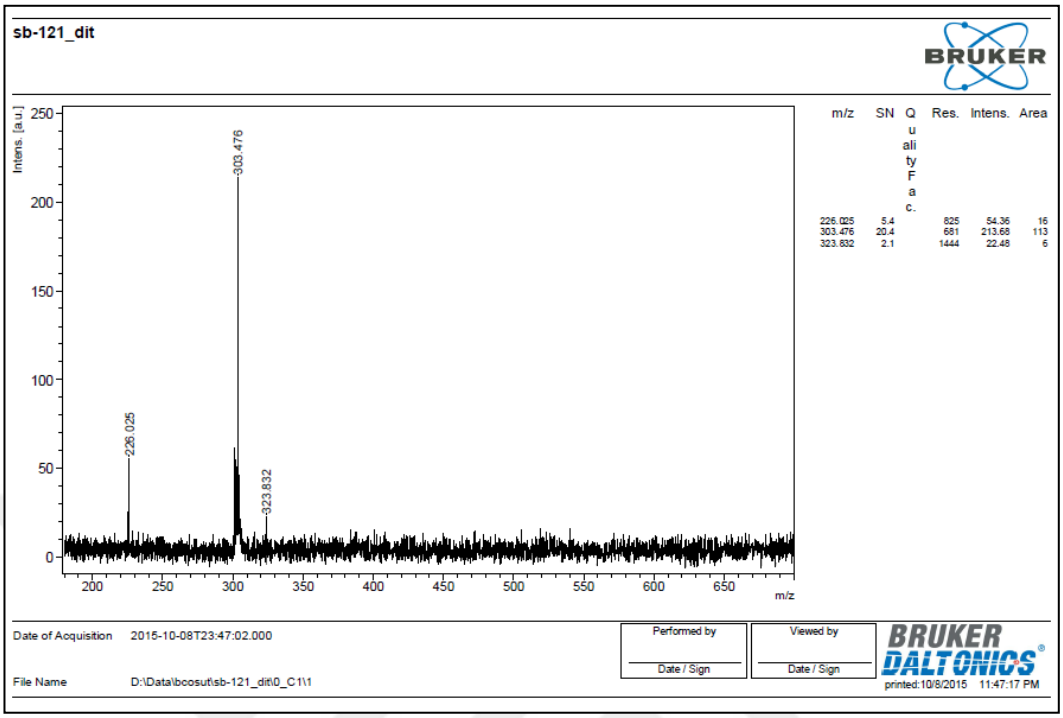

Figure B1.1: Mass spectrum of compound 1.

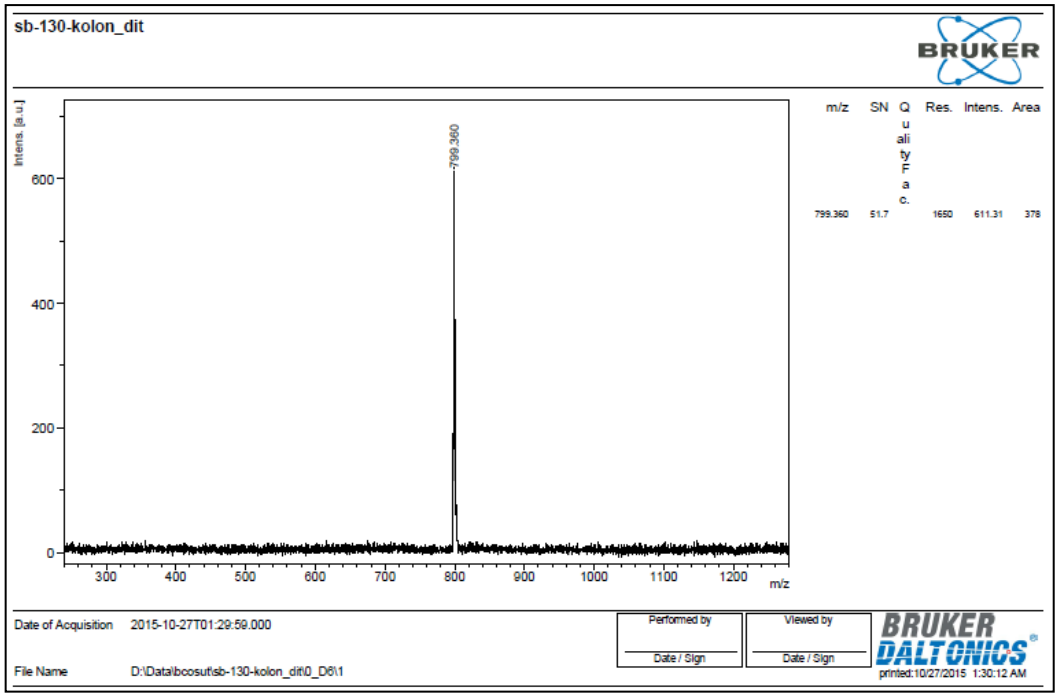

Figure B1.2: Mass spectrum of compound 2.

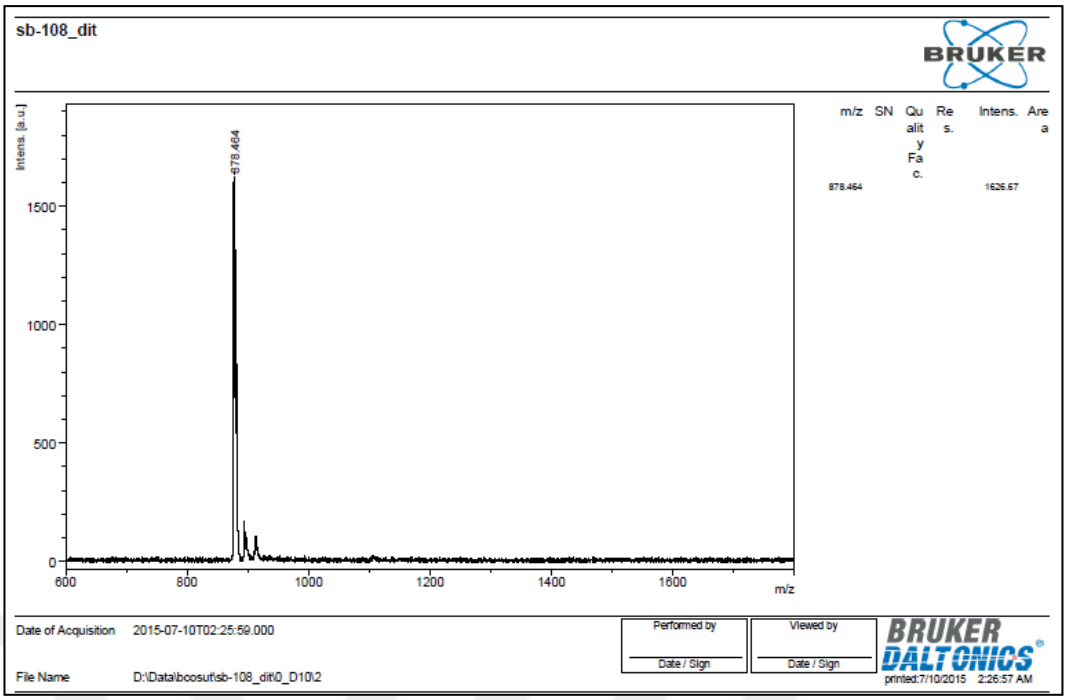

Figure B1.3: Mass spectrum of compound 3.

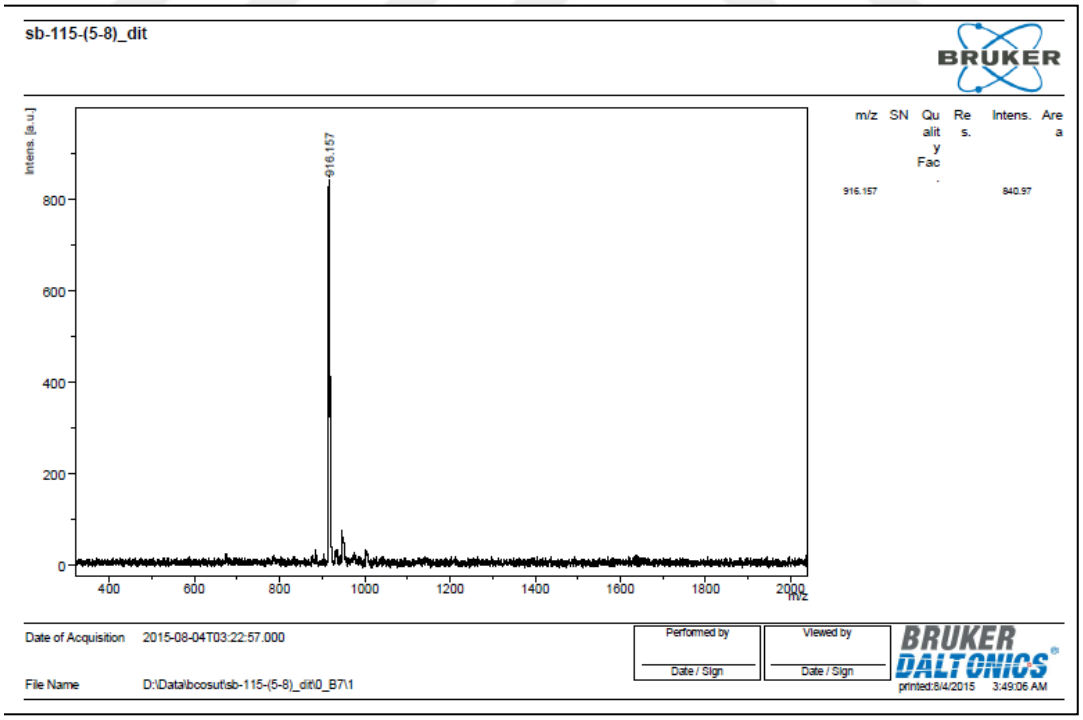

Figure B1.4: Mass spectrum of compound 4.